

48 Crepant Paths to $SU(2) \times SU(3)$

Mboyo Esole[♡], Ravi Jagadeesan^{♣, ♢}, and Monica Jinwoo Kang[♣]

♡ Department of Mathematics, Northeastern University
360 Huntington Avenue, Boston, MA 02115, USA

♣ Harvard Business School
Wyss Hall, Soldiers Field, Boston, MA 02163, USA

♢ Department of Economics, Harvard University
1805 Cambridge St, Cambridge, MA 02138, USA

♣ Department of Physics, Harvard University
17 Oxford Street, Cambridge, MA 02138, U.S.A

j.esole@northeastern.edu, ravi.jagadeesan@gmail.com, jkang@fas.harvard.edu

Abstract

We study crepant resolutions of Weierstrass models of $SU(2) \times SU(3)$ -models, whose gauge group describes the non-abelian sector of the Standard Model. The $SU(2) \times SU(3)$ -models are elliptic fibrations characterized by the collision of two Kodaira fibers with dual graphs that are affine Dynkin diagrams of type \tilde{A}_1 and \tilde{A}_2 . Once we eliminate those collisions that do not have crepant resolutions, we are left with six distinct collisions that are related to each other by deformations. Each of these six collisions has eight distinct crepant resolutions whose flop diagram is a hexagon with two legs attached to two adjacent nodes. Hence, we consider 48 distinct resolutions that are connected to each other by deformations and flops. We determine topological invariants—such as Euler characteristics, Hodge numbers, and triple intersections of fibral divisors—for each of the crepant resolutions. We analyze the physics of these fibrations when used as compactifications of M-theory and F-theory on Calabi–Yau threefolds yielding 5d $\mathcal{N} = 1$ and 6d $\mathcal{N} = (1, 0)$ supergravity theories respectively. We study the 5d prepotential in the Coulomb branch of the theory and check that the six-dimensional theory is anomaly-free and compatible with a 6d uplift from a 5d theory.

Contents

1	Introduction	2
1.1	Matter representation and connection to the Standard Model	3
1.2	Geography of crepant resolutions of G -models and hyperplane arrangements	4
1.3	Topological invariants	5
1.4	Compactification of M-theory to $5d \mathcal{N} = 1$ supergravity	5
1.5	Compactification of F-theory to $6d \mathcal{N} = (1, 0)$ supergravity and cancellation of anomalies	6
1.6	Organization of this paper	7
2	The many faces of the $SU(2) \times SU(3)$-model	7
3	Geometry	9
3.1	Crepant resolutions	10
3.2	Intersection theory and blowups	11
3.3	Euler characteristics and Hodge numbers	12
3.4	Triple intersection numbers	13
3.5	Non-Kodaira fibers	15
4	Hyperplane arrangements and geography of flops	15
4.1	Geometric weights and matter representations	15
4.2	Hyperplane arrangement	16
4.3	Correspondence between the geometry and the representation theory	17
5	The $I_2^s + I_3^s$ Model	20
5.1	Resolution I	20
5.2	Resolution II	22
5.3	Resolution III	25
5.4	Resolution IV	27
5.5	Flops	29
6	The $III + IV^s$ Model	30
6.1	Resolution I	31
6.2	Resolution II	33
6.3	Resolution III	35
6.4	Resolution IV	37
7	$5d$ and $6d$ supergravity theories with eight supercharges	38
7.1	$5d \mathcal{N} = 1$ supergravity theory with a gauge group $SU(2) \times SU(3)$	38
7.2	Anomaly cancellations in general $6d \mathcal{N} = (1, 0)$ supergravity theory	40
7.3	Anomaly cancellations in $6d \mathcal{N} = (1, 0)$ supergravity theory	43
A	Fiber enhancement	46

1 Introduction

One of the most powerful consequences of string theory dynamics is that gauge theories can be geometrically engineered by singularities [4, 41, 80]. In F-theory, the singularities are given by the degenerations of the fiber of an elliptic fibration [11, 67]. The F-theory picture naturally associates to an elliptic fibration a reductive Lie group G , a Lie algebra $\mathfrak{g} = \text{Lie}(G)$, and a representation \mathbf{R} of G . Such an elliptic fibration is called a G -model. The dual graphs of the singular fibers over the generic points of the discriminant locus of the elliptic fibration determine the gauge algebra \mathfrak{g} .

The Lie group G is semi-simple when the discriminant of the elliptic fibration contains at least two irreducible components Δ_1 and Δ_2 such that the dual graph of the singular fiber over the generic point of Δ_i ($i = 1, 2$) is reducible. These are called *collisions of singularities* and were first studied by Bershadsky and Johanson [12]. The gauge group G depends on the gauge algebra and the Mordell–Weil group of the elliptic fibration [62]. When the Mordell–Weil group is trivial, the gauge group G is the unique compact, connected, and simply-connected Lie group with Lie algebra \mathfrak{g} . The compact simply connected semi-simple Lie groups with rank 2 or 3 are

$$\text{SU}(2) \times \text{SU}(2), \quad \text{SU}(2) \times \text{G}_2, \quad \text{SU}(2) \times \text{Sp}(4), \quad \text{and} \quad \text{SU}(2) \times \text{SU}(3).$$

The $\text{SU}(2) \times \text{SU}(2)$ -, $\text{SU}(2) \times \text{G}_2$ -, and $\text{SU}(2) \times \text{SU}(3)$ -models could be realized by non-Higgsable clusters [66] as in [29, 30, 43]. There are subtleties in realizing an $\text{SU}(3)$ as a non-Higgsable group as discussed in Remark 2.1. The $\text{SU}(2) \times \text{SU}(2)$ -model, the $\text{SU}(2) \times \text{G}_2$ -model, and the $\text{Sp}(4)$ -model are studied respectively in [30], [29], and [31]. The individual $\text{SU}(2)$ and $\text{SU}(3)$ -models are studied in [34, 35] and the $\text{SU}(2) \times \text{SU}(3)$ -model (realized by the collision III+IV^s) has been studied from the point of view of string junctions in [43]. While the group $\text{SU}(2) \times \text{SU}(3)$ is famously the non-Abelian gauge sector of the Standard Model of particle physics [8, §2.4], the $\text{SU}(2) \times \text{SU}(3)$ -model has never been constructed explicitly as a nonsingular variety.

The purpose of this paper is to study the $\text{SU}(2) \times \text{SU}(3)$ -model with associated Lie algebra

$$E_3 = A_1 \oplus A_2.$$

We define elliptic fibrations with collisions of singularities corresponding to a Lie algebra of type E_3 , we study their geometry and topology, and explore the physics of compactifications of M-theory and F-theory on such varieties when the elliptic fibration is a Calabi–Yau threefold. By definition, an $\text{SU}(2) \times \text{SU}(3)$ -model is an elliptic fibration with a trivial Mordell–Weil group and a discriminant locus containing two irreducible smooth components S and T such that the generic fiber over S and T have respectively dual graphs of affine Dynkin type \tilde{A}_1 and \tilde{A}_2 , while the Kodaira type of the fiber over the generic point of any other irreducible component of the discriminant locus is of type I_1 or II . The $\text{SU}(2) \times \text{SU}(3)$ -models examined in this paper are defined by singular Weierstrass models, given in Section 2, for which we construct explicit crepant resolutions in Section 3.1. Weierstrass models provide convenient canonical birational models for elliptic fibrations since any elliptic fibration over a smooth base is birational to a possibly singular Weierstrass model [18, 19, 68].

We show that there are six distinct types of *collisions of singularities* that define Weierstrass models for $\text{SU}(2) \times \text{SU}(3)$ -models with crepant resolutions, namely:

$$I_2^s + I_3^s, \quad I_2^{\text{ns}} + I_3^s, \quad \text{III} + I_3^s, \quad I_2^s + \text{IV}^s, \quad I_2^{\text{ns}} + \text{IV}^s, \quad \text{III} + \text{IV}^s.$$

We show that each of the corresponding Weierstrass models has eight distinct crepant resolutions.

These six $SU(2)\times SU(3)$ -models are deformation of each other, where the deformations commute with the resolutions in a way such that the same eight sequences of three blowups are used for each of the six realizations of the $SU(2)\times SU(3)$ -model. In total, we have a network of 48 distinct elliptic fibrations connected by deformations and flops. All the crepant resolutions of the $SU(2)\times SU(3)$ -models are listed in Section (3.1).

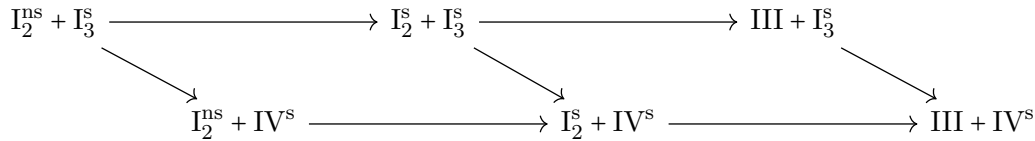


Figure 1: The six collisions of singularities that give Weierstrass models whose crepant resolutions are smooth $SU(2)\times SU(3)$ -models. In this graph, each arrow indicates a specialization of a Weierstrass model to another. The only collision that correspond to a non-Higgsable model is $III + IV^{\text{s}}$.

1.1 Matter representation and connection to the Standard Model

The gauge group of the $SU(2)\times SU(3)$ -model is the non-Abelian sector of the Standard Model of particle physics [8, §2.4]. In this paper, we consider this gauge theory in the context of five and six-dimensional supergravity theories with minimal supersymmetry resulting from a compactification of M-theory or F-theory on a Calabi–Yau threefold Y that corresponds to an elliptic fibration giving an $SU(2)\times SU(3)$ -model. The representation \mathbf{R} of the resulting 5d and 6d theory is reminiscent of the representations of fermions of the Standard Model once we ignore the Abelian sector.

The weights of vertical curves over codimension-one loci of the discriminant locus determine a representation \mathbf{R} of \mathfrak{g} called the *matter representation*. See [23] and reference therein for details on Weierstrass models, weights of curves, dual graphs, and G -models. We show that $SU(2)\times SU(3)$ -models, defined over a base of dimension-two or higher, have vertical rational curves carrying the weights of the following quaternionic representation \mathbf{R} reminiscent of the representation \mathbf{F} of fermions of the Standard Model transforming non-trivially under $SU(2)\times SU(3)$:

$$\begin{aligned}
\mathbf{R} &= (\mathbf{2}, \mathbf{1}) \oplus (\mathbf{1}, \mathbf{3}) \oplus (\mathbf{1}, \bar{\mathbf{3}}) \oplus (\mathbf{2}, \mathbf{3}) \oplus (\mathbf{2}, \bar{\mathbf{3}}) \oplus (\mathbf{3}, \mathbf{1}) \oplus (\mathbf{1}, \mathbf{8}), \\
\mathbf{F} &= (\mathbf{2}, \mathbf{1}) \oplus (\mathbf{1}, \mathbf{3}) \oplus (\mathbf{1}, \bar{\mathbf{3}}) \oplus (\mathbf{2}, \mathbf{3}) \oplus (\mathbf{2}, \bar{\mathbf{3}}),
\end{aligned}$$

where $(\mathbf{r}_1, \mathbf{r}_2)$ is the product of the representation \mathbf{r}_1 of the Lie algebra of type A_1 and the representation \mathbf{r}_2 of A_2 , and $\bar{\mathbf{r}}$ is the complex conjugate representation of \mathbf{r} .¹

In the Standard Model, left-handed leptons transform in the representation $(\mathbf{2}, \mathbf{1})$ of $SU(2)\times SU(3)$, left-handed quarks transform in the representation $(\mathbf{2}, \mathbf{3})$, and right-handed up and down quarks transform in the representation $(\mathbf{1}, \mathbf{3})$. Right-handed leptons are neutral under $SU(2)\times SU(3)$ in the Standard Model, and we also have $n_H^0 = h^{2,1}(Y) + 1$ neutral hypermultiplets in the $SU(2)\times SU(3)$ -model (see equation (7.29)).

There are also differences: the $SU(2)\times SU(3)$ -model has hypermultiplets transforming under the adjoints representations $(\mathbf{3}, \mathbf{1})$ and $(\mathbf{1}, \mathbf{8})$ while the Standard Model does not have fermions

¹In particular, $(\mathbf{3}, \mathbf{1})$ is the adjoint representation of A_1 , $(\mathbf{1}, \mathbf{8})$ is the adjoint representation of A_2 , $(\mathbf{2}, \mathbf{1})$ is the fundamental representation of A_1 , $(\mathbf{1}, \mathbf{3})$ is the fundamental representation of A_2 , and $(\mathbf{2}, \mathbf{3})$ is the bifundamental representation of $A_1 \oplus A_2$.

transforming in adjoint representations.

1.2 Geography of crepant resolutions of G -models and hyperplane arrangements

A crepant resolution is a resolution of singularities that preserves the canonical class. In the case of surfaces, a crepant resolution is necessarily unique and always exists for du Val singularities. Starting from dimension-three, crepant resolutions (when they exist) are not necessarily unique. For normal threefolds with canonical singularities, the number of crepant resolutions is finite [53] and two crepant resolutions are connected by flops [50]. A substitute for crepant resolutions are terminal varieties and they always exist for varieties with canonical singularities [14]. In light of the result of Kawamata [50], it follows from the celebrated results of [14] that minimal models are connected by flops. \mathbb{Q} -factorial terminal singularities are obstructions to the existence of crepant resolutions as \mathbb{Q} -factoriality implies that the exceptional set of any birational map is a divisor, and being terminal implies that all the discrepancies are positive [56]. Canonical singularities, \mathbb{Q} -factorial singularities, terminal singularities, crepant resolutions, and flops are defined for example in [55, 61].

For G -models, the geography of flops can be described by the hyperplane arrangement $I(\mathfrak{g}, \mathbf{R})$ defined inside the dual fundamental Weyl chamber of \mathfrak{g} and whose hyperplanes are the kernel of the weights of the representation \mathbf{R} [21, 22, 46]. In stringy geometry, this is a conjecture motivated by the structure of the Coulomb branches of a five-dimensional $\mathcal{N} = 1$ supergravity theory with a gauge group G and matter transforming in the representation \mathbf{R} [47]. As each Coulomb phase corresponds to a unique crepant resolution of the Weierstrass model, flops corresponds to phase transitions [79], and the different Coulomb phases correspond to the different connected domains in which the prepotential is differentiable; the study of the structure of the 5d Coulomb branches boils down to identifying the chambers of a hyperplane arrangement (see Section 7.1). Mathematically, this fact can be understood by subdivision of a relative movable cone of any of the crepant resolution over the Weierstrass model of a G -model into nef cones of each particular crepant resolution in the spirit of [51, 52, 60] and [61, Theorem 12-2-7].

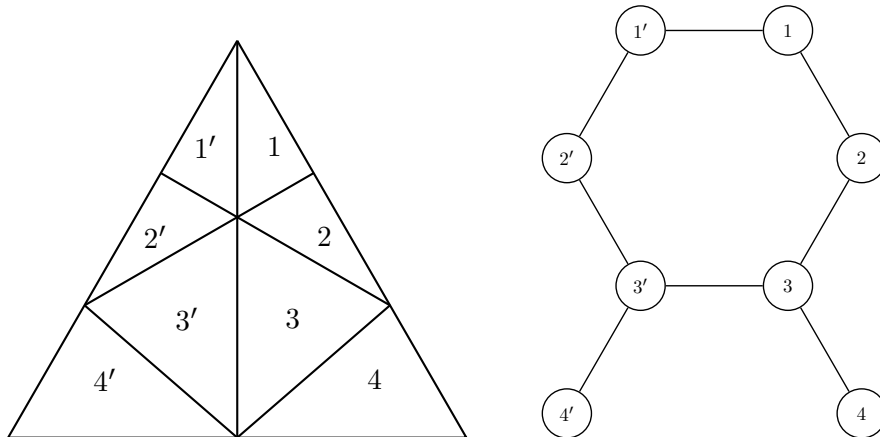


Figure 2: The chamber structure of $I(E_3 = A_1 \oplus A_2, (\mathbf{1}, \mathbf{3}) \oplus (\mathbf{2}, \mathbf{3}))$ and its adjacency graph. This also represents the structure of the extended Kähler cone of an $SU(2) \times SU(3)$ -model. See Figure 3 for more details on the walls separating the chambers.

The network of flops of the $SU(2) \times SU(3)$ -model matches the hyperplane arrangement $I(E_3 = A_1 \oplus A_2, (\mathbf{1}, \mathbf{3}) \oplus (\mathbf{2}, \mathbf{3}))$, where $(\mathbf{1}, \mathbf{3}) \oplus (\mathbf{2}, \mathbf{3})$ is the direct sum of the bifundamental representation of $SU(2) \times SU(3)$ and the fundamental representation of $SU(3)$. The chamber structure of this hyperplane arrangement is represented in Figure 2.

1.3 Topological invariants

The Euler characteristic of the elliptically-fibered Calabi–Yau threefold Y is instrumental in the discussion of the gravitational anomalies of the six-dimensional supergravity theory when F-theory is compactified on such Y [44]. The Hodge numbers of Y determines the number of vector multiplets and neutral hypermultiplets in an M-theory compactification on Y [15]. In the case of Calabi–Yau fourfolds, the Euler characteristic is relevant to the cancellation of the D3-brane tadpole [2,3,17,74]. The triple intersection numbers of divisors of a Calabi–Yau threefold Y give the Chern–Simons terms of an M-theory compactification on Y .

While the Euler characteristic and the Betti numbers, are independent of the choice of a crepant resolution as shown by Batyrev [9], the triple intersection numbers are not preserved by flops and depend on a choice of a crepant resolution [47]. We compute the Euler characteristic of an $SU(2) \times SU(3)$ -model over a base of arbitrary dimension in Theorem 3.5 in the spirit of [25,27,28]. Denoting by B the base of the fibration, by S and T the divisors supporting respectively the fiber with dual graphs \tilde{A}_1 and \tilde{A}_2 , and by L the first Chern class of the line bundle \mathcal{L} of the Weierstrass model (see Theorem 3.3), we have

$$\chi(Y) = 6 \frac{S^2 - 2L - 3SL + 2(S^2 - 3SL + S - 2L)T + (3S + 2)T^2}{(1 + S)(1 + T)(-1 - 6L + 2S + 3T)} c(TB).$$

We also determine the Hodge numbers of an $SU(2) \times SU(3)$ -model and the triple intersection numbers in the case of the Calabi–Yau threefolds. Since the triple intersection numbers depend on a choice of a resolution, we compute them for each of the crepant resolutions in Theorem 3.4.

$$h^{1,1}(Y) = 14 - K^2, \quad h^{2,1}(Y) = 29K^2 + 15KS + 24KT + 3S^2 + 6ST + 6T^2 + 14,$$

where K is the canonical class of the base B .

1.4 Compactification of M-theory to 5d $\mathcal{N} = 1$ supergravity

We analyze the physics of the compactifications of M-theory and F-theory on elliptically-fibered Calabi–Yau threefolds corresponding to $SU(2) \times SU(3)$ -models. These give five and six-dimensional gauge theories coupled to supergravity theories with eight supercharges respectively. For the five-dimensional supergravity theory, we compute the one-loop prepotential in the Coulomb branch (see Theorem 7.1), and determine the Chern–Simons couplings, the number of vector multiplets, tensor multiplets, and hypermultiplets. The Chern–Simons couplings are computed geometrically as triple intersection numbers of fibral divisors in each Coulomb chamber (see Theorem 3.11).

The Chern–Simons levels are given by triple intersection numbers of divisors of the Calabi–Yau threefolds and determine the prepotential of a five-dimensional supergravity theory from an M-theory compactification on such Calabi–Yau threefolds [15]. Using such relation, we match the triple intersection polynomial with the one-loop prepotential in each Coulomb chamber to obtain

constraints on the number of charged hypermultiplets (see equation (7.2)). In many cases, such a method will completely fix the number of multiplets [23, 24, 30, 31, 34]; however for the $SU(2) \times SU(3)$ -model, we get linear constraints that does not fully determine the number of multiplets.² However, they can completely be fixed by using Witten’s genus formula, which is a five-dimensional result. In the five-dimensional theory, we also determine the structure of the Coulomb chambers. Each chamber corresponds to a specific crepant resolution that we determine explicitly.

If we denote the number of hypermultiplets transforming in the irreducible representation \mathbf{R} as $n_{\mathbf{R}}$ and denote the curve supporting the gauge group $SU(2)$ and $SU(3)$ by S and T respectively, and write K for the canonical class of the base of the elliptic threefold,³ we have:

$$\begin{aligned} n_{\mathbf{3},1} &= \frac{1}{2}(K \cdot S + S^2 + 2), & n_{\mathbf{1},8} &= \frac{1}{2}(K \cdot T + T^2 + 2), \\ n_{\mathbf{2},1} &= -S \cdot (8K + 2S + 3T), & n_{\mathbf{1},\mathbf{3}} + n_{\mathbf{1},\bar{\mathbf{3}}} &= -T \cdot (9K + 3T + 2S), & n_{\mathbf{2},\mathbf{3}} + n_{\mathbf{2},\bar{\mathbf{3}}} &= S \cdot T. \end{aligned}$$

Interpreting the number of charged hypermultiplets with the genus of the supporting curves of S and T , denoted as $g(S)$ and $g(T)$ respectively, we get

$$\begin{aligned} n_{\mathbf{3},1} &= g(S), & n_{\mathbf{1},8} &= g(T), \\ n_{\mathbf{2},1} &= 16(1 - g(S)) + 6S^2 - 3S \cdot T, & n_{\mathbf{1},\mathbf{3}} + n_{\mathbf{1},\bar{\mathbf{3}}} &= 18(1 - g(T)) + 6T^2 - 2S \cdot T, & n_{\mathbf{2},\mathbf{3}} + n_{\mathbf{2},\bar{\mathbf{3}}} &= S \cdot T. \end{aligned}$$

1.5 Compactification of F-theory to $6d \mathcal{N} = (1, 0)$ supergravity and cancellation of anomalies

We also study in detail the anomaly cancellations of the six-dimensional theory. Considering the set of equations from requiring the local anomalies in the six-dimensional theory to cancel, we determine the unique solution of the number of charged hypermultiplets in each irreducible representation. Using Sadoy’s techniques [71], we check that anomalies are canceled explicitly by the Green-Schwarz mechanism. The number of hypermultiplets in each irreducible representations for an anomaly-free six-dimensional theory matches with those we get from the five-dimensional theories (see Section 7.3 for the discussion). This ensures that the five-dimensional theory can be uplifted to an anomaly-free six-dimensional theory.

Furthermore, in this paper we show that the matter content of the 6d gauge theory is anomaly-free. This theory can be still anomaly-free after an additional compactification on a Riemann surface to four-dimensions if we impose the condition $n_{\mathbf{3}} = n_{\bar{\mathbf{3}}}$, which will naturally follow from the CPT condition. For local gauge anomalies in four-dimensional spacetime, $SU(2)$ is always anomaly-free as all its representation are (pseudo)-real whereas the triangle diagram of $SU(3)$ is anomaly-free only when the number of matter transforming in the $\mathbf{3}$ and $\bar{\mathbf{3}}$ are equal to each other, which will naturally be satisfied if the CPT invariance is respected.

For global anomalies in four spacetime dimensions, one has to worry about $SU(2)$ as it is subject to Witten anomaly [81]. This is a direct consequence of the fact that the fourth homotopy group for $SU(N)$ is zero for N greater than two whereas for $SU(2)$ it is a \mathbb{Z}_2 . Thus, Witten anomalies from $SU(2)$ only vanishes when there is an even number of $SU(2)$ doublet. Similarly, the global anomaly

²When we consider a model with a semisimple Lie algebra and a trivial Mordell–Weil group, we always get linear constraints that does not fully determine the number of multiplets by matching the prepotential and the triple intersection polynomial [29, 30, 30, 31].

³The genus $g(S)$ of a supporting curve of S in a surface of canonical class K satisfies $2 - 2g(S) = -S \cdot K - S^2$. The same holds for the case of T as well.

contributions from $SU(2)$ and $SU(3)$ in six-dimensions can be discussed by looking into the sixth homotopy group for $SU(2)$ and $SU(3)$, which are given by \mathbb{Z}_{12} and \mathbb{Z}_6 respectively. Bershadsky and Vafa has shown that this yields the linear constraints on the number of hypermultiplets [13]. Considering these conditions only give a constraint on the genus of the curve S supporting the $SU(2)$ group: $g(S) = 0 \pmod 3$, as derived in Section 7.2.

1.6 Organization of this paper

The rest of the paper is structured as follows. In Section 2, we introduce the possible collisions of fibers that produce $SU(2) \times SU(3)$ -models and define their Weierstrass models. In Section 3, we describe the eight crepant resolutions of each of the six Weierstrass models introduced in Section 2. We also compute the Euler characteristic of the crepant resolutions and the triple intersection of the fibral divisors. In the case of Calabi–Yau threefolds, we also compute the Hodge numbers. In Section 4, we discuss the matter representations of the five and six-dimensional supergravity theories with a gauge group $SU(2) \times SU(3)$, compute the adjacency graph of the hyperplane arrangement associated with an $SU(2) \times SU(3)$ -model, and match the structure of the hyperplane arrangement with the flopping curves of the crepant resolutions. In Sections 5 and 6, we study in detail the crepant resolutions of the $I_2^s + I_3^s$ -models and the $III + IV^s$ -models respectively. In Section 7, we study the consequences of our geometric results for the physics of F-theory and M-theory compactified on an $SU(2) \times SU(3)$ -model. We first explain the number of multiplets of the five-dimensional theory using geometric data. We further derive the unique number of charged hypes in each irreducible representations in the uplifted six-dimensional theory canceling the local anomalies and show that it matches that of the five-dimensional theory. We also study the global anomaly contributions of the gauge group $SU(2) \times SU(3)$ [13].

2 The many faces of the $SU(2) \times SU(3)$ -model

In algebraic geometry, the notion of an irreducible variety depends on the choice of the underlying field. A variety is said to be *geometrically irreducible* when it stays irreducible after any field extension. Kodaira has introduced symbols to classify the type of the singular fibers of a minimal elliptic surface [54]. Kodaira symbols can be used more generally to classify the geometric fibers over generic points of the discriminant locus of an elliptic fibration of arbitrary dimension. The types of the fibers over generic points of the discriminant locus of an elliptic fibration are classified by decorated Kodaira fibers, as the Kodaira type classifies only the geometric fiber [19, §7.4.2]. The decoration tracks the minimal field extension under which all fiber components of the generic fiber become geometrically irreducible. Following [11], we use the decoration *non-split* (“ns”), *semi-split* (“ss”), and *split* (“s”). The fibers of type I_1 , II , III , II^* , and III^* are always well-defined without the need of a field extension. The fiber of type I_n ($n \geq 2$), IV , IV^* , and I_n^* can be split or non-split. The Kodaira fiber of type I_0^* can come from three distinct type: I_0^{*s} , I_0^{*ss} , and I_0^{*ns} with respective dual graphs \tilde{D}_4 , \tilde{B}_3 , and \tilde{G}_2 . The fiber I_0^{*ns} comes in two types as the minimal field extension can be the cyclic group \mathbb{Z}_3 or the permutation group of three elements S_3 [23].

There is a subtlety about the fiber I_2 : the fiber I_2^s and I_2^{ss} both have two geometrically irreducible components intersecting at two geometric points forming a divisor of degree two on the curve. The fiber I_2^{ss} corresponds to the case where the two distinct points are well defined only after a quadratic field extension while the fiber of type I_2^s does not require a field extension to define the two points of intersection.

There are several inequivalent decorated Kodaira fibers that have the same dual graph. The $SU(2) \times SU(3)$ -model involves the only two root systems that are dual graphs of several distinct Kodaira fibers. The dual graph of type \tilde{A}_1 is shared by two different Kodaira fibers, while there are five different Kodaira fibers with the dual graph \tilde{A}_2 , which is presented in Table 1.

Fibers	Dual graph
$I_2^s, I_2^{ns}, I_3^{ns}, III, IV^{ns}$	\tilde{A}_1
I_3^s, IV^s	\tilde{A}_2

Table 1: Decorated Kodaira fibers with dual graph of \tilde{A}_1 or \tilde{A}_2 .

The affine root system $\tilde{A}_1 \oplus \tilde{A}_2$ is the dual graph of ten different pairs of decorated Kodaira fibers. It follows that there are ten distinct ways to realize an $SU(2) \times SU(3)$ -model. Using Tate's algorithm, we realize these collisions as singular Weierstrass models by introducing specific valuations of the coefficients with respect to the divisors over which the singular fibers are defined. The minimal multiplicities for the coefficients a_i are reproduced in Table 2.

	a_1	a_2	a_3	a_4	a_6	Δ
I_2^s	0	1	1	1	2	2
I_2^{ns}	0	0	1	1	2	2
I_3^{ns}	0	0	2	2	3	3
III	1	1	1	1	2	3
IV^{ns}	1	1	1	2	2	4
I_3^s	0	1	1	2	3	3
IV^s	1	1	1	2	3	4

Table 2: Valuations of the coefficients of the Weierstrass models used in this paper for the Kodaira fibers of type $I_2^s, I_2^{ns}, I_3^{ns}, III, IV^{ns}, I_3^s,$ and IV^s to define $SU(2)$ and $SU(3)$ -models [11, 19, 48, 77]. The valuation of the discriminant Δ follows from the other valuations.

However, not all corresponding Weierstrass models have a crepant resolution. In this paper, we only consider those Weierstrass models that have crepant resolutions. In particular, we do not use I_3^{ns} or IV^{ns} to realize \tilde{A}_1 , as the Kodaira fibers of type I_3^{ns} and IV^{ns} have \mathbb{Q} -factorial terminal singularities. Such singularities are obstructions for the existence of crepant resolutions⁴ (this follows, for example, from [14, Lemma 3.6.2]). Thus, we consider only the following six cases of collisions:

$$I_2^s + I_3^s, \quad I_2^{ns} + I_3^s, \quad III + I_3^s, \quad I_2^s + IV^s, \quad I_2^{ns} + IV^s, \quad III + IV^s.$$

⁴The possible physical relevance of \mathbb{Q} -factorial terminal singularities in F-theory is explored in [6, 42].

The corresponding Weierstrass models are listed in equation (2.1):

$$\begin{aligned}
\text{I}_2^{\text{ns}} + \text{I}_3^{\text{s}} : \quad & y(y + a_1x + \tilde{a}_3st) = x^3 + \tilde{a}_2tx^2 + \tilde{a}_4st^2x + \tilde{a}_6s^2t^3, \\
\text{I}_2^{\text{s}} + \text{I}_3^{\text{s}} : \quad & y(y + a_1x + \tilde{a}_3st) = x^3 + \tilde{a}_2stx^2 + \tilde{a}_4st^2x + \tilde{a}_6s^2t^3, \\
\text{I}_2^{\text{s}} + \text{IV}^{\text{s}} : \quad & y(y + \tilde{a}_1tx + \tilde{a}_3st) = x^3 + \tilde{a}_2stx^2 + \tilde{a}_4st^2x + \tilde{a}_6s^2t^3, \\
\text{I}_2^{\text{ns}} + \text{IV}^{\text{s}} : \quad & y(y + \tilde{a}_1tx + \tilde{a}_3st) = x^3 + \tilde{a}_2tx^2 + \tilde{a}_4st^2x + \tilde{a}_6s^2t^3, \\
\text{III} + \text{I}_3^{\text{s}} : \quad & y(y + \tilde{a}_1sx + \tilde{a}_3st) = x^3 + \tilde{a}_2stx^2 + \tilde{a}_4st^2x + \tilde{a}_6s^2t^3, \\
\text{III} + \text{IV}^{\text{s}} : \quad & y(y + \tilde{a}_1stx + \tilde{a}_3st) = x^3 + \tilde{a}_2stx^2 + \tilde{a}_4st^2x + \tilde{a}_6s^2t^3.
\end{aligned} \tag{2.1}$$

We assume that the coefficients a_1 and \tilde{a}_i ($i = 1, 2, 3, 4, 6$) are algebraically independent and $S = V(s)$ and $T = V(t)$ are smooth divisors intersecting transversally. The variables s (resp. t) is a section of the normal bundle of the divisor S (resp. T). In each case, the Kodaira fiber over the generic point of S (resp. T) has a dual graph of type $\tilde{\text{A}}_1$ (resp. $\tilde{\text{A}}_2$). The difference between these models are the valuations of the Weierstrass coefficients a_1 and a_2 with respect to S and T , which are listed in Table 2. The discriminant locus of each Weierstrass model is given by

$$\Delta = s^{2+a}t^{3+b}(\dots),$$

where a is related to $S = V(s)$ and b to $T = V(t)$, $a = 0$ for Kodaira fibers of types I_2^{s} and I_2^{ns} , $a = 1$ for Kodaira fibers of type III , $b = 0$ for Kodaira fibers of type I_3^{s} , and $b = 1$ for Kodaira fibers of type IV^{s} . We observe that the reduced discriminant locus is composed of three irreducible components. The fiber degenerates further at the intersection of these three components and we study them to determine the type of matter.

Remark 2.1. As seen on Table 2, the fiber IV^{s} becomes the fiber IV^{ns} when the Weierstrass coefficient a_6 is deformed by a term of valuation two. Such a deformation does not commute with the resolution and changes the gauge group from $\text{SU}(3)$ to $\text{SU}(2)$. However, the resulting $\text{SU}(2)$ has \mathbb{Q} -factorial terminal singularities. Moreover, these groups $\text{SU}(2)$ and $\text{SU}(3)$ coming from fibers IV^{ns} and IV^{s} are strongly coupled and related to Argyres-Douglas theories [5, 67], both give in the weak coupling limit of type IIB string theory an $\text{SO}(6)$ gauge theory [33]. The non-Higgsable group corresponding to a fiber of type IV is $\text{SU}(2)$ as generically a fiber of type IV is a IV^{ns} . A non-Higgsable model of type IV^{s} will require a very particular setting to avoid the existence of a deformation to the fiber IV^{ns} as it will break the gauge group from $\text{SU}(3)$ to $\text{SU}(2)$.

3 Geometry

In this section, we collect the geometric data – crepant resolutions, Euler characteristic, Hodge numbers, triple intersection numbers– of the $\text{SU}(2) \times \text{SU}(3)$ -models. In Section 3.1, we present eight sequences of blowups that each give crepant resolutions of all six Weierstrass models from equation (2.1). In total, this results in 48 distinct $\text{SU}(2) \times \text{SU}(3)$ -models. In Section 3.2, we summarize the main pushforward theorems we use to compute the geometric data of $\text{SU}(2) \times \text{SU}(3)$ -models. Since two smooth n -dimensional projective algebraic variety over \mathbb{C} connected by a crepant birational map have the same Betti numbers [9, Theorem 4.2], all the crepant resolutions of Weierstrass models of an $\text{SU}(2) \times \text{SU}(3)$ -model have the same Euler characteristic. In Section 3.3, we give a generating

function for the Euler characteristic of an $SU(2) \times SU(3)$ -model. In the case of Calabi–Yau threefolds, we also compute the Hodge numbers of the $SU(2) \times SU(3)$ -models. In the case of a threefold, we also compute the Hodge numbers and the triple intersection numbers in Section 3.4. In Section 3.5, we discuss the various non-Kodaira fibers obtain from the resolutions of the $SU(2) \times SU(3)$ -models, we summarize them in Table 3.

3.1 Crepant resolutions

We use the following convention. Let X be a nonsingular variety. Let $Z \subset X$ be a complete intersection defined by the transverse intersection of r hypersurfaces $Z_i = V(g_i)$, where g_i is a section of the line bundle \mathcal{S}_i and (g_1, \dots, g_r) is a regular sequence. We denote the blowup of a nonsingular variety X along the complete intersection Z by

$$X \xleftarrow{(g_1, \dots, g_r | e_1)} \tilde{X}.$$

The exceptional divisor is $E_1 = V(e_1)$. We abuse notation and use the same symbols for x, y, s, e_i and their successive proper transforms. We also do not write the obvious pullbacks.

Assuming some mild regularity conditions on the coefficients of the Weierstrass equations, each of the following eight sequences of blowups gives a different crepant resolution of any of the $SU(2) \times SU(3)$ -model given by the Weierstrass models in equation (2.1):

$$\begin{aligned}
\text{Resolution I : } & X_0 \xleftarrow{(x, y, s | e_1)} X_1 \xleftarrow{(x, y, t | w_1)} X_2 \xleftarrow{(y, w_1 | w_2)} X_3 , \\
\text{Resolution II : } & X_0 \xleftarrow{(x, y, p_0 | p_1)} X_1 \xleftarrow{(y, p_1, t | w_1)} X_2 \xleftarrow{(p_0, t | w_2)} X_3 , \\
\text{Resolution III : } & X_0 \xleftarrow{(x, y, t | w_1)} X_1 \xleftarrow{(x, y, s | e_1)} X_2 \xleftarrow{(y, w_1 | w_2)} X_3 , \\
\text{Resolution IV : } & X_0 \xleftarrow{(x, y, t | w_1)} X_1 \xleftarrow{(y, w_1 | w_2)} X_2 \xleftarrow{(x, y, s | e_1)} X_3 , \\
\text{Resolution I' : } & X_0 \xleftarrow{(x, q, s | e_1)} X_1 \xleftarrow{(x, q, t | w_1)} X_2 \xleftarrow{(q, w_1 | w_2)} X_3 , \\
\text{Resolution II' : } & X_0 \xleftarrow{(x, q, p_0 | p_1)} X_1 \xleftarrow{(q, p_1, t | w_1)} X_2 \xleftarrow{(p_0, t | w_2)} X_3 , \\
\text{Resolution III' : } & X_0 \xleftarrow{(x, q, t | w_1)} X_1 \xleftarrow{(x, q, s | e_1)} X_2 \xleftarrow{(q, w_1 | w_2)} X_3 , \\
\text{Resolution IV' : } & X_0 \xleftarrow{(x, q, t | w_1)} X_1 \xleftarrow{(q, w_1 | w_2)} X_2 \xleftarrow{(x, q, s | e_1)} X_3 ,
\end{aligned} \tag{3.1}$$

where $q = y + a_1x + a_3$ and $p_0 = st$.

We observe that the sequences of blowups that define the first four resolutions are exactly the same as the sequence of blowups that define the resolutions of the $SU(2) \times G_2$ -model [29].

The birational map connecting the resolution I to I' (resp. II to II', III to III', and IV to IV') is induced by the involution $\sigma : [x : y : z] \rightarrow [-q : x : z]$ of the Weierstrass model. Fiberwise, the involution σ is the inverse map of the Mordell–Weil group: it maps a point P to its opposite $-P$

with respect to the Mordell–Weil group law. This is familiar from [35–37]. The birational maps induced by σ are *pseudo-isomorphisms* of the crepant resolutions over the Weierstrass model, as they are isomorphisms in codimension-one.

With the exceptions of resolutions II and II', all of the resolutions are defined by sequences of blowups around centers that are smooth, complete intersections. The resolutions II and II' are also defined by a sequence of blowups; however, one of the blowups does not have a smooth center but still defines a regular sequence. Fortunately, this condition is enough to use the pushforward theorems and compute the topological invariants as in the other cases.

3.2 Intersection theory and blowups

We compute geometric data of the $SU(2) \times SU(3)$ -models using intersection theory. Our computations rely on three theorems. Each crepant resolution of $SU(2) \times SU(3)$ -models is given as a sequence of three blowups, which is listed in equation (3.1). The first is a theorem of Aluffi that gives the Chern class of a blowup along a local complete intersection. The second theorem is a pushforward theorem that provides a user-friendly method to compute invariants of the resolved space in terms of the original space. The last theorem gives a simple method to pushforward analytic expressions in the Chow ring of a projective bundle to the Chow ring of its base.

Theorem 3.1 (Aluffi, [1, Lemma 1.3]). *Let $Z \subset X$ be the complete intersection of d nonsingular hypersurfaces Z_1, \dots, Z_d meeting transversally in X . Let $f: \tilde{X} \rightarrow X$ be the blowup of X centered at Z . We denote the exceptional divisor of f by E . The total Chern class of \tilde{X} is then:*

$$c(T\tilde{X}) = (1 + E) \left(\prod_{i=1}^d \frac{1 + f^*Z_i - E}{1 + f^*Z_i} \right) f^*c(TX). \quad (3.2)$$

Theorem 3.2 (Esole–Jefferson–Kang, see [25]). *Let the nonsingular variety $Z \subset X$ be a complete intersection of d nonsingular hypersurfaces Z_1, \dots, Z_d meeting transversally in X . Let E be the class of the exceptional divisor of the blowup $f: \tilde{X} \rightarrow X$ centered at Z . Let $\tilde{Q}(t) = \sum_a f^*Q_a t^a$ be a formal power series with $Q_a \in A_*(X)$. We define the associated formal power series $Q(t) = \sum_a Q_a t^a$, whose coefficients pullback to the coefficients of $\tilde{Q}(t)$. Then the pushforward $f_*\tilde{Q}(E)$ is*

$$f_*\tilde{Q}(E) = \sum_{\ell=1}^d Q(Z_\ell)M_\ell, \quad \text{where} \quad M_\ell = \prod_{\substack{m=1 \\ m \neq \ell}}^d \frac{Z_m}{Z_m - Z_\ell}.$$

Theorem 3.3 (Esole–Jefferson–Kang, see [25] and [2, 3, 32, 40]). *Let \mathcal{L} be a line bundle over a variety B and $\pi: X_0 = \mathbb{P}[\mathcal{O}_B \oplus \mathcal{L}^{\otimes 2} \oplus \mathcal{L}^{\otimes 3}] \rightarrow B$ a projective bundle over B . Let $\tilde{Q}(t) = \sum_a \pi^*Q_a t^a$ be a formal power series in t such that $Q_a \in A_*(B)$. Define the auxiliary power series $Q(t) = \sum_a Q_a t^a$. Then*

$$\pi_*\tilde{Q}(H) = -2 \frac{Q(H)}{H^2} \Big|_{H=-2L} + 3 \frac{Q(H)}{H^2} \Big|_{H=-3L} + \frac{Q(0)}{6L^2},$$

where $L = c_1(\mathcal{L})$ and $H = c_1(\mathcal{O}_{X_0}(1))$ is the first Chern class of the dual of the tautological line bundle of $\pi: X_0 = \mathbb{P}(\mathcal{O}_B \oplus \mathcal{L}^{\otimes 2} \oplus \mathcal{L}^{\otimes 3}) \rightarrow B$.

3.3 Euler characteristics and Hodge numbers

When an elliptic fibration is defined by the resolution of a singular Weierstrass model by a sequence of blowups with smooth centers defining regular embeddings, there are powerful pushforward theorems to compute its Euler characteristic in few simple algebraic manipulations [25].

Remark 3.4. All the Weierstrass models of the $SU(2) \times SU(3)$ -models and the $SU(2) \times G_2$ -models [29] share four crepant resolutions that are given by the same sequences of blowups (Resolutions I, II, III, and IV). Hence, the $SU(2) \times SU(3)$ -model for a choice of (B, S, T, \mathcal{L}) and the $SU(2) \times G_2$ -model defined with the same choice of (B, S, T, \mathcal{L}) , have the same Euler characteristics as formal expressions in $S, T, L, c(TB)$. Likewise, since $SU(2) \times SU(3)$ and $SU(2) \times G_2$ have the same rank, their Hodge numbers are also identical in the Calabi–Yau threefold case.

Theorem 3.5. *The generating polynomial of the Euler characteristic of an $SU(2) \times SU(3)$ -model obtained by a crepant resolution of a Weierstrass model given in Section 3.1:*

$$\chi(Y) = 6 \frac{S^2 - 2L - 3SL + 2(S^2 - 3SL + S - 2L)T + (3S + 2)T^2}{(1 + S)(1 + T)(-1 - 6L + 2S + 3T)} c(TB).$$

Proof. See [29, Theorem 2.5]. □

By direct expansion and specialization, we have the following three lemmas [29]:

Lemma 3.6. *For an elliptic threefold, the Euler characteristic is*

$$\chi(Y_3) = -6(-2c_1L + 12L^2 + S^2 - 5SL + 2ST - 8LT + 2T^2).$$

Lemma 3.7. *In the case of a Calabi–Yau threefold, by applying $c_1 = L = -K$, we have*

$$\chi(Y_3) = -6(10K^2 + S^2 + 5SK + 2ST + 8KT + 2T^2).$$

Lemma 3.8. *The Euler characteristic for an elliptic fourfold is given by*

$$\begin{aligned} \chi(Y_4) = & -6(-2c_2L - 72L^3 + 12c_1L^2 + c_1S^2 - 5c_1SL + 2c_1ST - 8c_1LT + 2c_1T^2 \\ & + S^3 - 15S^2L + 6S^2T + 54SL^2 - 44SLT + 9ST^2 + 84L^2T - 34LT^2 + 4T^3). \end{aligned}$$

Lemma 3.9. *The same Calabi–Yau condition $c_1 = L = -K$ is applied to get the Euler characteristic for a Calabi–Yau fourfold:*

$$\chi(Y_4) = -6(2c_2K + 60K^3 + S^3 + 14S^2K + 6S^2T + 49SK^2 + 42SKT + 9ST^2 + 76K^2T + 32KT^2 + 4T^3).$$

Theorem 3.10. *In the Calabi–Yau case, the Hodge numbers of an $SU(2) \times SU(3)$ -model given by the crepant resolution of a Weierstrass model given in Section 3.1 are*

$$h^{1,1}(Y) = 14 - K^2, \quad h^{2,1}(Y) = 29K^2 + 15KS + 24KT + 3S^2 + 6ST + 6T^2 + 14.$$

Proof. See [29, Theorem 2.10]. □

3.4 Triple intersection numbers

Let Y be a crepant resolution of an $SU(2) \times SU(3)$ -model defined by one of the crepant resolutions $f : Y \rightarrow Y_0$ given in Section 3.1. Assuming that Y is a threefold, the triple intersection polynomial of Y is a polynomial containing the divisors $(D_a \cdot D_b \cdot D_c) \cap [Y]$. We express a triple intersection polynomial of the $SU(2) \times SU(3)$ -model as a polynomial in $\psi_0, \psi_1, \phi_0, \phi_1$, and ϕ_2 that couples respectively with the fibral divisors $D_0^s, D_1^s, D_0^t, D_1^t$, and D_2^t . The pushforward is expressed in the base by pushing forward to the Chow ring of X_0 and then to the base B . We recall that $\pi : X_0 \rightarrow B$ is the projective bundle in which the Weierstrass model is defined. Then,

$$\mathcal{F}_{trip} = \int_Y \left[\left(\psi_0 D_0^s + \psi_1 D_1^s + \phi_0 D_0^t + \phi_1 D_1^t + \phi_2 D_2^t \right)^3 \right] = \int_B \pi_* f_* \left[\left(\psi_0 D_0^s + \psi_1 D_1^s + \phi_0 D_0^t + \phi_1 D_1^t + \phi_2 D_2^t \right)^3 \right].$$

Once the classes of the fibral divisors are determined, all that is left is to compute the pushforward to the base B using the pushforward theorems of Section 3.2.

Theorem 3.11. *The triple intersection polynomial of an $SU(2) \times SU(3)$ -model defined by the crepant resolutions in Section 3.1 is*

- *Resolution I:*

$$\begin{aligned} \mathcal{F}_{trip}^{(I)} = & -2S(2L+S)\psi_1^3 - 6ST\psi_1(\phi_1^2 - \phi_2\phi_1 + \phi_2^2) - 4T(T-L)\phi_1^3 \\ & - 3T(5L-S-2T)\phi_1^2\phi_2 - 3T(-4L+S+T)\phi_1\phi_2^2 - T(5L-2S+T)\phi_2^3 \\ & + 4S(L-S)\psi_0^3 + 6S(S-2L)\psi_0^2\psi_1 + 12LS\psi_0\psi_1^2 \\ & - 2T\phi_0^3(-2L+S+2T) + \phi_0^2(3T(\phi_1+\phi_2)(-2L+S+T) - 6ST\psi_1) \\ & + 3T\phi_0(2\phi_1(L\phi_2+S\psi_1) + \phi_1^2(L-S) + \phi_2^2(L-S) - 2S(\psi_0-\psi_1)^2 + 2S\psi_1\phi_2) \end{aligned}$$

- *Resolution II:*

$$\begin{aligned} \mathcal{F}_{trip}^{(II)} = & -S(4L+2S-T)\psi_1^3 + 3T(-5L+S+2T)\phi_1^2\phi_2 - 3T(-4L+S+T)\phi_1\phi_2^2 + 4T(L-T)\phi_1^3 \\ & + T(-5L+S-T)\phi_2^3 - 3ST\psi_1^2\phi_2 - 3ST\psi_1(2\phi_1^2 - 2\phi_1\phi_2 + \phi_2^2) \\ & - S(-4L+4S+T)\psi_0^3 + 3S(-4L+2S+T)\psi_0^2\psi_1 + 3S(4L-T)\psi_0\psi_1^2 - T(-4L+S+4T)\phi_0^3 \\ & + 3T\phi_0^2(-S(\psi_0+\psi_1) - (2L-T)\phi_2) + 3T\phi_0(L\phi_2^2 - S(\psi_0-\psi_1)^2 + 2S\psi_0\phi_2) \\ & + 3T\phi_0^2\phi_1(-2L+S+T) + 3T\phi_0\phi_1(\phi_1(L-S) + 2L\phi_2 + 2S\psi_1) - 3ST\psi_0\phi_2(\psi_0 - 2\psi_1 + \phi_2). \end{aligned}$$

- *Resolution III:*

$$\begin{aligned} \mathcal{F}_{trip}^{(III)} = & -2S(2L+S-T)\psi_1^3 - T(-4L+S+4T)\phi_1^3 - 3T(5L-S-2T)\phi_1^2\phi_2 \\ & - 3T(-4L+S+T)\phi_1\phi_2^2 - T(5L-S+T)\phi_2^3 - 3ST\psi_1(\phi_1 - \phi_2)^2 - 3ST\psi_1^2(\phi_1 + \phi_2) \\ & - 2S(-2L+2S+T)\psi_0^3 + \psi_0^2(6S\psi_1(-2L+S+T) - 3ST(\phi_1 + \phi_2)) \\ & + \psi_0(-6S\psi_1^2(T-2L) + 6ST\psi_1(\phi_1 + \phi_2) - 3ST(\phi_1^2 + \phi_2^2)) + 4T\phi_0^3(L-T) \\ & + \phi_0^2(3T(\phi_1 + \phi_2)(T-2L) - 6ST\psi_0) + 3T\phi_0(\phi_1 + \phi_2)(L(\phi_1 + \phi_2) + 2S\psi_0) \end{aligned}$$

• *Resolution IV:*

$$\begin{aligned}
\mathcal{F}_{trip}^{(IV)} &= S(-4L - 2S + 3T)\psi_1^3 - 4T(T - L)\phi_1^3 - 3T(5L - 2T)\phi_1^2\phi_2 \\
&\quad - 3T(T - 4L)\phi_1\phi_2^2 - T(5L + T)\phi_2^3 - 6ST\psi_1^2\phi_2 \\
&\quad + \psi_0^2(3S\psi_1(-4L + 2S + 3T) - 6ST\phi_2) + 3S\psi_0(\psi_1^2(4L - 3T) + 4T\psi_1\phi_2) \\
&\quad - 6ST\psi_0(\phi_1^2 - \phi_2\phi_1 + \phi_2^2) + S(4L - 4S - 3T)\psi_0^3 + 4T\phi_0^3(L - T) \\
&\quad + \phi_0^2(3T(\phi_1 + \phi_2)(T - 2L) - 6ST\psi_0) + 3T\phi_0(\phi_1 + \phi_2)(L(\phi_1 + \phi_2) + 2S\psi_0)
\end{aligned}$$

The triple intersection polynomials for the resolutions I', II', III', and IV' are respectively derived from those of the resolutions I, II, III, and IV by the involution $\phi_1 \leftrightarrow \phi_2$.

Proof. We give the proof for the case of Resolution I discussed in detail in Section 5.1, the other cases follow the same pattern.

$$\begin{aligned}
\mathcal{F}_{trip} &= \int_Y \left[\left(\psi_0 D_0^s + \psi_1 D_1^s + \phi_0 D_0^t + \phi_1 D_1^t + \phi_2 D_2^t \right)^3 \right] \\
&= \int_{X_3} \left[\left(\psi_0 D_0^s + \psi_1 D_1^s + \phi_0 D_0^t + \phi_1 D_1^t + \phi_2 D_2^t \right)^3 (3H + 6L - 2E_1 - 2W_1 - W_2) \right] \\
&= \int_{X_0} f_{1*} f_{2*} f_{3*} \left[\left(\psi_0 D_0^s + \psi_1 D_1^s + \phi_0 D_0^t + \phi_1 D_1^t + \phi_2 D_2^t \right)^3 (3H + 6L - 2E_1 - 2W_1 - W_2) \right] \\
&= \int_B \pi_* f_{1*} f_{2*} f_{3*} \left[\left(\psi_0 D_0^s + \psi_1 D_1^s + \phi_0 D_0^t + \phi_1 D_1^t + \phi_2 D_2^t \right)^3 (3H + 6L - 2E_1 - 2W_1 - W_2) \right].
\end{aligned}$$

The classes of the fibral divisors in the Chow ring of X_3 are

$$[D_0^s] = S - E_1, \quad [D_1^s] = E_1, \quad [D_0^t] = T - W_1, \quad [D_1^t] = W_1 - W_2, \quad [D_2^t] = W_2.$$

Denoting by M an arbitrary divisor in the class of the Chow ring of the base B , the nonzero intersection numbers of the products of M , H , E_1 , W_1 , and W_2 are

$$\begin{aligned}
\int_Y E_1^3 &= -2S(2L + S), & \int_Y W_1^3 &= -2T(2L - S + T), & \int_Y MW_1^2 &= -2TM, \\
\int_Y W_2^3 &= -T(5L - 2S + T), & \int_Y W_1^2 E_1 &= -2ST, & \int_Y W_1^2 W_2 &= T(-2L + S - T), & \int_Y ME_1^2 &= -2SM, \\
\int_Y W_2^2 E_1 &= -2ST, & \int_Y W_2^2 W_1 &= T(-L + S - 2T), & \int_Y E_1 W_1 W_2 &= -ST, \\
\int_Y HM &= 3M, & \int_Y H^2 M &= -9LM, & \int_Y H^3 &= 27L^2, & \int_Y MW_2^2 &= -2TM,
\end{aligned}$$

where the right-hand-side of each equality is computed in the Chow ring of the base B , the pushforward for f_{i*} ($i = 1, 2, 3$) are obtained via Theorem 3.2, the pushforward for π_* uses Theorem 3.3. The triple intersection numbers of the fibral divisors follow from these by simple linearity. \square

The triple intersection polynomials computed in Theorem 3.11 are very different from each other in chambers I, II, III, and IV. In chamber III, we get all possible ten homogeneous monomials in ψ_1 , ϕ_1 and ϕ_2 . In chamber II, we get nine of them ($\psi_1^2\phi_1$ is missing); in chamber I, we are missing two ($\psi_1^2\phi_1$ and $\psi_1^2\phi_2$); in chamber IV, we are missing four ($\psi_1^2\phi_1$, $\psi_1\phi_1^2$, $\psi_1\phi_2^2$ and $\psi_1\phi_1\phi_2$). These facts become handy when comparing the triple intersection polynomials with the prepotentials in Section 7.1.

3.5 Non-Kodaira fibers

The $SU(2) \times SU(3)$ -models have a particularly rich fiber structure with various types of non-Kodaira fibers. We have identified a total of thirteen non-Kodaira fibers over points in codimension-two or three in the base, which are all summarized in Table 3. The fiber structure of each models studied in this paper is described in Appendix A. Two of these non-Kodaira fibers appear for the first time in the literature. They are contraction of the fiber I_2^* appearing over codimension codimension-three points in the base in the crepant resolution II or IV of the collision $I_2 + IV^s$. They are related to the sequence $A_1 + A_2 \rightarrow D_5 \rightarrow D_6$. All the non-Kodaira fibers obtained at the collision of S and T can be derived by removing certain nodes on the Kodaira fibers I_0^* , I_1^* , I_2^* , IV^* , or III^* . Away from $S \cap T$, there is also a non-Kodaira fiber that appears in the specialization of the fiber of type III. The phenomena that non-Kodaira fibers of a flat fibration are contractions of Kodaira fibers has been noticed by Miranda in the particular case of his regularization of elliptic threefolds [63] and also in generalizations of Miranda’s models to n -folds as studied by Szydło [75]. Cattaneo argues in [16] that this is always the case for flat elliptic threefolds that are crepant resolutions of Weierstrass models. The study of crepant resolutions of singular Weierstrass models and the geography of their flops is an essential endeavor in stringy geometry and has been studied for many models producing in this way most of the known non-Kodaira fibers [16, 20, 23, 24, 26, 29–32, 35–37, 57, 59, 63, 65, 75, 76].

4 Hyperplane arrangements and geography of flops

In Section 4.1, we discuss matter representations of the $SU(2) \times SU(3)$ -model in five and six-dimensional theories with eight supercharges from Katz-Vafa method and confirm its perfect match with the representations computed from the geometry.

In Section 4.2, we study the hyperplane arrangement $I(A_1 \oplus A_2, (\mathbf{1}, \mathbf{3}) \oplus (\mathbf{2}, \mathbf{3}))$. The full representation of the $SU(2) \times SU(3)$ -model is $\mathbf{R} = (\mathbf{2}, \mathbf{1}) \oplus (\mathbf{1}, \mathbf{3}) \oplus (\mathbf{1}, \bar{\mathbf{3}}) \oplus (\mathbf{2}, \mathbf{3}) \oplus (\mathbf{2}, \bar{\mathbf{3}}) \oplus (\mathbf{3}, \mathbf{1}) \oplus (\mathbf{1}, \mathbf{8})$. However, the hyperplane arrangement $I(A_1 \oplus A_2, \mathbf{R})$ has the same chamber structure as $I(A_1 \oplus A_2, (\mathbf{1}, \mathbf{3}) \oplus (\mathbf{2}, \mathbf{3}))$ since the adjoints only define the exterior walls of the dual fundamental Weyl chamber, taking care of the redundancy, and noticing that $((\mathbf{2}, \mathbf{1}))$ does not contribute interior walls, it is sufficient to consider $(\mathbf{1}, \mathbf{3}) \oplus (\mathbf{2}, \mathbf{3})$ only.

In Section 4.3, we match the chamber of the hyperplane arrangement $I(A_1 \oplus A_2, (\mathbf{1}, \mathbf{3}) \oplus (\mathbf{2}, \mathbf{3}))$ with the crepant resolutions as inspired by their interpretation as Coulomb branches of a five-dimensional gauge theory discussed in Section 7.1.

4.1 Geometric weights and matter representations

An important geometric data is the representation \mathbf{R} under which the matter fields transform. This representation is characterized by its weights, which are computed geometrically by intersection numbers of fibral divisors with vertical curves over codimension-two points. We do not add by hand the chiral conjugates of representations; all representations are seen explicitly by their weights via fibers given by the geometry. Starting from a collection of weights, we determine the representation by using the notion of *saturated set of weights* borrowed from Bourbaki. See [23, 24] for more information.

The representation \mathbf{R} that we obtain from purely geometric considerations is consistent with what one would indirectly guess using the Katz-Vafa method [49]. But the Katz-Vafa method can

fail for certain models such as the $SU(2) \times G_2$ model, while the method of saturations of weight still provides the correct representation \mathbf{R} as discussed in [29]. The sector of \mathbf{R} that does not contain fundamental representations can be derived from the branching rule of the adjoint representation of maximal embedding $A_1 \oplus A_2 \rightarrow A_4$ while the fundamental representations follow from the branching rule of the adjoints of the maximal embedding $A_1 \rightarrow A_2$ and $A_2 \rightarrow A_3$:

$$\begin{cases} \mathbf{24} & \longrightarrow (\mathbf{3}, \mathbf{1}) \oplus (\mathbf{1}, \mathbf{8}) \oplus (\mathbf{2}, \mathbf{3}) \oplus (\mathbf{2}, \bar{\mathbf{3}}) \oplus (\mathbf{1}, \bar{\mathbf{1}}), \\ \mathbf{15} & \longrightarrow \mathbf{8} \oplus \mathbf{3} \oplus \bar{\mathbf{3}} \oplus \mathbf{1}, \\ \mathbf{8} & \longrightarrow \mathbf{3} \oplus \mathbf{2} \oplus \bar{\mathbf{2}} \oplus \mathbf{1}. \end{cases} \quad (4.1)$$

A frozen representation is a representation ρ whose weights are carried by certain curves of the elliptic fibration over codimension-two points in the base, but no hypermultiplet is charged under ρ [24, 29]. When compactified to a five-dimensional or six-dimensional supergravity theory with eight supercharges, matter in these adjoint representations are frozen when the curves supporting the components of the gauge group are smooth rational curves since the number of adjoint hypermultiplets is given by the arithmetic genus of the curve supporting the gauge group.

4.2 Hyperplane arrangement

We consider the semi-simple Lie algebra

$$\mathfrak{g} = A_1 \oplus A_2.$$

An irreducible representation of $A_1 \oplus A_2$ is the tensor product $\mathbf{r}_1 \otimes \mathbf{r}_2$, where \mathbf{r}_1 and \mathbf{r}_2 are respectively irreducible representations of A_1 and A_2 . Following a common convention in physics, we denote a representation of A_n by its dimension in bold character. The weights are denoted by ϖ_j^I where the upper index I denotes the representation \mathbf{R}_I and the lower index j denotes a particular weight of the representation \mathbf{R}_I . A weight of a representation of $A_1 \oplus A_2$ is denoted by a triple $(a; b, c)$ such that (a) is a weight of A_1 and (b, c) is a weight of A_2 , all in the basis of fundamental weights. We use the same notation for coroots. Let $\phi = (\psi_1; \phi_1, \phi_2)$ be a vector of the coroot space of $A_1 \oplus A_2$ in the basis of the fundamental coroots. Each weight ϖ defines a linear form $\phi \cdot \varpi$ defined by the natural evaluation on a coroot. We recall that fundamental coroots are dual to fundamental weights. Hence, with our choice of conventions, $\phi \cdot \varpi$ is the usual Euclidian scalar product.

To study the hyperplane arrangement, it is not necessary to consider the full representation $\mathbf{R} = (\mathbf{2}, \mathbf{1}) \oplus (\mathbf{1}, \mathbf{3}) \oplus (\mathbf{1}, \bar{\mathbf{3}}) \oplus (\mathbf{2}, \mathbf{3}) \oplus (\mathbf{2}, \bar{\mathbf{3}}) \oplus (\mathbf{3}, \mathbf{1}) \oplus (\mathbf{1}, \mathbf{8})$ since the adjoints only define the dual fundamental Weyl chamber and $\mathbf{3}$ and $\bar{\mathbf{3}}$ differ only by a sign. Thus, we use without loss of generality the representation \mathbf{R} as:

$$\mathbf{R} = (\mathbf{2}, \mathbf{1}) \oplus (\mathbf{1}, \mathbf{3}) \oplus (\mathbf{2}, \mathbf{3}), \quad (4.2)$$

which is the sum of the fundamental of A_1 , the fundamental of A_2 , and the bifundamental representations of A_1 and A_2 . We study the arrangement of hyperplanes perpendicular to the weights of the representation \mathbf{R} inside the dual fundamental Weyl chamber of $A_1 \oplus A_2$.

The open dual fundamental Weyl chamber is the half cone defined by the the positivity of the linear form induced by the simple roots:

$$\psi_1 > 0, \quad 2\phi_1 - \phi_2 > 0, \quad -\phi_1 + 2\phi_2 > 0. \quad (4.3)$$

The weight system of the representation $\mathbf{2}$ of A_1 and the representation $\mathbf{3}$ of A_2 are

$$\mathbf{2}: \quad \varpi_1^2 = 1, \quad \varpi_2^2 = -1 \quad (4.4)$$

$$\mathbf{3}: \varpi_1^{\mathbf{3}} = (1, 0), \quad \varpi_2^{\mathbf{3}} = (-1, 1), \quad \varpi_3^{\mathbf{3}} = (0, -1). \quad (4.5)$$

The weights of the representation $(\mathbf{2}, \mathbf{1})$, $(\mathbf{1}, \mathbf{3})$ and $(\mathbf{2}, \mathbf{3})$ are (in the Cartan's basis of fundamental weights). All the relevant weights are given in Table 4.

Theorem 4.1. *The hyperplane arrangement $I(A_1 \oplus A_2, (\mathbf{1}, \mathbf{3}) \oplus (\mathbf{2}, \mathbf{3}))$ has eight chambers whose sign vectors (with respect to the forms $(\varpi_2^{(\mathbf{1}, \mathbf{3})}, \varpi_5^{(\mathbf{2}, \mathbf{3})}, \varpi_4^{(\mathbf{2}, \mathbf{3})}, \varpi_3^{(\mathbf{2}, \mathbf{3})}, \varpi_2^{(\mathbf{2}, \mathbf{3})})$) are as listed in Table 5. The corresponding adjacency graph is given in Figure 3.*

Proof. There are five hyperplanes intersecting the interior of the dual fundamental Weyl chamber: $\varpi_2^{(\mathbf{1}, \mathbf{3})}$, $\varpi_2^{(\mathbf{2}, \mathbf{3})}$, $\varpi_3^{(\mathbf{2}, \mathbf{3})}$, $\varpi_4^{(\mathbf{2}, \mathbf{3})}$, and $\varpi_5^{(\mathbf{2}, \mathbf{3})}$. We use them in the order $(\varpi_2^{(\mathbf{1}, \mathbf{3})}, \varpi_5^{(\mathbf{2}, \mathbf{3})}, \varpi_4^{(\mathbf{2}, \mathbf{3})}, \varpi_3^{(\mathbf{2}, \mathbf{3})}, \varpi_2^{(\mathbf{2}, \mathbf{3})})$, the sign vector is $(-\phi_1 + \phi_2, -\psi_1 - \phi_1 + \phi_2, -\psi_1 + \phi_1, \psi_1 - \phi_2, \psi_1 - \phi_1 + \phi_2)$. Keeping in mind the conditions in equation (4.3) defining the open dual fundamental Weyl chamber, the results follow from a direct check of all possible signs and the chambers are listed on Table 5. \square

4.3 Correspondence between the geometry and the representation theory

In this section, we match the crepant resolutions of Section 3.1 and the chambers of the hyperplane arrangement $I(\mathfrak{g}, \mathbf{R})$ of Table 5. The graph of flops between the crepant resolutions is isomorphic to the adjacency graph of the chambers of the hyperplane arrangement, but the isomorphism is not canonical since the graph has a \mathbb{Z}_2 automorphism. A simple way to fix the identification is to compare the triple intersection numbers in each resolution, which are given by Theorem 3.11, and the prepotentials computed in each chamber, which are given by Theorem 7.1.

In Section 3, we described eight different possible resolutions. There is a \mathbb{Z}_2 symmetry in the the structures of the resolutions mapping resolutions I, II, III, IV and the resolutions I', II', III', IV' and induced by the inverse map of the Mordell–Weil group. Similarly, we see the \mathbb{Z}_2 symmetry in the adjacent graph of the chambers between the chambers 1, 2, 3, 4 and the chambers 1', 2', 3', 4'. This can be observed easily in Figure 3.

We see the explicit correspondence between the chambers and the resolutions as

$$\begin{aligned} \text{I} &\leftrightarrow 1, & \text{II} &\leftrightarrow 2, & \text{III} &\leftrightarrow 3, & \text{IV} &\leftrightarrow 4, \\ \text{I}' &\leftrightarrow 1', & \text{II}' &\leftrightarrow 2', & \text{III}' &\leftrightarrow 3', & \text{IV}' &\leftrightarrow 4'. \end{aligned} \quad (4.6)$$

We can also compute the weight of the flopping curve between pairs of resolutions connected by a flop, and compare it with the weight of the wall between the adjacent chambers. As an illustration, we treat the case of $I_2^s + I_3^s$ -models and show that that the weights of the flopping curves, which are derived in Section 5.5, match the weights of the walls in Figure 3. This solidifies the duality between the chambers and the resolutions, which is represented by the complete structure of the resolutions and the adjacent graph of the chambers juxtaposed in Figure 3.

The dual fundamental Weyl chamber is identified with the relative movable cone of a crepant resolution $Y \rightarrow Y_0$ over the Weierstrass model Y_0 . This cone is an invariant of minimal models in the same birational class [61, §12-2]. The nef cone of any crepant resolution is then identified with a chamber of the hyperplane arrangement $I(\mathfrak{g}, \mathbf{R})$. In particular, two nef cones whose interior coincide represent the same crepant resolution. An interior walls of $I(\mathfrak{g}, \mathbf{R})$ corresponds to a geometric weight observed up to a sign between two distinct crepant resolutions separated by a flop. Two crepant resolutions have nef cones separated by an interior wall they they are connected by an extremal flop [61, Propostion 12-2-2].

I_0^*	
I_1^*	
I_2^*	
IV^*	
III^*	

Table 3: These are the non-Kodaira fibers observed for the $SU(2) \times SU(3)$ -models organized by the type of the resulting Kodaira fibers with contracted nodes. When there is a possible ambiguity, the node that touches the zero section is colored in black. The last two fibers in the row of I_2^* are observed for the first time.

Representation	Weights		
$(\mathbf{2}, \mathbf{1})$	$\varpi_1^{(\mathbf{2}, \mathbf{1})} = (1; 0, 0)$	$\varpi_2^{(\mathbf{2}, \mathbf{1})} = (-1; 0, 0)$	
$(\mathbf{1}, \mathbf{3})$	$\varpi_1^{(\mathbf{1}, \mathbf{3})} = (0; 1, 0)$	$\varpi_2^{(\mathbf{1}, \mathbf{3})} = (0; -1, 1)$	$\varpi_3^{(\mathbf{2}, \mathbf{1})} = (0; 0, -1)$
$(\mathbf{2}, \mathbf{3})$	$\varpi_1^{(\mathbf{2}, \mathbf{3})} = (1; 1, 0)$	$\varpi_2^{(\mathbf{2}, \mathbf{3})} = (1; -1, 1)$	$\varpi_3^{(\mathbf{2}, \mathbf{3})} = (1; 0, -1)$
	$\varpi_4^{(\mathbf{2}, \mathbf{3})} = (-1; 1, 0)$	$\varpi_5^{(\mathbf{2}, \mathbf{3})} = (-1; -1, 1)$	$\varpi_6^{(\mathbf{2}, \mathbf{3})} = (-1; 0, -1)$

Table 4: Weights of the representations

Subchambers	$\varpi_2^{(1,3)}$	$\varpi_5^{(2,3)}$	$\varpi_4^{(2,3)}$	$\varpi_3^{(2,3)}$	$\varpi_2^{(2,3)}$	Explicit description
①	+	-	-	+	+	$0 < \phi_2 - \phi_1 < \phi_1 < \phi_2 < \psi_1$
②	+	-	-	-	+	$0 < \phi_2 - \phi_1 < \phi_1 < \psi_1 < \phi_2$
③	+	-	+	-	+	$0 < \phi_2 - \phi_1 < \psi_1 < \phi_1 < \phi_2$
④	+	+	+	-	+	$0 < \psi_1 < \phi_2 - \phi_1 < \phi_1 < \phi_2$
①	-	-	-	+	+	$0 < \phi_1 - \phi_2 < \phi_2 < \phi_1 < \psi_1$
②	-	-	+	+	+	$0 < \phi_1 - \phi_2 < \phi_2 < \psi_1 < \phi_1$
③	-	-	+	-	+	$0 < \phi_1 - \phi_2 < \psi_1 < \phi_2 < \phi_1$
④	-	-	+	-	-	$0 < \psi_1 < \phi_1 - \phi_2 < \phi_2 < \phi_1$

Table 5: Chambers of the hyperplane arrangement $I(A_1 \oplus A_2, \mathbf{R})$ with $\mathbf{R} = (\mathbf{1}, \mathbf{3}) \oplus (\mathbf{2}, \mathbf{3})$. We will get exactly the same structure if we take the representation $\mathbf{R} = (\mathbf{2}, \mathbf{1}) \oplus (\mathbf{1}, \mathbf{3}) \oplus (\mathbf{2}, \mathbf{3})$ since the representation $(\mathbf{2}, \mathbf{1})$ does not contribute any hyperplane intersecting the interior of the dual fundamental Weyl chamber.

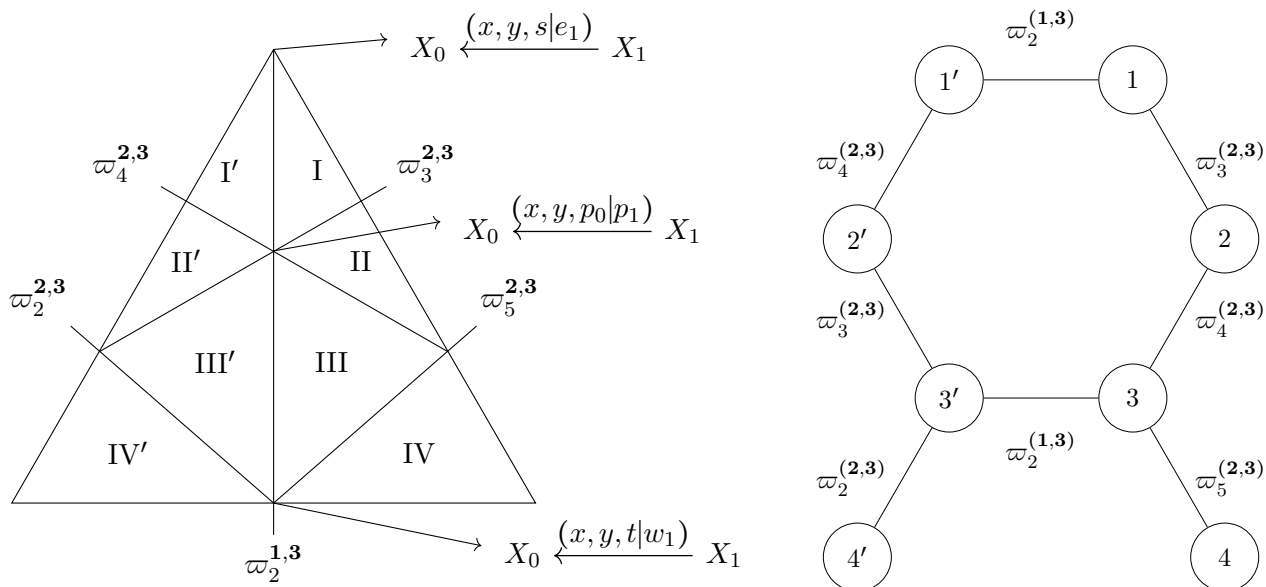


Figure 3: **Left:** the complete structure of the resolutions of $SU(2) \times SU(3)$. This is a two-dimensional patch of the entire three-dimensional cones. Hence, every point (resp. line) on this picture represents a line (resp. surface). Accordingly, these eight triangles are the three-dimensional triangular cones. The point in the top of the triangle is the resolution that resolves the $SU(2)$, and the bottom-middle point of the triangle is the first resolution that resolves $SU(3)$ only. The point in the middle of the triangle is the point that describes the blow-up that mixes both $SU(2)$ and $SU(3)$. All these three points are connected as expected and it works as the plane of the mirrors. **Right:** the adjacent graph of the eight chambers of $I(\mathfrak{g}, \mathbf{R})$ with $\mathfrak{g} = A_1 \oplus A_2$ and $\mathbf{R} = (\mathbf{1}, \mathbf{3}) \oplus (\mathbf{2}, \mathbf{3})$.

5 The $\mathbf{I}_2^s + \mathbf{I}_3^s$ Model

In this section, we study the fiber structure of the crepant resolutions of the $\mathbf{I}_2^s + \mathbf{I}_3^s$ model defined by the following Weierstrass equation:

$$Y_0 : y^2 + a_1xy + \tilde{a}_3sty = x^3 + \tilde{a}_2stx^2 + \tilde{a}_4st^2x + \tilde{a}_6s^2t^3. \quad (5.1)$$

5.1 Resolution I

Resolution I is defined by the following sequence of blowups:

$$X_0 = \mathbb{P}(\mathcal{O}_B \oplus \mathcal{L}^{\otimes 2} \oplus \mathcal{L}^{\otimes 3}) \xleftarrow{(x, y, s|e_1)} X_1 \xleftarrow{(x, y, t|w_1)} X_2 \xleftarrow{(y, w_1|w_2)} X_3, \quad (5.2)$$

where X_0 is the projective bundle in which the Weierstrass model is defined; each successive blowup produces a projective bundle over the center of the blowup. The projective coordinates of the fibers of the successive projective bundles are

$$[e_1w_1w_2x; e_1w_1w_2^2y; z = 1][w_1w_2x; w_1w_2^2y; s][x; w_2y; t][y; w_1]. \quad (5.3)$$

The proper transform of Y_0 is denoted Y and is a smooth elliptic fibration:

$$Y : y(w_2y + a_1x + \tilde{a}_3st) = w_1(e_1x^3 + \tilde{a}_2se_1tx^2 + \tilde{a}_4st^2x + \tilde{a}_6s^2t^3). \quad (5.4)$$

We denote by D_a^s and D_a^t the irreducible fibral divisors that project to S and T :

$$\mathbf{I}_2^s : \begin{cases} D_0^s : s = y(w_2y + a_1x) - w_1e_1x^3 = 0 \\ D_1^s : e_1 = y(w_2y + a_1x + \tilde{a}_3st) - w_1(\tilde{a}_4st^2x + \tilde{a}_6s^2t^3) = 0 \end{cases} \quad (5.5)$$

$$\mathbf{I}_3^s : \begin{cases} D_0^t : t = y(w_2y + a_1x) - w_1e_1x^3 = 0 \\ D_1^t : w_1 = w_2y + a_1x + \tilde{a}_3st = 0 \\ D_2^t : w_2 = y(a_1x + \tilde{a}_3st) - w_1(e_1x^3 + \tilde{a}_2se_1tx^2 + \tilde{a}_4st^2x + \tilde{a}_6s^2t^3) = 0 \end{cases} \quad (5.6)$$

The generic fiber of D_a^s (resp. D_a^t) over S (resp. T) is denoted as C_a^s (resp. C_a^t). The fiber structure away from the intersection $S \cap T$ is well understood from the study of the individual $\text{SU}(2)$ and $\text{SU}(3)$ -models [35]. The generic fiber over the intersection of S and T is of type \mathbf{I}_5^s as in Figure 4, which is produced by the following splittings of C_a^s and C_a^t .

$$\text{On } S \cap T : \begin{cases} C_0^s \longrightarrow \eta_0^0 \\ C_1^s \longrightarrow \eta_1^{0A} + \eta_1^{0B} + \eta_1^1 + \eta_1^2 \\ C_0^t \longrightarrow \eta_1^{0A} + \eta_1^{0B} + \eta_0^0 \\ C_1^t \longrightarrow \eta_1^1 \\ C_2^t \longrightarrow \eta_1^2 \end{cases} \quad (5.7)$$

$$\text{On } S \cap T : \begin{cases} C_0^s \cap C_0^t \rightarrow \eta_0^0 : s = t = y(w_2y + a_1x) - w_1e_1x^3 = 0 \\ C_1^s \cap C_0^t \rightarrow \eta_1^{0A} : e_1 = t = y = 0, \quad \eta_1^{0B} : e_1 = t = w_2y + a_1x = 0 \\ C_1^s \cap C_1^t \rightarrow \eta_1^1 : e_1 = w_1 = w_2y + a_1x + \tilde{a}_3st = 0 \\ C_1^s \cap C_2^t \rightarrow \eta_1^2 : e_1 = w_2 = y(a_1x + \tilde{a}_3st) - st^2w_1(\tilde{a}_4x + \tilde{a}_6st) = 0 \end{cases} \quad (5.8)$$

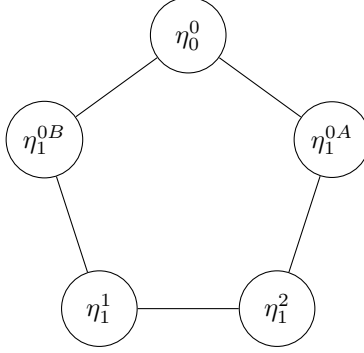


Figure 4: Fiber over the generic point of the locus $S \cap T$ in Resolution I of the $I_2^s + I_3^s$ -model.

The curves η_0^0 , η_1^1 , and η_1^2 have the same weights as C_0^s , C_1^t , and C_2^t , respectively. The curves η_1^{0A} (resp. η_1^{0B}) has zero intersection with D_1^t (resp. D_2^t). The intersection of the curves composing the fiber I_5^s with the fibral divisors are listed on Table 6.

	D_0^s	D_1^s	D_0^t	D_1^t	D_2^t	Weight	Representation
η_0^0	-2	2	0	0	0	$[-2;0,0]$	$(\mathbf{3}, \mathbf{1})$
η_1^2	0	0	1	1	-2	$[0;-1,2]$	$(\mathbf{1}, \mathbf{8})$
η_1^1	0	0	1	-2	1	$[0;2-1]$	$(\mathbf{1}, \mathbf{8})$
η_1^{0A}	1	-1	-1	0	1	$[1;0,-1]$	$(\mathbf{2}, \mathbf{3})$
η_1^{0B}	1	-1	-1	1	0	$[1;-1,0]$	$(\mathbf{2}, \bar{\mathbf{3}})$

Table 6: Weights of vertical curves and representations in the resolution I of the $I_2^s + I_3^s$ -model.

The weights of the curves η_0^0 , η_1^2 , and η_1^1 are among the weights of the adjoint representation while the weights of the curves η_1^{0A} and η_1^{0B} are respectively in the bifundamental representation $(\mathbf{2}, \mathbf{3})$ and $(\mathbf{2}, \bar{\mathbf{3}})$.

The fiber I_5^s can degenerate in two different ways by following the degenerations of η_1^{0B} and η_1^2 . The curve η_1^{0B} degenerates at $V(a_1)$, and η_1^2 is a conic that degenerates at the zero locus of its discriminant. The generic fiber over $S \cap T \cap V(a_1)$ is a non-Kodaira fiber corresponding to a contracted fiber of type IV^* described in Figure 5. The generic fiber over $S \cap T \cap V(a_1 \tilde{a}_6 - \tilde{a}_3 \tilde{a}_4)$ is an I_6^2 fiber obtained by the degeneration of the conic η_1^2 into two lines intersecting transversally (see Figure 6).

$$\text{On } S \cap T \cap V(a_1) : \begin{cases} \eta_0^0 & \longrightarrow \eta_0^0 : s = t = w_2 y^2 - w_1 e_1 x^3 = 0 \\ \eta_1^{0A} & \longrightarrow \eta_1^{0A} : e_1 = t = y = 0 \\ \eta_1^{0B} & \longrightarrow \eta_1^{0A} : e_1 = t = y = 0, \eta_1^{02} : e_1 = t = w_2 = 0 \\ \eta_1^1 & \longrightarrow \eta_1^1 : e_1 = w_1 = w_2 y + \tilde{a}_3 s t = 0 \\ \eta_1^2 & \longrightarrow \eta_1^{02} : e_1 = w_2 = t = 0, \eta_1^2 : e_1 = w_2 = \tilde{a}_3 y - t w_1 (\tilde{a}_4 x + \tilde{a}_6 s t) = 0 \end{cases} \quad (5.9)$$

$$\text{On } S \cap T \cap V(a_1 \tilde{a}_6 - \tilde{a}_3 \tilde{a}_4) : \eta_1^2 \longrightarrow \begin{cases} \eta_1^{2A} : a_1 x + \tilde{a}_3 s t = 0, \\ \eta_1^{2B} : \tilde{a}_3 y - \tilde{a}_6 s t^2 w_1 = 0 \end{cases} \quad (5.10)$$

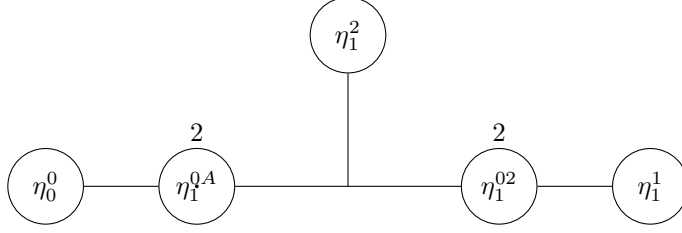


Figure 5: Fiber over the generic point of the locus $S \cap T \cap V(a_1)$ in Resolution I of the $\mathbb{I}_2^s + \mathbb{I}_3^s$ -model.

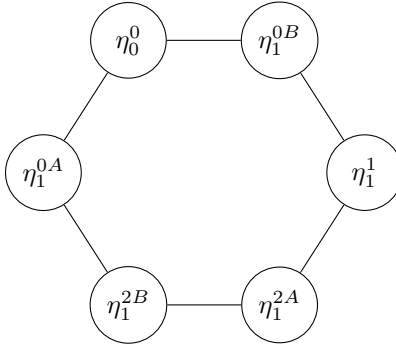


Figure 6: Fiber over the generic point of the locus $S \cap T \cap V(a_1 \tilde{a}_6 - \tilde{a}_3 \tilde{a}_4)$ in Resolution I of the $\mathbb{I}_2^s + \mathbb{I}_3^s$ -model.

As it is clear from equation (5.10), the curve η_1^{2A} will degenerate to a surface over $S \cap T \cap V(a_1, \tilde{a}_3)$. For that reason, we assume that the base is at most a threefold to ensure that the fibration is flat.

5.2 Resolution II

In this section, we study the resolution II. In contrast to the other resolutions, some of the centers of the blowups that define resolutions II and II' are singular. In particular, the first blowup in the sequence of blowups that defines resolution II has a singular center. In order to describe the first blowup, it is useful to rewrite the equation (5.1) as

$$Y_0 : \begin{cases} y(y + a_1 x + \tilde{a}_3 p_0) = x^3 + \tilde{a}_2 p_0 x^2 + \tilde{a}_4 p_0 t x + \tilde{a}_6 p_0^2 t \\ p_0 = st \end{cases} . \quad (5.11)$$

The resolution II is then given by the following sequence of blowups

$$X_0 \xrightarrow{(x, y, p_0 | p_1)} X_1 \xrightarrow{(y, t, p_1 | w_1)} X_2 \xleftarrow{(t, p_0 | w_2)} X_3 , \quad (5.12)$$

where $X_0 = \mathbb{P}[\mathcal{O}_B \oplus \mathcal{L}^{\otimes 2} \oplus \mathcal{L}^{\otimes 3}]$. The projective coordinates on X_3 are then

$$[p_1 w_1 x : p_1 w_1^2 y : z = 1][x : w_1 y : p_0 w_2][y : t w_2 : p_1][t : p_0], \quad (5.13)$$

and the proper transform is

$$Y : \begin{cases} y(w_1y + a_1x + \tilde{a}_3p_0w_2) = p_1x^3 + \tilde{a}_2p_0p_1w_2x^2 + \tilde{a}_4p_0tw_2^2x + \tilde{a}_6p_0^2tw_2^3 \\ p_0p_1 = st \end{cases} . \quad (5.14)$$

The variety $X_1 = Bl_{(x,y,p_0)}X_0$ has double point singularities at $p_0 = p_1 = s = t = 0$. The fibral divisors of Y are

$$I_2^s : \begin{cases} D_0^s : s = p_0 = y(w_1y + a_1x) - p_1x^3 = 0 \\ D_1^s : s = p_1 = y(w_1y + a_1x + \tilde{a}_3p_0w_2) - tw_2^2(\tilde{a}_4p_0x + \tilde{a}_6p_0^2w_2) = 0 \end{cases} \quad (5.15)$$

$$I_3^s : \begin{cases} D_0^t : w_2 = p_0p_1 - st = y(w_1y + a_1x) - p_1x^3 = 0 \\ D_1^t : t = p_1 = w_1y + a_1x + \tilde{a}_3p_0w_2 = 0 \\ D_2^t : w_1 = p_0p_1 - st = y(a_1x + \tilde{a}_3p_0w_2) - (p_1x^3 + \tilde{a}_2p_0p_1w_2x^2 + \tilde{a}_4p_0tw_2^2x + \tilde{a}_6p_0^2tw_2^3) = 0 \end{cases} \quad (5.16)$$

At the intersection of S and T the fiber enhances to an I_5^s . This is realized by the following splittings of the curves.

$$\text{On } S \cap T : \begin{cases} C_0^s \longrightarrow \eta_0^0 + \eta_0^2 \\ C_1^s \longrightarrow \eta_1^0 + \eta_1^1 + \eta_1^2 \\ C_0^t \longrightarrow \eta_0^0 + \eta_1^0 \\ C_1^t \longrightarrow \eta_1^1 \\ C_2^t \longrightarrow \eta_0^2 + \eta_1^2 \end{cases} \quad (5.17)$$

The curves at the intersection are given by

$$\text{On } S \cap T : \begin{cases} C_0^s \cap C_0^t \rightarrow \eta_0^0 : s = p_0 = w_2 = y(w_1y + a_1x) - p_1x^3 = 0, \\ C_0^s \cap C_2^t \rightarrow \eta_0^2 : s = p_0 = w_1 = a_1y - p_1x^2 = 0, \\ C_1^s \cap C_0^t \rightarrow \eta_1^0 : s = p_1 = w_2 = w_1y + a_1x = 0, \\ C_1^s \cap C_1^t \rightarrow \eta_1^1 : s = p_1 = t = w_1y + a_1x + \tilde{a}_3p_0w_2 = 0, \\ C_1^s \cap C_2^t \rightarrow \eta_1^2 : s = p_1 = w_1 = y(a_1x + \tilde{a}_3p_0w_2) - p_0tw_2^2(\tilde{a}_4x + \tilde{a}_6p_0w_2) = 0. \end{cases} \quad (5.18)$$

This corresponds to I_5^s as in Figure 7. The curve η_1^2 is quadratic in x, y , and p_0 with the discriminant $a_1(a_1\tilde{a}_6 - \tilde{a}_3\tilde{a}_4)$.

	D_0^s	D_1^s	D_0^t	D_1^t	D_2^t	Weight	Representation
η_0^0	-1	1	-1	0	1	[-1;0,-1]	(2, 3)
η_0^2	-1	1	1	0	-1	[-1;0,1]	(2, $\bar{3}$)
η_1^1	0	0	1	-2	1	[0;2,-1]	(1, 8)
η_1^0	1	-1	-1	1	0	[1;-1,0]	(2, $\bar{3}$)
η_1^2	1	-1	0	1	-1	[1;-1,1]	(2, 3)

Table 7: Weights of vertical curves and representations in the resolution II of the $I_2^s+I_3^s$ -model.

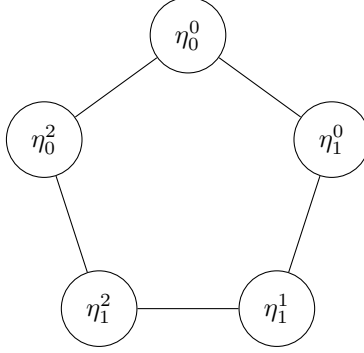


Figure 7: Fiber over the generic point of the locus $S \cap T$ in Resolution II of the $I_2^s + I_3^s$ -model.

There are two enhancements when the discriminant of the curve η_1^2 vanishes. First enhancement is when $a_1 = 0$:

$$\text{On } S \cap T \cap V(a_1) : \begin{cases} \eta_0^2 \longrightarrow \eta_{01}^2 \\ \eta_1^0 \longrightarrow \eta_1^{02} \\ \eta_1^2 \longrightarrow \eta_{01}^2 + \eta_1^{02} + \eta_1^2 \end{cases}, \quad (5.19)$$

where the new curves are given by

$$\begin{cases} \eta_{01}^2 : & s = p_0 = p_1 = w_1 = 0 \\ \eta_1^{02} : & s = p_1 = w_2 = w_1 = 0 \\ \eta_1^2 : & s = p_1 = w_1 = \tilde{a}_3 y - \tilde{a}_4 t w_2 x - \tilde{a}_6 p_0 t w_2^2 = 0 \end{cases}. \quad (5.20)$$

For this codimension-three enhancement, we get a non-Kodaira fiber that is an incomplete fiber of type IV^* , as illustrated in Figure 8.

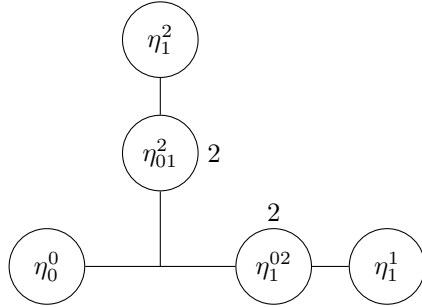


Figure 8: Fiber over the generic point of the locus $S \cap T \cap V(a_1)$ in Resolution II of the $I_2^s + I_3^s$ -model.

The other specialization is when $(a_1 \tilde{a}_6 - \tilde{a}_3 \tilde{a}_4)$, where η_1^2 splits into two curves that intersect each other such that

$$\text{on } S \cap T \cap V(a_1 \tilde{a}_6 - \tilde{a}_3 \tilde{a}_4) : \eta_1^2 \longrightarrow \eta_1^{2A} + \eta_1^{2B}, \quad (5.21)$$

while all the other fibers are the same. except η_1^2 . The resulting fiber is a Kodaira fiber of type I_6 as in Figure 9.

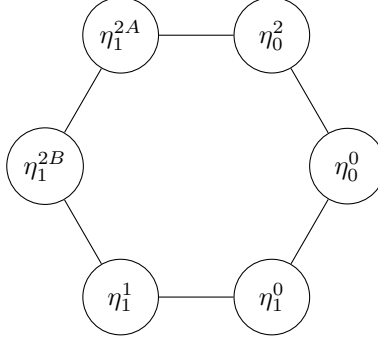


Figure 9: Fiber over the generic point of the locus $S \cap T \cap V(a_1\tilde{a}_6 - \tilde{a}_3\tilde{a}_4)$ in Resolution II of the $I_2^s + I_3^s$ -model.

5.3 Resolution III

The resolution III is defined by the following sequence of blowups:

$$X_0 \xleftarrow{(x, y, t|w_1)} X_1 \xleftarrow{(x, y, s|e_1)} X_2 \xleftarrow{(y, w_1|w_2)} X_3 \quad (5.22)$$

The projective coordinates are then given by

$$[e_1w_1w_2x; e_1w_1w_2^2y; z = 1][e_1x; e_1w_2y; t][x; w_2y; s][y; w_1]. \quad (5.23)$$

The proper transform of the elliptic fibration for the resolution III is the same as equation (5.4) and the five fibral divisors are thus identical to those listed on the equation (5.6).

As before, we have a fiber of type I_2^s over the generic point of S and fiber of type I_3^s over the generic point of T . At the collision of S and T , the different curves are

$$\text{On } S \cap T : \begin{cases} C_0^s \cap C_0^t \rightarrow \eta_0^0 : s = t = y(w_2y + a_1x) - w_1e_1x^3 = 0 \\ C_0^s \cap C_1^t \rightarrow \eta_0^1 : s = w_1 = w_2y + a_1x = 0 \\ C_0^s \cap C_2^t \rightarrow \eta_0^2 : s = w_2 = a_1y - e_1w_1x^2 = 0 \\ C_1^s \cap C_1^t \rightarrow \eta_1^1 : e_1 = w_1 = w_2y + a_1x + \tilde{a}_3st = 0 \\ C_1^s \cap C_2^t \rightarrow \eta_1^2 : e_1 = w_2 = y(a_1x + \tilde{a}_3st) - st^2w_1(\tilde{a}_4x + \tilde{a}_6st) = 0 \end{cases} \quad (5.24)$$

The splittings of curves are

$$\text{On } S \cap T : \begin{cases} C_0^s \longrightarrow \eta_0^0 + \eta_0^1 + \eta_0^2 \\ C_1^s \longrightarrow \eta_1^1 + \eta_1^2 \\ C_0^t \longrightarrow \eta_0^0 \\ C_1^t \longrightarrow \eta_0^1 + \eta_1^1 \\ C_2^t \longrightarrow \eta_0^2 + \eta_1^2 \end{cases} \quad (5.25)$$

This corresponds to I_3^s , which is represented in Figure 10.

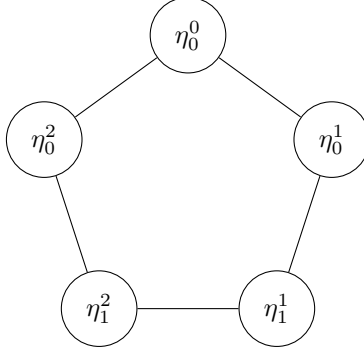


Figure 10: Fiber over the generic point of the locus $S \cap T$ in Resolution III of the $I_2^s + I_3^s$ -model.

From the splittings of the curves, we compute the intersection numbers to get the weight vectors and further deduce the representations.

	D_0^s	D_1^s	D_0^t	D_1^t	D_2^t	Weight	Representation
η_0^0	0	0	-2	1	1	$[0; -1, -1]$	$(\mathbf{1}, \mathbf{8})$
η_0^1	-1	1	1	-1	0	$[-1; 1, 0]$	$(\mathbf{2}, \mathbf{3})$
η_1^1	1	-1	0	-1	1	$[1; 1, -1]$	$(\mathbf{2}, \mathbf{\bar{3}})$
η_1^2	1	-1	0	1	-1	$[1; -1, 1]$	$(\mathbf{2}, \mathbf{3})$
η_0^2	-1	1	1	0	-1	$[-1; 0, 1]$	$(\mathbf{2}, \mathbf{\bar{3}})$

Table 8: Weights of vertical curves and representations in the resolution III of the $I_2^s + I_3^s$ -model.

This has two further specializations when the discriminant of η_1^2 vanishes. The first enhancement is when $a_1 = 0$. We observe the following splittings for the elliptical fibrations:

$$\text{On } S \cap T \cap V(a_1) : \begin{cases} \eta_0^0 & \longrightarrow \eta_0^0 : s = t = w_2 y^2 - w_1 e_1 x^3 = 0 \\ \eta_0^1 & \longrightarrow \eta_0^{12} : s = w_1 = w_2 = 0 \\ \eta_0^2 & \longrightarrow \eta_0^{12} : s = w_2 = w_1 = 0, \eta_{01}^2 : s = w_2 = e_1 = 0 \\ \eta_1^1 & \longrightarrow \eta_1^1 : e_1 = w_1 = w_2 y + \tilde{a}_3 s t = 0 \\ \eta_1^2 & \longrightarrow \eta_{01}^2 : e_1 = w_2 = s = 0, \eta_1^2 : e_1 = w_2 = \tilde{a}_3 y - t w_1 (\tilde{a}_4 x + \tilde{a}_6 s t) = 0 \end{cases} \quad (5.26)$$

The splittings from the five divisors to the codimension-three enhancement when $a_1 = 0$ is

$$\text{On } S \cap T \cap V(a_1) : \begin{cases} C_0^s & \longrightarrow \eta_0^0 + \eta_0^{12} + \eta_{01}^2 \\ C_1^s & \longrightarrow \eta_{01}^2 + \eta_1^1 + \eta_1^2 \\ C_0^t & \longrightarrow \eta_0^0 \\ C_1^t & \longrightarrow \eta_0^{12} + \eta_1^1 \\ C_2^t & \longrightarrow \eta_0^{12} + \eta_{01}^2 + \eta_1^2. \end{cases} \quad (5.27)$$

The generic fiber over $S \cap T \cap V(a_1)$ is a non-Kodaira fiber illustrated in Figure 11 and corresponding to an incomplete fiber of type IV^* .

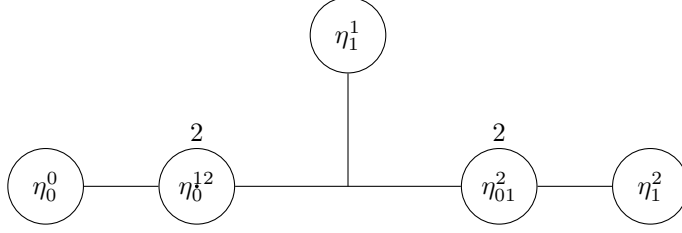


Figure 11: Fiber over the generic point of the locus $S \cap T \cap V(a_1)$ in Resolution III of the $I_2^s + I_3^s$ -model.

Now consider the other condition, $a_1 \tilde{a}_6 = \tilde{a}_3 \tilde{a}_4$, to get the other specialization. The curve η_1^2 splits into two fibers intersecting each other:

$$\text{on } S \cap T \cap V(a_1 \tilde{a}_6 - \tilde{a}_3 \tilde{a}_4) : \eta_1^2 \longrightarrow \eta_1^{2A} + \eta_1^{2B}. \quad (5.28)$$

Thus, we get a fiber enhancement of type I_6^s , which is represented in Figure 12.

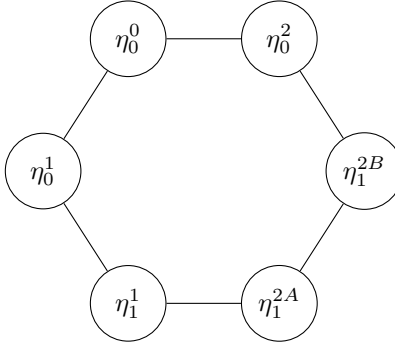


Figure 12: Fiber over the generic point of the locus $S \cap T \cap V(a_1 \tilde{a}_6 - \tilde{a}_3 \tilde{a}_4)$ in Resolution III of the $I_2^s + I_3^s$ -model.

5.4 Resolution IV

The resolution IV is given by the following sequence of blowups:

$$X_0 \xleftarrow{(x, y, t|w_1)} X_1 \xleftarrow{(y, w_1|w_2)} X_2 \xleftarrow{(x, y, s|e_1)} X_3. \quad (5.29)$$

Its projective coordinates are then given by

$$[e_1 w_1 w_2 x; e_1 w_1 w_2^2 y; z = 1][e_1 x; e_1 w_2 y; t][e_1 y; w_1][x; y; s]. \quad (5.30)$$

The proper transform of the elliptic fibration for the resolution III is the same as equation (5.4) and the five fibral divisors are thus identical to the equation (5.6). At the intersection of both divisors

S and T , we get the following curves:

$$\text{On } S \cap T \cap V(a_1) : \begin{cases} C_0^s \cap C_0^t \longrightarrow \eta_0^0 : s = t = y(w_2y + a_1x) - w_1e_1x^3 = 0, \\ C_0^s \cap C_1^t \longrightarrow \eta_0^1 : s = w_1 = w_2y + a_1x = 0, \\ C_0^s \cap C_2^t \longrightarrow \eta_0^{2A} : s = w_2 = x = 0, \eta_0^{2B} : s = w_2 = a_1y - w_1e_1x^2 = 0, \\ C_1^s \cap C_2^t \longrightarrow \eta_1^2 : e_1 = w_2 = y(a_1x + \tilde{a}_3st) - st^2w_1(\tilde{a}_4x + \tilde{a}_6st) = 0. \end{cases} \quad (5.31)$$

From the five fibral divisors, we summarize the splittings of the curves to be the following.

$$\text{On } S \cap T \cap V(a_1) : \begin{cases} C_0^s \longrightarrow \eta_0^0 + \eta_0^1 + \eta_0^{2A} + \eta_0^{2B} \\ C_1^s \longrightarrow \eta_1^2 \\ C_0^t \longrightarrow \eta_0^0 \\ C_1^t \longrightarrow \eta_0^1 \\ C_2^t \longrightarrow \eta_0^{2A} + \eta_0^{2B} + \eta_1^2. \end{cases} \quad (5.32)$$

This corresponds to I_2^s as it is represented in Figure 13.

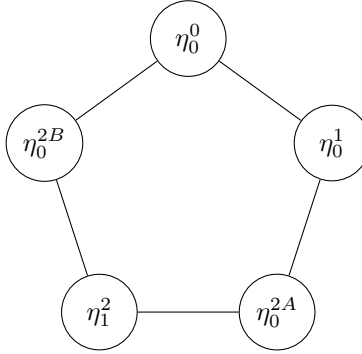


Figure 13: Fiber over the generic point of the locus $S \cap T$ in Resolution IV of the $I_2^s + I_3^s$ -model.

The intersection numbers are computed using the equation (5.32) to get the weights and the representations of the curves.

	D_0^s	D_1^s	D_0^t	D_1^t	D_2^t	Weight	Representation
η_0^0	0	0	-2	1	1	$[0;-1,-1]$	$(\mathbf{1}, \mathbf{8})$
η_0^1	0	0	1	-2	1	$[0;2,-1]$	$(\mathbf{1}, \mathbf{8})$
η_0^{2A}	-1	1	0	1	-1	$[-1;-1,1]$	$(\mathbf{2}, \mathbf{3})$
η_1^2	2	-2	0	0	0	$[2;0,0]$	$(\mathbf{3}, \mathbf{1})$
η_0^{2B}	-1	1	1	0	-1	$[-1;0,1]$	$(\mathbf{2}, \mathbf{3})$

Table 9: Weights of vertical curves and representations in the resolution IV of the $I_2^s + I_3^s$ -model.

This has two further specializations in codimension-three. The first specialization is when $a_1 = 0$.

We observe the following splittings for the elliptical fibrations

$$\text{on } S \cap T \cap V(a_1) : \begin{cases} \eta_0^0 & \longrightarrow \eta_0^0 : s = t = w_2 y^2 - w_1 e_1 x^3 = 0, \\ \eta_0^1 & \longrightarrow \eta_0^{12} : s = w_1 = w_2 = 0, \\ \eta_0^{2A} & \longrightarrow \eta_0^{2A} : s = w_2 = x = 0, \\ \eta_0^{2B} & \longrightarrow \eta_0^{12} : s = w_2 = w_1 = 0, \eta_{01}^2 : s = w_2 = e_1 = 0, \eta_0^{2A} : s = w_2 = x = 0, \\ \eta_1^2 & \longrightarrow \eta_{01}^2 : e_1 = w_2 = s = 0, \eta_1^2 : e_1 = w_2 = \tilde{a}_3 y - t w_1 (\tilde{a}_4 x + \tilde{a}_6 s t) = 0. \end{cases} \quad (5.33)$$

For this codimension-three fiber enhancement, we get a specialization of E_6 , as it is represented in Figure 14.

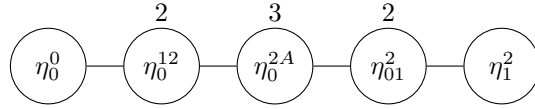


Figure 14: Fiber over the generic point of the locus $S \cap T \cap V(a_1)$ in Resolution IV of the $I_2^s + I_3^s$ -model.

The other specialization is when $a_1 \tilde{a}_6 = \tilde{a}_3 \tilde{a}_4$. Then all the other fibers are the same except η_1^2 , which splits into two curves intersecting each other:

$$\text{on } S \cap T \cap V(a_1 \tilde{a}_6 - \tilde{a}_3 \tilde{a}_4) : \eta_1^2 \longrightarrow \eta_1^{2A} + \eta_1^{2B}. \quad (5.34)$$

For this codimension-three enhancement, we get a fiber of type I_6^s as in Figure 15.

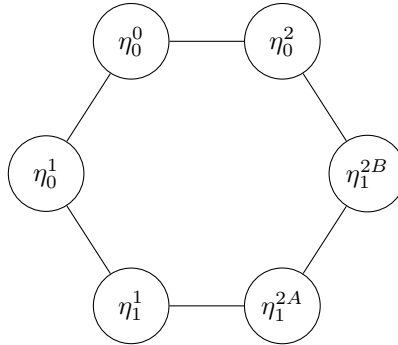


Figure 15: Fiber over the generic point of the locus $S \cap T \cap V(a_1 \tilde{a}_6 - \tilde{a}_3 \tilde{a}_4)$ in Resolution IV of the $I_2^s + I_3^s$ -model.

5.5 Flops

In this section, we discuss the flops between the resolutions I, II, III, and IV. We recall that the resolutions I' , II' , III' , IV' are their mirrors under the birational map induced by the involution

of the Mordell–Weil group. We consider the case of the $I_2^s+I_3^s$ model analyzed in Section 5. The other case follows the same scheme. When there is a simple flop between two resolutions, if the flopping curve has weights ω in one of the resolutions, is replaced in the other by a curve of weights $-\omega$. Each resolution corresponds to a minimal model over the Weierstrass model. Hence, in the hyperplane arrangement, each resolution corresponds to a specific chamber. When two resolutions are connected by a flop of a curve of weight ω , the hyperplane separating the corresponding chamber is exactly the hyperplane ω^\perp perpendicular to ω . It follows that a chamber is uniquely defined by its possible flopping curves. We determine in Table 10 all the flopping curves and show that their weights coincide with the hyperplanes separating two chambers of the hyperplane arrangement. These curves are identified with their corresponding weights from Table 4. This result matches with the analysis in Figure 3, which completes the correspondence between the geometry and the representation theory.

Flopping curves						Weight			
Resolution I:	η_1^{0A}	$[1; 0, -1]$	$(\mathbf{2}, \mathbf{3})$	\leftrightarrow	Resolution II:	η_0^2	$[-1; 0, 1]$	$(\mathbf{2}, \bar{\mathbf{3}})$	$\omega_3^{(\mathbf{2}, \mathbf{3})}$
Resolution II:	η_1^1	$[1; -1, 0]$	$(\mathbf{2}, \bar{\mathbf{3}})$	\leftrightarrow	Resolution III:	η_0^1	$[-1; 1, 0]$	$(\mathbf{2}, \mathbf{3})$	$\omega_4^{(\mathbf{2}, \mathbf{3})}$
Resolution III:	η_1^1	$[1; 1, -1]$	$(\mathbf{2}, \bar{\mathbf{3}})$	\leftrightarrow	Resolution IV:	η_0^{2A}	$[-1; -1, 1]$	$(\mathbf{2}, \mathbf{3})$	$\omega_5^{(\mathbf{2}, \mathbf{3})}$

Table 10: The fibers that is the one that separates between the chambers and thus responsible for flops in the $I_2^s+I_3^s$ -model. The weight of the contracted curve in a (terminal) flop connecting two resolutions is normal to the facet common to the closures of the corresponding chambers in the hyperplane arrangement.

6 The III+IV^s Model

In this section, we study the fiber structure of the crepant resolutions of the III + IV^s-model defined by the following Weierstrass equation:

$$Y_0 : y^2 + \tilde{a}_1 stxy + \tilde{a}_3 sty = x^3 + \tilde{a}_2 stx^2 + \tilde{a}_4 st^2x + \tilde{a}_6 s^2t^3, \quad (6.1)$$

where the fiber III and IV^s are the fibers over the generic point of $S = V(s)$ and $T = V(t)$ respectively. It corresponds to the low-right corner of Figure 1. In particular, the fiber over S and T cannot specialize further while preserving their dual graphs (and hence, the gauge group $SU(2) \times SU(3)$). In [43], this model was explored using the point of view of string junctions.

Here, we analyze the geometry of the crepant resolutions of the III + IV^s-model. The triple intersection numbers are the same as those of the $I_2^s+I_3^s$ -model. The fiber over the generic point of $S \cap T$ is a non-Kodaira fiber corresponding to a fiber of type IV* with some nodes contracted. Such a fiber enhances further over $S \cap T \cap V(\tilde{a}_3)$ to a non-Kodaira fiber corresponding to a fiber of type III* with some nodes contracted. The non-Kodaira fibers observed for the III+IV^s-model were already seen in the $I_2^s+I_3^s$ -model but one codimension higher.

6.1 Resolution I

The resolution I is defined by the following sequence of blowups:

$$X_0 \xleftarrow{(x, y, s|e_1)} X_1 \xleftarrow{(x, y, t|w_1)} X_2 \xleftarrow{(y, w_1|w_2)} X_3 \quad (6.2)$$

The proper transform of the III+IV^s-model is

$$Y : y(w_2y + \tilde{a}_1se_1tw_1w_2x + \tilde{a}_3st) = w_1(e_1x^3 + \tilde{a}_2se_1tx^2 + \tilde{a}_4st^2x + \tilde{a}_6s^2t^3). \quad (6.3)$$

The projective coordinates are then given by

$$[e_1w_1w_2x; e_1w_1w_2^2y; z = 1][w_1w_2x; w_1w_2^2y; s][x; w_2y; t][y; w_1]. \quad (6.4)$$

The fibral divisors are

$$I_2^s : \begin{cases} D_0^s : s = w_2y^2 - w_1e_1x^3 = 0, \\ D_1^s : e_1 = y(w_2y + \tilde{a}_3st) - st^2w_1(\tilde{a}_4x + \tilde{a}_6st) = 0, \end{cases} \quad (6.5)$$

$$I_3^s : \begin{cases} D_0^t : t = w_2y^2 - w_1e_1x^3 = 0, \\ D_1^t : w_1 = w_2y + \tilde{a}_3st = 0, \\ D_2^t : w_2 = \tilde{a}_3sty - w_1(e_1x^3 + \tilde{a}_2se_1tx^2 + \tilde{a}_4st^2x + \tilde{a}_6s^2t^3) = 0. \end{cases} \quad (6.6)$$

Over the generic point of the intersection of S and T , we get the following irreducible curves

$$\text{On } S \cap T : \begin{cases} C_0^s \cap C_0^t & \rightarrow \eta_0^0 : s = t = w_2y^2 - w_1e_1x^3 = 0, \\ C_1^s \cap C_0^t & \rightarrow \eta_1^{02} : e_1 = t = w_2 = 0, \eta_1^{0A} : e_1 = t = y = 0, \\ C_1^s \cap C_1^t & \rightarrow \eta_1^1 : e_1 = w_1 = w_2y + \tilde{a}_3st = 0, \\ C_1^s \cap C_2^t & \rightarrow \eta_1^{02} : e_1 = w_2 = t = 0, \eta_1^2 : e_1 = w_2 = \tilde{a}_3y - tw_1(\tilde{a}_4x + \tilde{a}_6st) = 0. \end{cases} \quad (6.7)$$

The fiber over the generic point of $S \cap T$ has a structure given by Figure 16, and corresponds to a fiber of type IV* with contracted nodes. At the collision $S \cap T$, the components of the fibers III and IV^s degenerate as follows.

$$\text{On } S \cap T : \begin{cases} C_0^s \longrightarrow \eta_0^0, \\ C_1^s \longrightarrow 2\eta_1^{02} + 2\eta_1^{0A} + \eta_1^1 + \eta_1^2, \\ C_0^t \longrightarrow \eta_0^0 + \eta_1^{02} + 2\eta_1^{0A}, \\ C_1^t \longrightarrow \eta_1^1, \\ C_2^t \longrightarrow \eta_1^{02} + \eta_1^2. \end{cases} \quad (6.8)$$

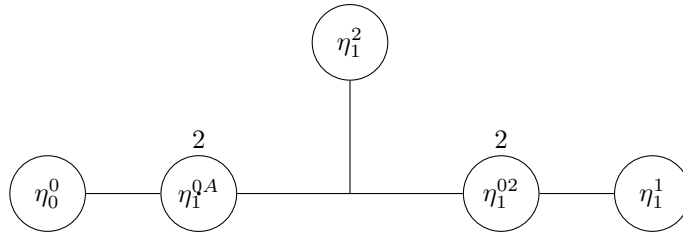


Figure 16: Fiber over the generic point of the locus $S \cap T$ in Resolution I of the III+IV^s-model.

We observe that this is identical to the fiber in the resolution I of the $\mathbb{I}_2^s + \mathbb{I}_3^s$ -model in codimension-three over $S \cap T \cap V(a_1)$.

In order to get the weights of the curves, the intersection numbers are computed between the codimension-two curves and the fibral divisors.

	D_0^s	D_1^s	D_0^t	D_1^t	D_2^t	Weight	Representation
η_0^0	-2	2	0	0	0	[-2;0,0]	(3, 1)
η_1^{0A}	1	-1	-1	0	1	[1;0,-1]	(2, 3)
η_1^2	0	0	1	0	-1	[0;0,1]	(1, $\bar{3}$)
η_1^{02}	0	0	0	1	-1	[0;-1,1]	(1, 3)
η_1^1	0	0	1	-2	1	[0;2,-1]	(1, 8)

Table 11: Weights of vertical curves and representations in the resolution I of the III+IV^s-model.

We note that the sum of the two curves $\eta_1^{02} + \eta_1^{0A}$ produce the weight [1; -1, 0] of the representation **(2, $\bar{3}$)**. In the resolution I of the $\mathbb{I}_2^s + \mathbb{I}_3^s$ -model, the weight [1; -1, 0] corresponds to η_1^{0B} in codimension-two, which splits into the two curves in codimension-three with the same weights as η_1^{02} and η_1^{0A} .

The fiber over the generic point of $S \cap T$ shown on Figure 16 specializes further when $\tilde{a}_3 = 0$:

$$\text{on } S \cap T \cap V(\tilde{a}_3) : \begin{cases} \eta_1^1 & \longrightarrow \eta_1^{12}, \\ \eta_1^2 & \longrightarrow \eta_1^{02} + \eta_1^{12} + \eta_1^2, \end{cases} \quad (6.9)$$

where the new curves are given by

$$\begin{cases} \eta_1^{12} : & e_1 = w_1 = w_2 = 0, \\ \eta_1^{02} : & e_1 = w_2 = t = 0, \\ \eta_1^2 : & e_1 = w_2 = \tilde{a}_4 x + \tilde{a}_6 st = 0. \end{cases} \quad (6.10)$$

The fiber over the generic point $S \cap T \cap V(\tilde{a}_3)$ is illustrated in Figure 17, and corresponds to a fiber of type III* with contracted nodes.

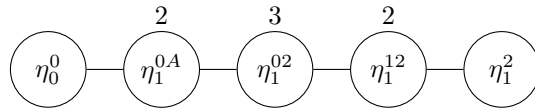


Figure 17: Fiber over the generic point of the locus $S \cap T \cap V(\tilde{a}_3)$ in Resolution I of the III+IV^s-model.

6.2 Resolution II

In this section, we study the resolution II in detail. As the resolution II requires making a first blowup around a singular center, it is useful to rewrite equation (6.1) as

$$Y_0 : \begin{cases} y(y + \tilde{a}_1 p_0 x + \tilde{a}_3 p_0) = x^3 + \tilde{a}_2 p_0 x^2 + \tilde{a}_4 p_0 t x + \tilde{a}_6 p_0^2 t \\ p_0 = st \end{cases} . \quad (6.11)$$

The resolution II is then given by the following sequence of blowups

$$X_0 \xrightarrow{\langle x, y, p_0 | p_1 \rangle} X_1 \xrightarrow{\langle y, t, p_1 | w_1 \rangle} X_2 \xleftarrow{\langle t, p_0 | w_2 \rangle} X_3 . \quad (6.12)$$

Where $X_0 = \mathbb{P}[\mathcal{O}_B \oplus \mathcal{L}^{\otimes 2} \oplus \mathcal{L}^{\otimes 3}]$. The projective coordinates are then

$$[p_1 w_1 x : p_1 w_1^2 y : z = 1][x : w_1 y : p_0 w_2][y : t w_2 : p_1][t : p_0], \quad (6.13)$$

and the proper transform is

$$Y : \begin{cases} y(w_1 y + \tilde{a}_1 p_0 w_2 x + \tilde{a}_3 p_0 w_2) = p_1 x^3 + \tilde{a}_2 p_0 p_1 w_2 x^2 + \tilde{a}_4 p_0 t w_2^2 x + \tilde{a}_6 p_0^2 t w_2^3 \\ p_0 p_1 = st \end{cases} . \quad (6.14)$$

The variety $X_1 = Bl_{(x, y, p_0)} X_0$ has double point singularities on $p_0 = p_1 = s = t = 0$. The fibral divisors are:

$$\text{III} : \begin{cases} D_0^s : s = p_0 = w_1 y^2 - p_1 x^3 = 0 \\ D_1^s : s = p_1 = y(w_1 y + \tilde{a}_1 p_0 w_2 x + \tilde{a}_3 p_0 w_2) - (p_1 x^3 + \tilde{a}_4 p_0 t w_2^2 x + \tilde{a}_6 p_0^2 t w_2^3) = 0 \end{cases} \quad (6.15)$$

$$\text{IV}^s : \begin{cases} D_0^t : w_2 = p_0 p_1 - st = w_1 y^2 - p_1 x^3 = 0 \\ D_1^t : t = p_1 = w_1 y + \tilde{a}_1 p_0 w_2 x + \tilde{a}_3 p_0 w_2 = 0 \\ D_2^t : w_1 = p_0 p_1 - st = y(\tilde{a}_1 p_0 w_2 x + \tilde{a}_3 p_0 w_2) - (p_1 x^3 + \tilde{a}_2 p_0 p_1 w_2 x^2 + \tilde{a}_4 p_0 t w_2^2 x + \tilde{a}_6 p_0^2 t w_2^3) = 0 \end{cases} \quad (6.16)$$

At the intersection of S and T , the fiber enhances to a non-Kodaira fiber presented in Figure 18. This is realized by the following splitting of curves.

$$\text{On } S \cap T : \begin{cases} C_0^s \longrightarrow \eta_0^0 + \eta_{01}^2 \\ C_1^s \longrightarrow \eta_{01}^2 + 2\eta_1^{02} + \eta_1^1 + \eta_1^2 \\ C_0^t \longrightarrow \eta_0^0 + \eta_1^{02} \\ C_1^t \longrightarrow \eta_1^1 \\ C_2^t \longrightarrow 2\eta_{01}^2 + \eta_1^{02} + \eta_1^2 \end{cases} \quad (6.17)$$

The curves at the intersection are given by

$$\text{On } S \cap T : \begin{cases} C_0^s \cap C_1^t \longrightarrow \eta_0^0 : s = p_0 = w_2 = w_1 y^2 - p_1 x^3 = 0 \\ C_0^s \cap C_2^t \longrightarrow \eta_0^2 : s = p_0 = w_1 = p_1 = 0 \\ C_1^s \cap C_0^t \longrightarrow \eta_1^{02} : s = p_1 = w_2 = w_1 = 0 \\ C_1^s \cap C_1^t \longrightarrow \eta_1^1 : s = p_1 = t = w_1 y + \tilde{a}_3 p_0 w_2 = 0 \\ C_1^s \cap C_2^t \longrightarrow \eta_1^{02} : s = p_1 = w_1 = w_2 = 0, \eta_{01}^2 : s = p_1 = w_1 = p_0 = 0, \\ \eta_1^2 : s = p_1 = w_1 = \tilde{a}_3 y - \tilde{a}_4 t w_2 x + \tilde{a}_6 p_0 t w_2^2 = 0 \end{cases} \quad (6.18)$$

Note that we had the same fiber earlier in the resolution I of the $I_2^s + I_3^s$ -model in codimension-three with a condition $a_1 = 0$.

	D_0^s	D_1^s	D_0^t	D_1^t	D_2^t	Weight	Representation
η_0^0	-1	1	-1	0	1	$[-1;0,-1]$	$(\mathbf{2}, \mathbf{3})$
η_{01}^2	-1	1	1	0	-1	$[-1;0,1]$	$(\mathbf{2}, \bar{\mathbf{3}})$
η_1^1	0	0	1	-2	1	$[0;2,-1]$	$(\mathbf{1}, \mathbf{8})$
η_1^{02}	1	-1	-1	1	0	$[1;-1,0]$	$(\mathbf{2}, \bar{\mathbf{3}})$
η_1^2	1	-1	0	0	0	$[1;0,0]$	$(\mathbf{2}, \mathbf{1})$

Table 12: Weights of vertical curves and representations in the resolution II of the III+IV^s-model.

The chain $\eta_1^{02} + \eta_{01}^2 + \eta_1^2$ produces the weight $[1; -1, 1]$ of the representation $(\mathbf{2}, \mathbf{3})$. In the case of the resolution II of the $I_2^s + I_3^s$ -model, the sum of the curves corresponds to η_1^2 in codimension-two, which splits into the three curves in codimension-three.

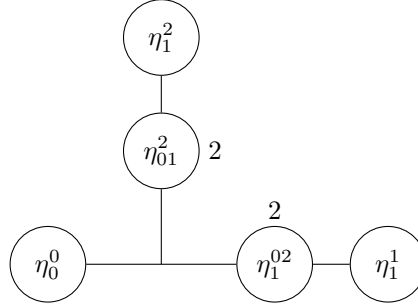


Figure 18: Fiber over the generic point of the locus $S \cap T$ in Resolution II of the III+IV^s-model.

There is an enhancement when \tilde{a}_3 as the two curves η_1^1 and η_1^2 degenerate as follows:

$$\text{on } S \cap T \cap V(\tilde{a}_3) : \begin{cases} \eta_1^1 \longrightarrow \eta_1^{12}, \\ \eta_1^2 \longrightarrow \eta_1^{02} + \eta_1^{12} + \eta_1^2, \end{cases} \quad (6.19)$$

where the new curves are given by

$$\begin{cases} \eta_1^{12} : & s = p_1 = t = w_1 = 0, \\ \eta_1^{02} : & s = p_1 = w_1 = w_2 = 0, \\ \eta_1^2 : & s = p_1 = w_1 = \tilde{a}_4 x - \tilde{a}_6 p_0 w_2 = 0. \end{cases} \quad (6.20)$$

For this codimension-three enhancement, we get a non-Kodaira fiber corresponding to a non-Kodaira fiber corresponding to a contracted fiber of type IV* as in Figure 19.

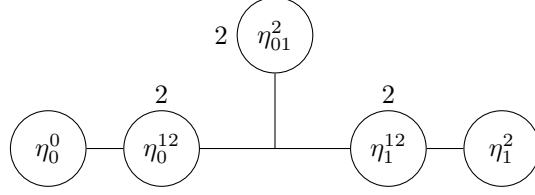


Figure 19: Fiber over the generic point of the locus $S \cap T \cap V(\tilde{\alpha}_3)$ in Resolution II of the III+IV^s-model.

6.3 Resolution III

The Resolution III is defined by the following sequence of blowups:

$$X_0 \xleftarrow{(x, y, t|w_1)} X_1 \xleftarrow{(x, y, s|e_1)} X_2 \xleftarrow{(y, w_1|w_2)} X_3 \quad (6.21)$$

The projective coordinates are then given by

$$[e_1 w_1 w_2 x; e_1 w_1 w_2^2 y; z = 1][e_1 x; e_1 w_2 y; t][x; w_2 y; s][y; w_1]. \quad (6.22)$$

The proper transform is identical to equation (6.3).

On the intersection of S and T , we see the following curves:

$$\text{On } S \cap T : \begin{cases} C_0^s \cap C_0^t & \longrightarrow \eta_0^0 : s = t = w_2 y^2 - w_1 e_1 x^3 = 0, \\ C_0^s \cap C_1^t & \longrightarrow \eta_0^{12} : s = w_1 = w_2 = 0, \\ C_0^s \cap C_2^t & \longrightarrow \eta_{01}^2 : s = w_2 = e_1 = 0, \quad \eta_0^{12} : s = w_2 = w_1 = 0, \\ C_1^s \cap C_1^t & \longrightarrow \eta_1^1 : e_1 = w_1 = w_2 y + \tilde{a}_3 s t = 0, \\ C_1^s \cap C_2^t & \longrightarrow \eta_{01}^2 : e_1 = w_2 = s = 0, \quad \eta_1^2 : e_1 = w_2 = \tilde{a}_3 y - t w_1 (\tilde{a}_4 x + \tilde{a}_6 s t) = 0. \end{cases} \quad (6.23)$$

Hence, we can deduce that the five fibral divisors split in the following way to produce the fiber in codimension-two, which is presented in Figure 20.

$$\text{On } S \cap T : \begin{cases} C_0^s & \longrightarrow \eta_0^0 + 2\eta_0^{12} + \eta_{01}^2, \\ C_1^s & \longrightarrow \eta_{01}^2 + \eta_1^1 + \eta_1^2, \\ C_0^t & \longrightarrow \eta_0^0, \\ C_1^t & \longrightarrow \eta_0^{12} + \eta_1^1, \\ C_2^t & \longrightarrow \eta_0^{12} + 2\eta_{01}^2 + \eta_1^2. \end{cases} \quad (6.24)$$

We observe that we had the same fiber earlier in the resolution III of the $I_2^s + I_3^s$ -model in codimension-three with a condition $a_1 = 0$.

In order to get the weights of the curves, the intersection numbers are computed between the codimension-two curves and the fibral divisors.

	D_0^s	D_1^s	D_0^t	D_1^t	D_2^t	Weight	Representation
η_0^0	0	0	-2	1	1	[0;-1,-1]	(1, 8)
η_0^{12}	-1	1	1	-1	0	[-1;1,0]	(2, 3)
η_1^1	1	-1	0	-1	1	[1;1,-1]	(2, 3)
η_{01}^2	0	0	0	1	-1	[0;-1,1]	(1, 3)
η_1^2	1	-1	0	0	0	[1;0,0]	(2, 1)

Table 13: Weights of vertical curves and representations in the resolution III of the III+IV^s-model at the III+IV^s collision.

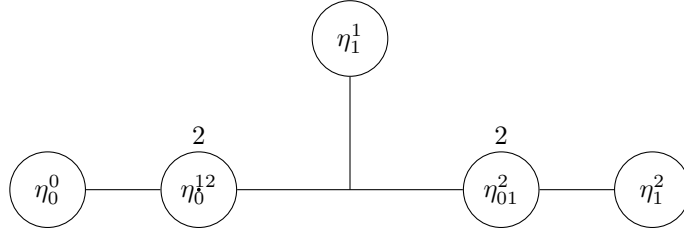


Figure 20: Fiber over the generic point of the locus $S \cap T$ in Resolution III of the III+IV^s-model.

The sum of the two curves $\eta_0^{12} + \eta_{01}^2$ produce the weight $[-1; 0, 1]$ of the representation (**2, $\bar{3}$**). Moreover, the sum of $\eta_{01}^2 + \eta_1^2$ produce the weight $[1; -1, 1]$, which corresponds to a representation (**2, 3**). In the case of the resolution III of the $\mathbb{I}_2^s + \mathbb{I}_3^s$ -model, the former sum corresponds to η_0^2 and the latter sum corresponds to η_1^2 in codimension-two.

Over $S \cap T \cap V(\tilde{a}_3)$ the curve η_1^2 splits as:

$$\text{on } S \cap T \cap V(\tilde{a}_3) : \begin{cases} \eta_1^1 \longrightarrow \eta_1^{12}, \\ \eta_1^2 \longrightarrow \eta_1^{12} + \eta_1^2, \end{cases} \quad (6.25)$$

where the new curves are given by

$$\begin{cases} \eta_1^{12} : & e_1 = w_1 = w_2 = 0, \\ \eta_1^2 : & e_1 = w_2 = \tilde{a}_4 x + \tilde{a}_6 st = 0. \end{cases} \quad (6.26)$$

This corresponds to the codimension-three enhancement in Figure 21.

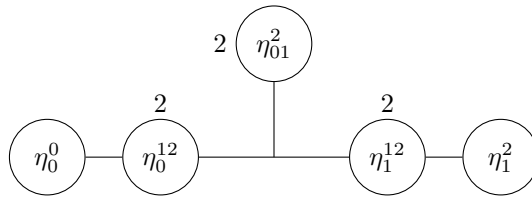


Figure 21: Fiber over the generic point of the locus $S \cap T \cap V(\tilde{a}_3)$ in Resolution III of the III+IV^s-model.

6.4 Resolution IV

The Resolution IV is defined by the following sequence of blowups

$$X_0 \xleftarrow{(x, y, t|w_1)} X_1 \xleftarrow{(y, w_1|w_2)} X_2 \xleftarrow{(x, y, s|e_1)} X_3. \quad (6.27)$$

Its projective coordinates are then given by

$$[e_1 w_1 w_2 x; e_1 w_1 w_2^2 y; z = 1][e_1 x; e_1 w_2 y; t][e_1 y; w_1][x; y; s]. \quad (6.28)$$

The proper transform is identical to equation (6.3).

Over the generic point of the intersection of S and T , we see the following irreducible vertical curves.

$$\text{On } S \cap T: \begin{cases} C_0^s \cap C_0^t & \longrightarrow \eta_0^0 : s = t = w_2 y^2 - w_1 e_1 x^3 = 0, \\ C_0^s \cap C_1^t & \longrightarrow \eta_0^{12} : s = w_1 = w_2 = 0, \\ C_0^s \cap C_2^t & \longrightarrow \eta_0^{2A} : s = w_2 = x = 0, \eta_{01}^2 : s = w_2 = e_1 = 0, \eta_0^{12} : s = w_2 = w_1 = 0 \\ C_1^s \cap C_2^t & \longrightarrow \eta_{01}^2 : e_1 = w_2 = s = 0, \eta_1^2 : e_1 = w_2 = \tilde{a}_3 y - t w_1 (\tilde{a}_4 x + \tilde{a}_6 s t) = 0. \end{cases} \quad (6.29)$$

The collision gives the following splitting of curves from the fiber III and IV^s resulting in the fiber illustrated in Figure 22:

$$\text{On } S \cap T: \begin{cases} C_0^s & \longrightarrow \eta_0^0 + 2\eta_0^{12} + 3\eta_0^{2A} + \eta_{01}^2, \\ C_1^s & \longrightarrow \eta_{01}^2 + \eta_1^2, \\ C_0^t & \longrightarrow \eta_0^0, \\ C_1^t & \longrightarrow \eta_0^{12}, \\ C_2^t & \longrightarrow \eta_0^{12} + 3\eta_0^{2A} + 2\eta_{01}^2 + \eta_1^2. \end{cases} \quad (6.30)$$

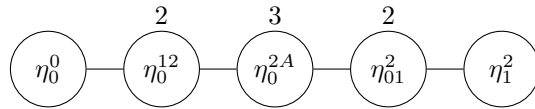


Figure 22: Fiber over the generic point of the locus $S \cap T$ in Resolution IV of the III+IV^s-model.

Note that we had the same fiber earlier in the resolution III of the $I_2^s + I_3^s$ -model in codimension-three with a condition $a_1 = 0$.

The weights of these vertical curves and the corresponding representations are collected in Table 14. In order to get the weights of the curves, the intersection numbers are computed between the codimension-two curves and the fibral divisors.

The sum of the three curves $\eta_1^{02} + \eta_{01}^2 + \eta_1^2$ produce the weight $[1; -1, 1]$, which yields a representation **(2, 3)**. In the case of the resolution IV of the $I_2^s + I_3^s$ -model, the sum of the curves corresponds to η_1^2 in codimension-two, which splits into the three curves in codimension-three.

	D_0^s	D_1^s	D_0^t	D_1^t	D_2^t	Weight	Representation
η_0^0	0	0	-2	1	1	$[0;-1,-1]$	$(\mathbf{1}, \mathbf{8})$
η_0^{12}	0	0	1	-2	1	$[0;2,-1]$	$(\mathbf{1}, \mathbf{8})$
η_0^{2A}	-1	1	0	1	-1	$[-1;-1,1]$	$(\mathbf{2}, \mathbf{3})$
η_{01}^2	1	-1	0	0	0	$[1;0,0]$	$(\mathbf{2}, \mathbf{1})$
η_1^2	1	-1	0	0	0	$[1;0,0]$	$(\mathbf{2}, \mathbf{1})$

Table 14: Weights of vertical curves and representations in the resolution IV of the III+IV^s.

The fiber specialize further over $S \cap T \cap V(\tilde{a}_3)$ as the curve η_1^2 becomes

$$\text{on } S \cap T \cap V(\tilde{a}_3) : \eta_1^2 \rightarrow \eta_1^2 : e_1 = w_2 = \tilde{a}_4 x + \tilde{a}_6 st = 0. \quad (6.31)$$

What is now different from other points of $S \cap T$ is that the curve η_1^2 now intersect both η_{01}^2 and η_0^{2A} at the same point resulting in a different fiber structure represented in Figure 23.

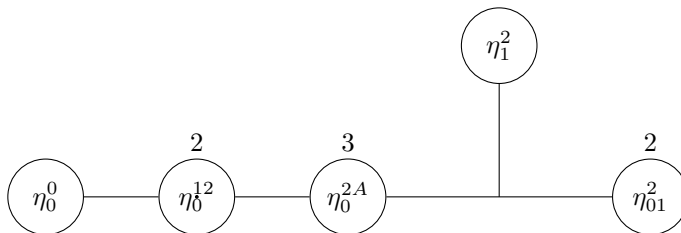


Figure 23: Fiber over the generic point of the locus $S \cap T \cap V(\tilde{a}_3)$ in Resolution IV of the III+IV^s-model.

7 $5d$ and $6d$ supergravity theories with eight supercharges

In this section, we discuss the five and six-dimensional theories with eight supercharges via Calabi–Yau compactification of M-theory and F-theory on an $SU(2) \times SU(3)$ -model. We first compute the one-loop prepotentials of the $SU(2) \times SU(3)$ -model in all eight chambers and match them with the triple intersection numbers of the corresponding crepant resolutions to get the number of charged hypermultiplets in each irreducible representations (fundamentals, adjoints, and bifundamental) in Section 7.1. We then describe in Section 7.2 how the anomaly cancellation conditions in six-dimensional theory with a gauge group can be derived with geometric data with number of charged hypermultiplets as the unknowns. We return to our case for the gauge group $SU(2) \times SU(3)$ in Section 7.3 and show that we get a unique solution of number of hyps for the six-dimensional theory and find it to match with the result we got for the five-dimensional theory in Section 7.1.

7.1 $5d$ $\mathcal{N} = 1$ supergravity theory with a gauge group $SU(2) \times SU(3)$

M-theory (an eleven-dimensional supergravity theory) compactified on a Calabi–Yau threefold yields a low energy physics that describes five-dimensional $\mathcal{N} = 1$ supergravity. The field content

and interactions of such a 5d theory are determined by the topology and intersection ring of the Calabi–Yau threefold [15, 39]. When the Calabi–Yau threefold is a G -model, the resulting five-dimensional supergravity has a gauge group G .

In the Coulomb phase of an $\mathcal{N} = 1$ supergravity theory in five-dimensional spacetime, the scalar fields of the vector multiplets are restricted to the Cartan sub-algebra of the Lie group as the Lie group is broken to $U(1)^r$ where r is the rank of the group. It follows that the charge of a hypermultiplet is simply given by a weight of the representation under which it transforms. When the representation has zero weights, only the hypermultiplets charged by non-zero weights are considered charged hypermultiplets. Let ϕ be in the Cartan subalgebra of a Lie algebra \mathfrak{g} . The one-loop prepotential obtained by integrating out the charged hypermultiplets is [47]

$$6\mathcal{F}_{\text{IMS}} = \frac{1}{2} \left(\sum_{\alpha} |\langle \alpha, \phi \rangle|^3 - \sum_i \sum_{\varpi \in \mathbf{R}_i} n_{\mathbf{R}_i} |\langle \varpi, \phi \rangle|^3 \right), \quad (7.1)$$

where α are the simple roots, \mathbf{R}_i are the irreducible representations of the gauge group, ϖ are the weights of \mathbf{R}_i . This one-loop prepotential is the quantum contribution to the prepotential of a five-dimensional gauge theory with the matter fields in the representations of the gauge group. The prepotential depends on the choice of a Coulomb chamber to get rid of the absolute values. We compute it for each of the eight chambers of an $SU(2) \times SU(3)$ -model. The chambers are defined by Table 5.

Theorem 7.1. *The prepotential of an $SU(2) \times SU(3)$ -model in the eight phases defined by the chambers of Table 5 are*

- Chamber 1

$$\begin{aligned} 6\mathcal{F}_{\text{IMS}}^{(1)} = & -8(n_{1,8} - 1)\phi_1^3 - \frac{3}{2}(n_{1,3} + n_{1,\bar{3}} - 2n_{1,8} + 2)\phi_1^2\phi_2 \\ & + \frac{3}{2}(n_{1,3} + n_{1,\bar{3}} + 2n_{1,8} - 2)\phi_1\phi_2^2 + (-n_{1,3} - n_{1,\bar{3}} - 8n_{1,8} + 8)\phi_2^3 \\ & - (n_{2,1} + 3n_{2,3} + 3n_{2,\bar{3}} + 8n_{3,1} - 8)\psi_1^3 - 6(n_{2,3} + n_{2,\bar{3}})\psi_1(\phi_1^2 - \phi_1\phi_2 + \phi_2^2) \end{aligned}$$

- Chamber 2

$$\begin{aligned} 6\mathcal{F}_{\text{IMS}}^{(2)} = & -8(n_{1,8} - 1)\phi_1^3 - \frac{3}{2}(n_{1,3} + n_{1,\bar{3}} - 2n_{1,8} + 2)\phi_1^2\phi_2 + \frac{3}{2}(n_{1,3} + n_{1,\bar{3}} + 2n_{1,8} - 2)\phi_1\phi_2^2 \\ & - (n_{1,3} + n_{1,\bar{3}} + 8n_{1,8} + n_{2,3} + n_{2,\bar{3}} - 8)\phi_2^3 - (n_{2,1} + 2(n_{2,3} + n_{2,\bar{3}} + 4n_{3,1} - 4))\psi_1^3 \\ & - 3(n_{2,3} + n_{2,\bar{3}})\psi_1^2\phi_2 - 3(n_{2,3} + n_{2,\bar{3}})\psi_1(2\phi_1^2 - 2\phi_1\phi_2 + \phi_2^2) \end{aligned}$$

- Chamber 3

$$\begin{aligned} 6\mathcal{F}_{\text{IMS}}^{(3)} = & -(8n_{1,8} + n_{2,3} + n_{2,\bar{3}} - 8)\phi_1^3 - \frac{3}{2}(n_{1,3} + n_{1,\bar{3}} - 2n_{1,8} + 2)\phi_1^2\phi_2 \\ & + \frac{3}{2}(n_{1,3} + n_{1,\bar{3}} + 2n_{1,8} - 2)\phi_1\phi_2^2 + (-n_{1,3} - n_{1,\bar{3}} - 8n_{1,8} - n_{2,3} - n_{2,\bar{3}} + 8)\phi_2^3 \\ & + (-n_{2,1} - n_{2,3} - n_{2,\bar{3}} - 8n_{3,1} + 8)\psi_1^3 - 3(n_{2,3} + n_{2,\bar{3}})\psi_1^2(\phi_1 + \phi_2) \\ & - 3(n_{2,3} + n_{2,\bar{3}})\psi_1(\phi_1^2 - 2\phi_1\phi_2 + \phi_2^2) \end{aligned}$$

- Chamber 4

$$\begin{aligned}
6\mathcal{F}_{IMS}^{(4)} &= -8(n_{1,8} - 1)\phi_1^3 - \frac{3}{2}(n_{1,3} + n_{1,\bar{3}} - 2n_{1,8} + 2n_{2,3} + 2n_{2,\bar{3}} + 2)\phi_1^2\phi_2 \\
&\quad + \frac{3}{2}(n_{1,3} + n_{1,\bar{3}} + 2n_{1,8} + 2n_{2,3} + 2n_{2,\bar{3}} - 2)\phi_1\phi_2^2 \\
&\quad - (n_{1,3} + n_{1,\bar{3}} + 8n_{1,8} + 2n_{2,3} + 2n_{2,\bar{3}} - 8)\phi_2^3 \\
&\quad - (n_{2,1} + 8n_{3,1} - 8)\psi_1^3 - 6(n_{2,3} + n_{2,\bar{3}})\psi_1^2\phi_2
\end{aligned}$$

The prepotential $\mathcal{F}_{IMS}^{(i)}$ (for $i = 1, 2, 3, 4$) is obtained from $\mathcal{F}_{IMS}^{(i)}$ by the involution $\phi_1 \leftrightarrow \phi_2$.

Proof. Direct computation starting with equation (7.1) and using Table 5 to remove the absolute values. \square

Following [37], the number of hypermultiplets are computed by comparing the prepotential and the triple intersection polynomial given in Theorem 3.11. Comparing the triple intersection numbers obtained in the resolutions I, II, III, IV with the prepotentials computed respectively in chambers 1, 2, 3, 4, we get

$$\begin{aligned}
n_{2,1} + 8n_{3,1} &= 4LS + 2S^2 - 3ST + 8, & n_{1,8} &= \frac{1}{2}(-LT + T^2 + 2), \\
n_{2,3} + n_{2,\bar{3}} &= ST, & n_{1,3} + n_{1,\bar{3}} &= T(9L - 2S - 3T).
\end{aligned} \tag{7.2}$$

We see in particular that the numbers $n_{2,1}$ and $n_{3,1}$ are restricted by a linear relation but are not fixed by this method. In the case of Calabi–Yau threefolds, the vanishing of the first Chern class yields $K = -L$ where K is the canonical class of the base B . Using Witten’s genus formula [79], we get

$$n_{2,1} = -S(8K + 2S + 3T), \quad n_{3,1} = \frac{1}{2}(KS + S^2 + 2). \tag{7.3}$$

We notice that the number of (bi)fundamental matter is compatible with what is expected from the technique of intersecting branes, and when the threefold is Calabi–Yau, $K = -L$ and $n_{1,8}$ becomes the arithmetic genus of the curve T as expected from Witten’s genus formula.

7.2 Anomaly cancellations in general $6d \mathcal{N} = (1, 0)$ supergravity theory

F-theory compactified on a Calabi–Yau threefold gives a six-dimensional supergravity theory with eight supercharges coupled to n_V vector, n_T tensor, and n_H^0 neutral hypermultiplets [67]. When the Calabi–Yau variety is elliptically-fibered with a gauge group G and a representation \mathbf{R} [44, 69, 71],

- the number of vectors: $n_V = \dim G$,
- the number of tensors: $n_T = 9 - K^2$,
- the number of hypers: $n_H = n_H^0 + n_H^{ch}$ with neutral hypers $n_H^0 = h^{2,1} + 1$,

where K is the canonical class of the base $Bstg$ of the elliptic fibration, and we have charged hypermultiplets transforming in the representation \mathbf{R} of G . We consider the semisimple gauge group with simple components G_a such that $G = \sum_a G_a$.

Six-dimensional $\mathcal{N} = (1, 0)$ gauge theories can suffer from anomalies. We only care about local anomalies: pure gravitational anomalies, pure gauge anomalies, and mixed gravitational and gauge anomalies [44, 69, 71]. An effective way to address these anomalies are via using Green-Schwarz mechanism in six-dimensions [45, 72, 73]. The anomaly polynomial I_8 has a pure gravitational contribution from the term proportional to the $\mathbf{tr}R^4$, which is given by $\propto (n_H - n_V^{(6)} + 29n_T - 273)\mathbf{tr}R^4$, where R is the Riemann tensor thought of as a 6×6 real matrix of two-form values. In order to have vanishing gravitational anomalies, the coefficient of $\mathbf{tr}R^4$ has to vanish [70]:

$$n_H - n_V^{(6)} + 29n_T - 273 = 0. \quad (7.4)$$

The remainder terms of the anomaly polynomial I_8 is given by [44, 69, 71]

$$I_8 = \frac{K^2}{8}(\mathbf{tr}R^2)^2 + \frac{1}{6}\sum_a X_a^{(2)}\mathbf{tr}R^2 - \frac{2}{3}\sum_a X_a^{(4)} + 4\sum_{a<b} Y_{ab}, \quad (7.5)$$

where contributions from each simple gauge component $X_a^{(n)}$ for $n = 2, 4$ and the mixed contribution Y_{ab} are given by [44, 69, 71]

$$X_a^{(n)} = \mathbf{tr}_{\mathbf{adj}} F_a^n - \sum_i n_{\mathbf{R}_{i,a}} \mathbf{tr}_{\mathbf{R}_{i,a}} F_a^n, \quad Y_{ab} = \sum_{i,j} n_{\mathbf{R}_{i,a}, \mathbf{R}_{j,b}} \mathbf{tr}_{\mathbf{R}_{i,a}} F_a^2 \mathbf{tr}_{\mathbf{R}_{j,b}} F_b^2, \quad (7.6)$$

where $n_{\mathbf{R}_{i,a}, \mathbf{R}_{j,b}}$ is the number of hypermultiplets transforming in the representation $(\mathbf{R}_{i,a}, \mathbf{R}_{j,b})$ of the gauge group $G_a \times G_b$. Note that the mixed term by computing all possible pairs of the simple components of the gauge groups which are denoted by two indices.

It is important to note that when a representation is charged on both simple components of the group, it affects not only Y_{ab} but also $X_a^{(2)}$ and $X_a^{(4)}$. Consider a representation $(\mathbf{R}_1, \mathbf{R}_2)$ for of a semisimple group with two simple components $G = G_1 \times G_2$, where \mathbf{R}_a is a representation of G_a . Then this representation contributes $\dim \mathbf{R}_2$ times to $n_{\mathbf{R}_1}$, and contributes $\dim \mathbf{R}_1$ times to $n_{\mathbf{R}_2}$:

$$n_{\mathbf{R}_1} = \dots + \dim \mathbf{R}_2 n_{\mathbf{R}_1, \mathbf{R}_2}, \quad n_{\mathbf{R}_2} = \dots + \dim \mathbf{R}_1 n_{\mathbf{R}_1, \mathbf{R}_2}. \quad (7.7)$$

Since the hypermultiplets of zero weights are neutral, we have to remove the neutral hypermultiplet contributions to get the charged dimension of the hypermultiplets in each irreducible representation. By denoting the zero weights of a representation \mathbf{R}_i as $\mathbf{R}_i^{(0)}$, the charged dimension of the hypermultiplets in representation \mathbf{R}_i is given by [44]

$$\dim \mathbf{R}_i - \dim \mathbf{R}_i^{(0)}.$$

For a representation \mathbf{R}_i , $n_{\mathbf{R}_i}$ denotes the multiplicity of the representation \mathbf{R}_i . Then the number of charged hypermultiplets is given by [44]

$$n_H^{ch} = \sum_i n_{\mathbf{R}_i} (\dim \mathbf{R}_i - \dim \mathbf{R}_i^{(0)}). \quad (7.8)$$

The trace identities for a representation $\mathbf{R}_{i,a}$ of a simple group G_a are

$$\mathbf{tr}_{\mathbf{R}_{i,a}} F_a^2 = A_{\mathbf{R}_{i,a}} \mathbf{tr}_{\mathbf{F}_a} F_a^2, \quad \mathbf{tr}_{\mathbf{R}_{i,a}} F_a^4 = B_{\mathbf{R}_{i,a}} \mathbf{tr}_{\mathbf{F}_a} F_a^4 + C_{\mathbf{R}_{i,a}} (\mathbf{tr}_{\mathbf{F}_a} F_a^2)^2 \quad (7.9)$$

with respect to a reference representation \mathbf{F}_a for each simple component G_a of the gauge group.⁵ The coefficients $A_{\mathbf{R}_{i,a}}$, $B_{\mathbf{R}_{i,a}}$, and $C_{\mathbf{R}_{i,a}}$ depends on the gauge groups and are listed in [7, 38, 78].

⁵We denoted this representation as \mathbf{F}_a as we picked the fundamental representations for convenience. However, any representation can be used as a reference representation.

Then we can write the gauge contribution terms with respect to the coefficients from the trace identities:

$$X_a^{(2)} = \left(A_{a,\text{adj}} - \sum_i n_{\mathbf{R}_{i,a}} A_{\mathbf{R}_{i,a}} \right) \text{tr}_{\mathbf{F}_a} F_a^2, \quad (7.10)$$

$$X_a^{(4)} = \left(B_{a,\text{adj}} - \sum_i n_{\mathbf{R}_{i,a}} B_{\mathbf{R}_{i,a}} \right) \text{tr}_{\mathbf{F}_a} F_a^4 + \left(C_{a,\text{adj}} - \sum_i n_{\mathbf{R}_{i,a}} C_{\mathbf{R}_{i,a}} \right) (\text{tr}_{\mathbf{F}_a} F_a^2)^2, \quad (7.11)$$

$$Y_{ab} = \sum_{i,j} n_{\mathbf{R}_{i,a}, \mathbf{R}_{j,b}} A_{\mathbf{R}_{i,a}} A_{\mathbf{R}_{j,b}} \text{tr}_{\mathbf{F}_a} F_a^2 \text{tr}_{\mathbf{F}_b} F_b^2, \quad (a \neq b). \quad (7.12)$$

For each simple component G_a , the anomaly polynomial I_8 has a pure gauge contribution proportional to the quartic term $\text{tr} F_a^4$, which is contained in equation (7.11). In order to have a vanishing pure gauge anomalies, the coefficients of these terms have to vanish:

$$B_{a,\text{adj}} - \sum_i n_{\mathbf{R}_{i,a}} B_{\mathbf{R}_{i,a}} = 0.$$

When the coefficients of all quartic terms ($\text{tr} R^4$ and $\text{tr} F_a^4$) vanish, the remaining part of the anomaly polynomial I_8 is

$$\left\{ \begin{array}{l} I_8 = \frac{K^2}{8} (\text{tr} R^2)^2 + \frac{1}{6} \sum_a X_a^{(2)} \text{tr} R^2 - \frac{2}{3} \sum_a X_a^{(4)} + 4 \sum_{a < b} Y_{ab}, \\ X_a^{(2)} = \left(A_{a,\text{adj}} - \sum_i n_{\mathbf{R}_{i,a}} A_{\mathbf{R}_{i,a}} \right) \text{tr}_{\mathbf{F}_a} F_a^2, \quad X_a^{(4)} = \left(C_{a,\text{adj}} - \sum_i n_{\mathbf{R}_{i,a}} C_{\mathbf{R}_{i,a}} \right) (\text{tr}_{\mathbf{F}_a} F_a^2)^2, \\ Y_{ab} = \sum_{i,j} n_{\mathbf{R}_{i,a}, \mathbf{R}_{j,b}} A_{\mathbf{R}_{i,a}} A_{\mathbf{R}_{j,b}} \text{tr}_{\mathbf{F}_a} F_a^2 \text{tr}_{\mathbf{F}_b} F_b^2, \quad (a \neq b). \end{array} \right. \quad (7.13)$$

The anomalies are canceled by the Green-Schwarz mechanism when I_8 factorizes [45, 72, 73]. The modification of the field strength H of the antisymmetric tensor B is

$$H = dB + \frac{1}{2} K \omega_{3L} + 2 \sum_a \frac{S_a}{\lambda_a} \omega_{a,3Y}, \quad (7.14)$$

where ω_{3L} and $\omega_{a,3Y}$ are respectively the gravitational Yang–Mills and Chern–Simons terms. If I_8 factors as

$$I_8 = X \cdot X, \quad X = \frac{1}{2} K \text{tr} R^2 + \sum_a \frac{2}{\lambda_a} S_a \text{tr} F_a^2, \quad (7.15)$$

where the λ_a are normalization factors chosen such that the smallest topological charge of an embedded $SU(2)$ instanton in G_a is one [10, 58, 69]. This forces λ_a to be the Dynkin index of the fundamental representation of G_a as summarized in Table 15 [69].

\mathfrak{g}	A_n	B_n	C_n	D_n	E_8	E_7	E_6	F_4	G_2
λ	1	2	1	2	60	12	6	6	2

Table 15: The normalization factors for each simple gauge algebra. See [58].

When I_8 factors, the anomaly is canceled by adding the following Green-Schwarz counter-term

$$\Delta L_{GS} \propto \frac{1}{2} B \wedge X, \quad (7.16)$$

which implies that X carries string charges.

With all the local anomaly cancellation conditions in six-dimensions investigated, we can coalesce as the set of equations with number of charged hypermultiplets in each irreducible representations as unknowns. If the simple group G_a is supported on a divisor S_a , the local anomaly cancellation conditions are the following equations [44, 69, 71]:

$$n_T = 9 - K^2, \quad (7.17a)$$

$$n_H - n_V^{(6)} + 29n_T - 273 = 0, \quad (7.17b)$$

$$\left(B_{a,\text{adj}} - \sum_i n_{\mathbf{R}_{i,a}} B_{\mathbf{R}_{i,a}} \right) = 0, \quad (7.17c)$$

$$\lambda_a \left(A_{a,\text{adj}} - \sum_i n_{\mathbf{R}_{i,a}} A_{\mathbf{R}_{i,a}} \right) = 6K \cdot S_a, \quad (7.17d)$$

$$\lambda_a^2 \left(C_{a,\text{adj}} - \sum_i n_{\mathbf{R}_{i,a}} C_{\mathbf{R}_{i,a}} \right) = -3S_a^2, \quad (7.17e)$$

$$\lambda_a \lambda_b \sum_{i,j} n_{\mathbf{R}_{i,a}, \mathbf{R}_{j,b}} A_{\mathbf{R}_{i,a}} A_{\mathbf{R}_{j,b}} = S_a \cdot S_b, \quad (a \neq b). \quad (7.17f)$$

Assuming the first three equations hold, cancelling the anomalies is equivalent to factoring the anomaly polynomial [44, 69, 71]

$$I_8 = \frac{K^2}{8} (\text{tr} R^2)^2 + \frac{1}{6} (X_1^{(2)} + X_2^{(2)}) \text{tr} R^2 - \frac{2}{3} (X_1^{(4)} + X_2^{(4)}) + 4Y_{12}. \quad (7.18)$$

To summarize, for a compactification on an elliptically-fibered Calabi–Yau threefold Y , the number of multiplets is [44]

$$n_V^{(6)} = \dim G, \quad n_T = h^{1,1}(B) - 1 = 9 - K^2, \quad (7.19a)$$

$$n_H = n_H^0 + n_H^{ch} = h^{2,1}(Y) + 1 + \sum_i n_{\mathbf{R}_i} \left(\dim \mathbf{R}_i - \dim \mathbf{R}_i^{(0)} \right), \quad (7.19b)$$

where $n_{\mathbf{R}_i}$ is a number of hypermultiplets charged under each irreducible representation \mathbf{R}_i that satisfies equations (7.17).

7.3 Anomaly cancellations in $6d \mathcal{N} = (1, 0)$ supergravity theory

In this section, we check that the gravitational, gauge, and mixed gravitational-gauge anomalies of the six-dimensional supergravity are all canceled when the Lie algebra and the representation are

$$\mathfrak{g} = A_1 \oplus A_2, \quad \mathbf{R} = (\mathbf{2}, \mathbf{1}) \oplus (\mathbf{1}, \mathbf{3}) \oplus (\mathbf{1}, \bar{\mathbf{3}}) \oplus (\mathbf{2}, \mathbf{3}) \oplus (\mathbf{2}, \bar{\mathbf{3}}) \oplus (\mathbf{3}, \mathbf{1}) \oplus (\mathbf{1}, \mathbf{8}).$$

We follow the approach of Sadov [71] (see also [44] and [64]) and use the notation of [31]. The six-dimensional anomaly cancellation conditions put linear constraints on the number of charged hypermultiplets transforming in each irreducible representations.

First, we recall that the Euler characteristic of a Calabi–Yau threefold defined as a crepant resolution of the Weierstrass model of an $SU(2) \times SU(3)$ -model is

$$\chi(Y) = -6(10K^2 + 5KS + 8KT + S^2 + 2ST + 2T^2), \quad (7.20)$$

where S supports A_1 and T supports A_2 . We also assume that S and T are smooth divisors intersecting transversally.

We will use the anomaly cancellation conditions to explicitly compute the number of hypermultiplets transforming in each representation by requiring all anomalies to cancel. We will see that they are the same as those found in five-dimensional supergravity by comparing the triple intersection numbers of the fibral divisors and the cubic prepotentials in the Coulomb phase.

The Lie algebra of type A_1 (resp. A_2) only has a unique quartic Casimir invariant so that we don't have to impose the vanishing condition for the coefficients of $\text{tr } F_1^4$ (resp. $\text{tr } F_2^4$). We have the following trace identities

$$\text{tr}_3 F_1^2 = 4\text{tr}_2 F_2^2, \quad \text{tr}_3 F_1^4 = 8(\text{tr}_3 F_1^2)^2, \quad \text{tr}_2 F_1^4 = \frac{1}{2}(\text{tr}_2 F_1^2)^2, \quad (7.21)$$

$$\text{tr}_8 F_2^2 = 6\text{tr}_3 F_2^2, \quad \text{tr}_8 F_2^4 = 9(\text{tr}_3 F_2^2)^2, \quad \text{tr}_3 F_2^4 = \frac{1}{2}(\text{tr}_3 F_2^2)^2, \quad (7.22)$$

which give

$$\begin{aligned} X_1^{(2)} &= (4 - 4n_{3,1} - n_{2,1} - 3n_{2,3} - 3n_{2,\bar{3}}) \text{tr}_2 F_1^2, \\ X_2^{(2)} &= (6 - 6n_{1,8} - n_{1,3} - n_{1,\bar{3}} - 2n_{2,3} - 2n_{2,\bar{3}}) \text{tr}_3 F_2^2, \\ X_1^{(4)} &= (8 - 8n_{3,1} - \frac{1}{2}n_{2,1} - \frac{3}{2}n_{2,3} - \frac{3}{2}n_{2,\bar{3}})(\text{tr}_2 F_1^2)^2, \\ X_2^{(4)} &= (9 - 9n_{1,8} - \frac{1}{2}n_{1,3} - \frac{1}{2}n_{1,\bar{3}} - n_{2,3} - n_{2,\bar{3}})(\text{tr}_3 F_2^2)^2, \\ Y_{23} &= (n_{2,3} + n_{2,\bar{3}}) \text{tr}_3 F_2^2 \text{tr}_2 F_1^2. \end{aligned} \quad (7.23)$$

Following Sadov, the anomaly cancellation conditions are [71]:

$$\begin{aligned} X_1^{(2)} &= 6KS \text{tr}_2 F_1^2, & X_2^{(2)} &= 6KT \text{tr}_3 F_2^2, \\ X_1^{(4)} &= -3S^2(\text{tr}_2 F_1^2)^2, & X_2^{(4)} &= -3T^2(\text{tr}_3 F_2^2)^2, & Y_{23} &= ST \text{tr}_3 F_2^2 \text{tr}_2 F_1^2. \end{aligned} \quad (7.24)$$

Comparing the coefficients, we get the following linear equations

$$\begin{aligned} 6(1 - n_{1,8}) - (n_{1,3} + n_{1,\bar{3}}) - 2(n_{2,3} + n_{2,\bar{3}}) &= 6KT, & 4(1 - n_{3,1}) - n_{2,1} - 3(n_{2,3} + n_{2,\bar{3}}) &= 6KS, \\ 9(1 - n_{1,8}) - \frac{1}{2}(n_{1,3} + n_{1,\bar{3}}) - (n_{2,3} + n_{2,\bar{3}}) &= -3T^2, & 8(1 - n_{3,1}) - \frac{1}{2}n_{2,1} - \frac{3}{2}(n_{2,3} + n_{2,\bar{3}}) &= -3S^2, \\ n_{2,3} + n_{2,\bar{3}} &= ST. \end{aligned} \quad (7.25)$$

These linear equations have the following unique solution⁶

$$\begin{aligned} n_{1,8} &= \frac{1}{2}(KT + T^2 + 2), & n_{3,1} &= \frac{1}{2}(KS + S^2 + 2), \\ n_{2,1} &= -S(8K + 2S + 3T), & n_{1,3} + n_{1,\bar{3}} &= -T(9K + 2S + 3T), & n_{2,3} + n_{2,\bar{3}} &= ST. \end{aligned} \quad (7.26)$$

These numbers have simple geometric interpretations. The numbers $n_{1,8}$ and $n_{3,1}$ are respectively the genus of the curves T and S . The number $n_{2,3} + n_{2,\bar{3}}$ is the degree of $S \cdot T$ (intersection number

⁶We recall that Witten's genus formula asserts that the number of hypermultiplets charged under the adjoint representation is given by the genus of the curve supporting the corresponding gauge group.

of S and T). The number $n_{\mathbf{2},\mathbf{1}}$ is the intersection number of S and the discriminant of the generic fiber of D_1^s . The number $n_{\mathbf{1},\mathbf{3}} + n_{\mathbf{1},\bar{\mathbf{3}}}$ is the intersection number of T and the discriminant of D_2^t .

From here we can get the numbers of hypermultiplets $n_{\mathbf{2}}$ and $n_{\mathbf{3}} + n_{\bar{\mathbf{3}}}$ tracing back from equation (7.7):

$$n_{\mathbf{2}} = -2(4K + S), \quad n_{\mathbf{3}} + n_{\bar{\mathbf{3}}} = -3T(3K + T). \quad (7.27)$$

We recall that the Hodge numbers of a crepant resolution of an $SU(2) \times SU(3)$ -model are (see Theorem 3.10)

$$h^{1,1}(Y) = 14 - K^2, \quad h^{2,1}(Y) = 29K^2 + 15KS + 24KT + 3S^2 + 6ST + 6T^2 + 14. \quad (7.28)$$

The total number of hypermultiplets is the sum of the number of neutral hypermultiplets ($n_H^0 = h^{2,1}(Y) + 1$) and the number of charged hypermultiplets⁷.

$$n_H^0 = h^{2,1}(Y) + 1 = 29K^2 + 15KS + 24KT + 3S^2 + 6ST + 6T^2 + 15, \quad (7.29)$$

$$n_H^{ch} = 2n_{\mathbf{2},\mathbf{1}} + 6(n_{\mathbf{2},\mathbf{3}} + n_{\mathbf{2},\bar{\mathbf{3}}}) + 3(n_{\mathbf{1},\mathbf{3}} + n_{\mathbf{1},\bar{\mathbf{3}}}) + (8 - 2)n_{\mathbf{1},\mathbf{8}} + (3 - 1)n_{\mathbf{3},\mathbf{1}}. \quad (7.30)$$

Thus, the total number of hypermultiplets is

$$n_H = n_H^0 + n_H^{ch} = 29K^2 + 23. \quad (7.31)$$

The numbers of vector multiplets and tensor multiplets are

$$n_T = 9 - K^2, \quad n_V = \dim G = \dim SU(2) + \dim SU(3) = 3 + 8 = 11. \quad (7.32)$$

We can now check that the coefficient of $\text{tr } R^4$ vanishes [70]:

$$n_H - n_V + 29n_T - 273 = 0. \quad (7.33)$$

Finally, we show that the anomaly polynomial I_8 indeed factors as a perfect square:

$$\begin{aligned} I_8 &= \frac{K^2}{8} (\text{tr } R^2)^2 + \frac{1}{6} (X_1^{(2)} + X_2^{(2)}) \text{tr } R^2 - \frac{2}{3} (X_1^{(4)} + X_2^{(4)}) + 4Y_{\mathbf{23}}, \\ &= \frac{1}{2} \left(\frac{1}{2} K \text{tr } R^2 + 2S \text{tr}_2 F_1^2 + 2T \text{tr}_3 F_2^2 \right)^2. \end{aligned} \quad (7.34)$$

Hence, we conclude that all the local anomalies are canceled via Green-Schwarz mechanism.

The global anomalies for the Standard Model in 4d was discussed in Section 1.1 by examining the fourth homotopy group of $SU(2)$ and $SU(3)$. Similarly, the global anomaly contributions from $SU(2)$ and $SU(3)$ in six-dimensions can be discussed by looking into the sixth homotopy group for $SU(2)$ and $SU(3)$, which are given by \mathbb{Z}_{12} and \mathbb{Z}_6 respectively. Bershadsky and Vafa has shown that this yields the linear constraints on the number of hypermultiplets [13]. In the case of $SU(2)$ and $SU(3)$, we have:

$$\begin{cases} SU(2): & 4 - n_{\mathbf{2}} = 0 \pmod{6}, \\ SU(3): & n_{\mathbf{3}} = 0 \pmod{6}, \end{cases} \quad (7.35)$$

⁷To count the charged hypermultiplets, each irreducible representation \mathbf{R} contributes $\dim^{ch} \mathbf{R} \times n_{\mathbf{R}}$ where $\dim^{ch} \mathbf{R}$ is the number of non-zero weights of the representation \mathbf{R} and $n_{\mathbf{R}}$ is the number of hypermultiplets transforming in the representation \mathbf{R} [44].

where n_2 and n_3 are the number of hypermultiplets transforming in the fundamental representation of $SU(2)$ and $SU(3)$ respectively. Using equation (7.26), we immediately compute geometrically the number of charged hypermultiplets as

$$\begin{cases} n_2 = n_{2,1} + 3(n_{2,3} + n_{2,\bar{3}}) = -16(g(S) - 1) + 6S^2, \\ n_3 = n_{1,3} + n_{1,\bar{3}} + 2(n_{2,3} + n_{2,\bar{3}}) = -18(g(T) - 1) + 6T^2, \end{cases} \quad (7.36)$$

where $g(S)$ and $g(T)$ are the genus of the curves supporting S and T respectively. By using these conditions we find that the global anomalies of $SU(3)$ always vanishes whereas $SU(2)$ global anomaly canceling condition is found to be

$$g(S) = 0 \pmod{3}. \quad (7.37)$$

Acknowledgements

The authors are grateful to Prateek Agrawal, Paolo Aluffi, Patrick Jefferson, Kenji Matsuki, Washington Taylor and Shing-Tung Yau for helpful discussions. M.J.K. would like to thank Korean Institute for Advanced Studies for their hospitality during part of this work. M.E. is supported in part by the National Science Foundation (NSF) grant DMS-1701635 ‘‘Elliptic Fibrations and String Theory’’. M.J.K. is supported by the National Science Foundation (NSF) grant PHY-1352084. R.J. is supported by a National Science Foundation (NSF) Graduate Research Fellowship.

A Fiber enhancement

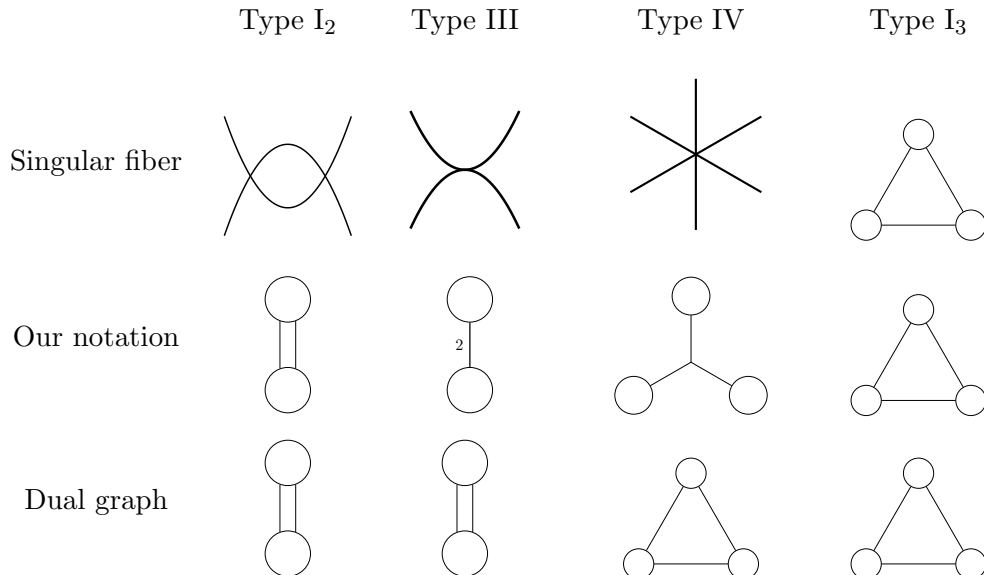


Figure 24: Convention for Kodaira fibers of type I_2 , III, IV, and I_3 .

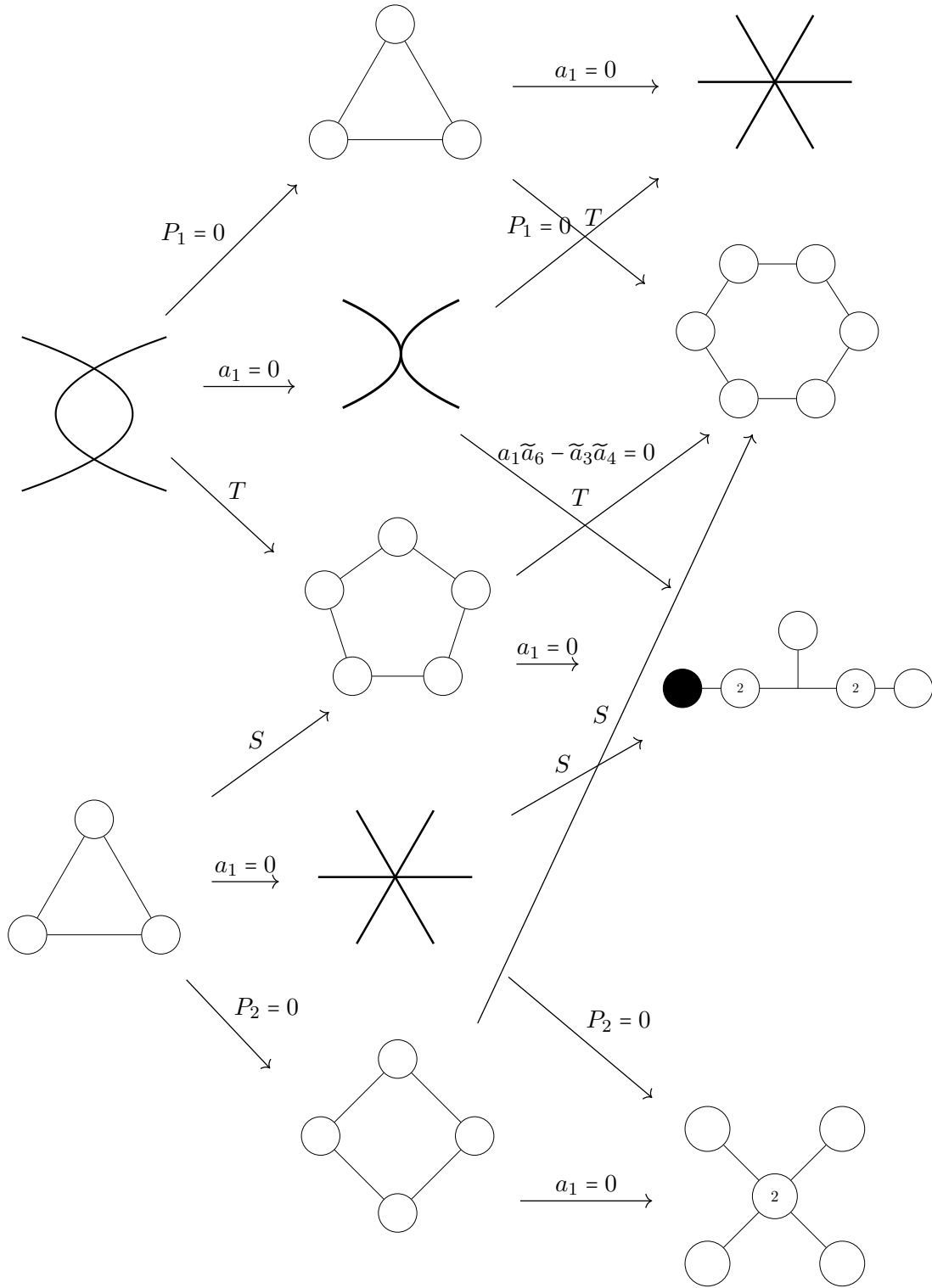


Table 16: $I_2^s + I_3^s$, Resolution I, II, and III. $P_1 = \tilde{a}_4^2 t - a_1^2 \tilde{a}_6$ and $P_2 = \tilde{a}_3^3 s - a_1 \tilde{a}_2 \tilde{a}_3^2 s + a_1^2 \tilde{a}_3 \tilde{a}_4 - a_1^3 \tilde{a}_6$. The non-Kodaira fiber in codimension-three is a contraction of a IV^* .

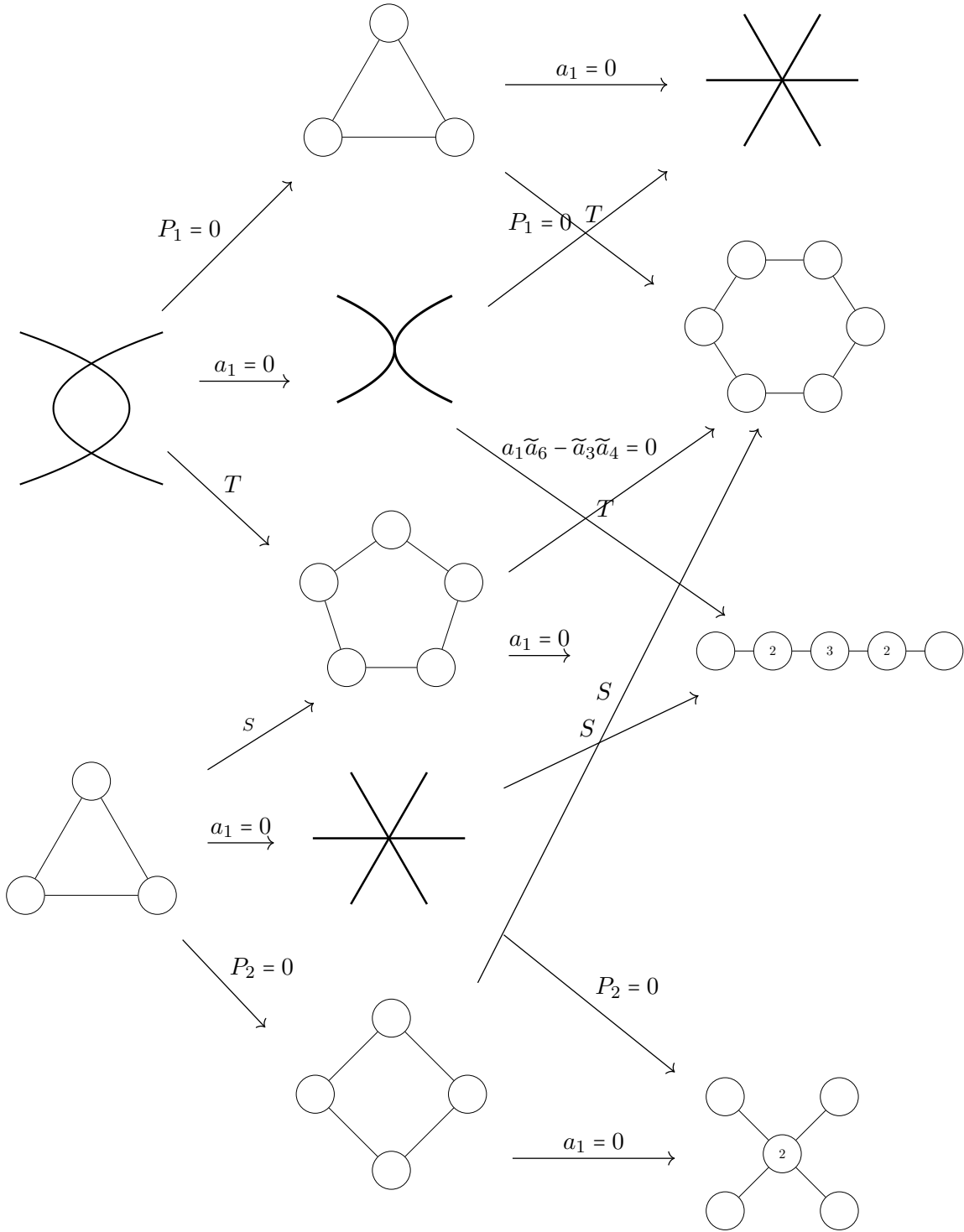


Table 17: $I_2^s + I_3^s$, Resolution IV. $P_1 = \tilde{a}_4^2 t - a_1^2 \tilde{a}_6$ and $P_2 = \tilde{a}_3^3 s - a_1 \tilde{a}_2 \tilde{a}_3^2 s + a_1^2 \tilde{a}_3 \tilde{a}_4 - a_1^3 \tilde{a}_6$. The non-Kodaira fiber is a contracted fiber of type IV*.

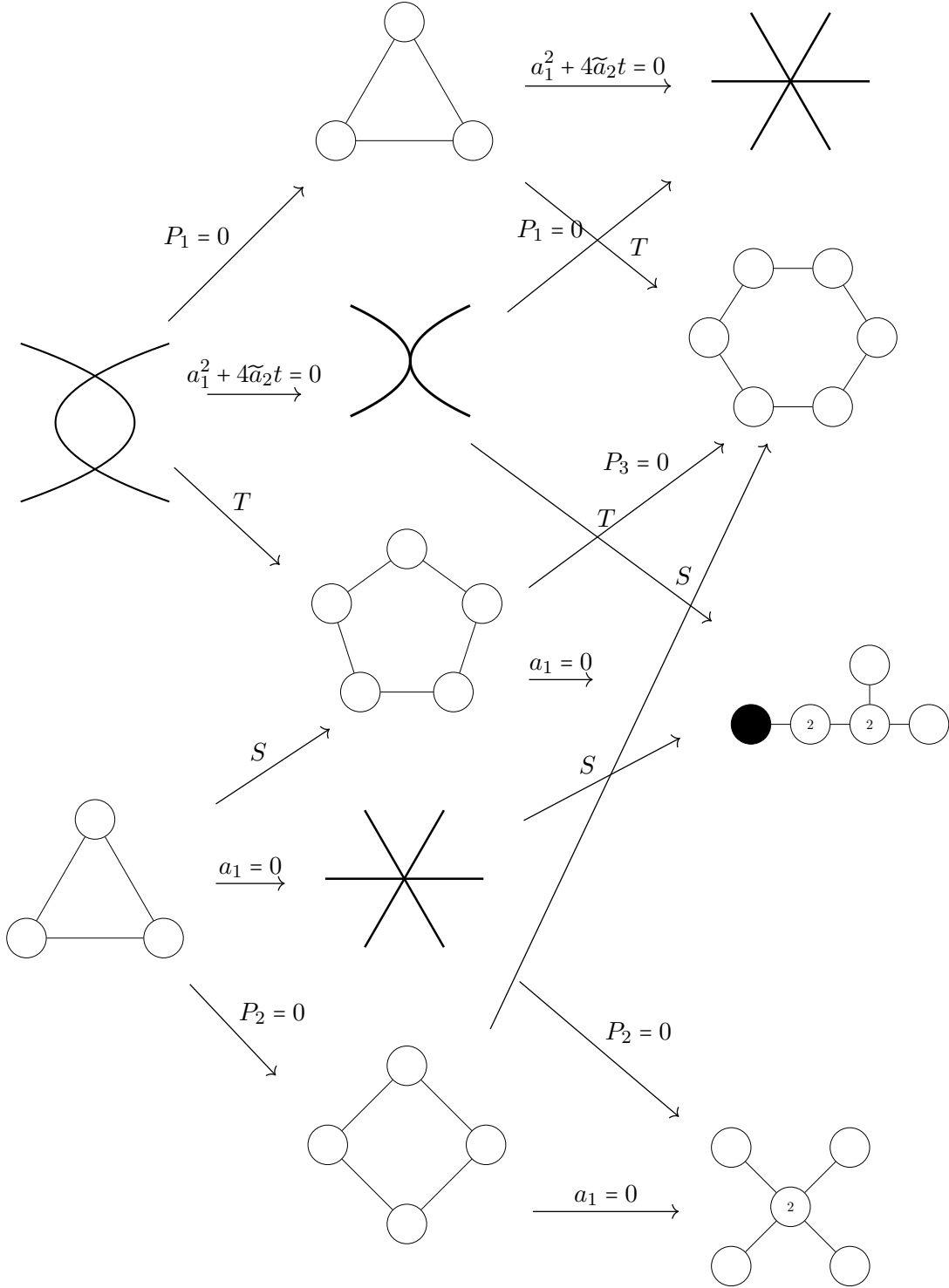


Table 18: $I_2^{\text{ns}} + I_3^{\text{s}}$ Resolution I and IV. $P_1 = -2\tilde{a}_1^2 t + 4\tilde{a}_2 \tilde{a}_6 t + a_1^2 \tilde{a}_6 - 2\tilde{a}_2 \tilde{a}_3^2$, $P_2 = \tilde{a}_3^3 s - a_1 \tilde{a}_2 \tilde{a}_3^2 + a_1^2 \tilde{a}_3 \tilde{a}_4 - a_1^3 \tilde{a}_6$, and $P_3 = \tilde{a}_2 \tilde{a}_3^2 s - a_1 (a_1 \tilde{a}_6 - \tilde{a}_3 \tilde{a}_4)$. The non-Kodaira fiber is a contraction of an I_1^* .

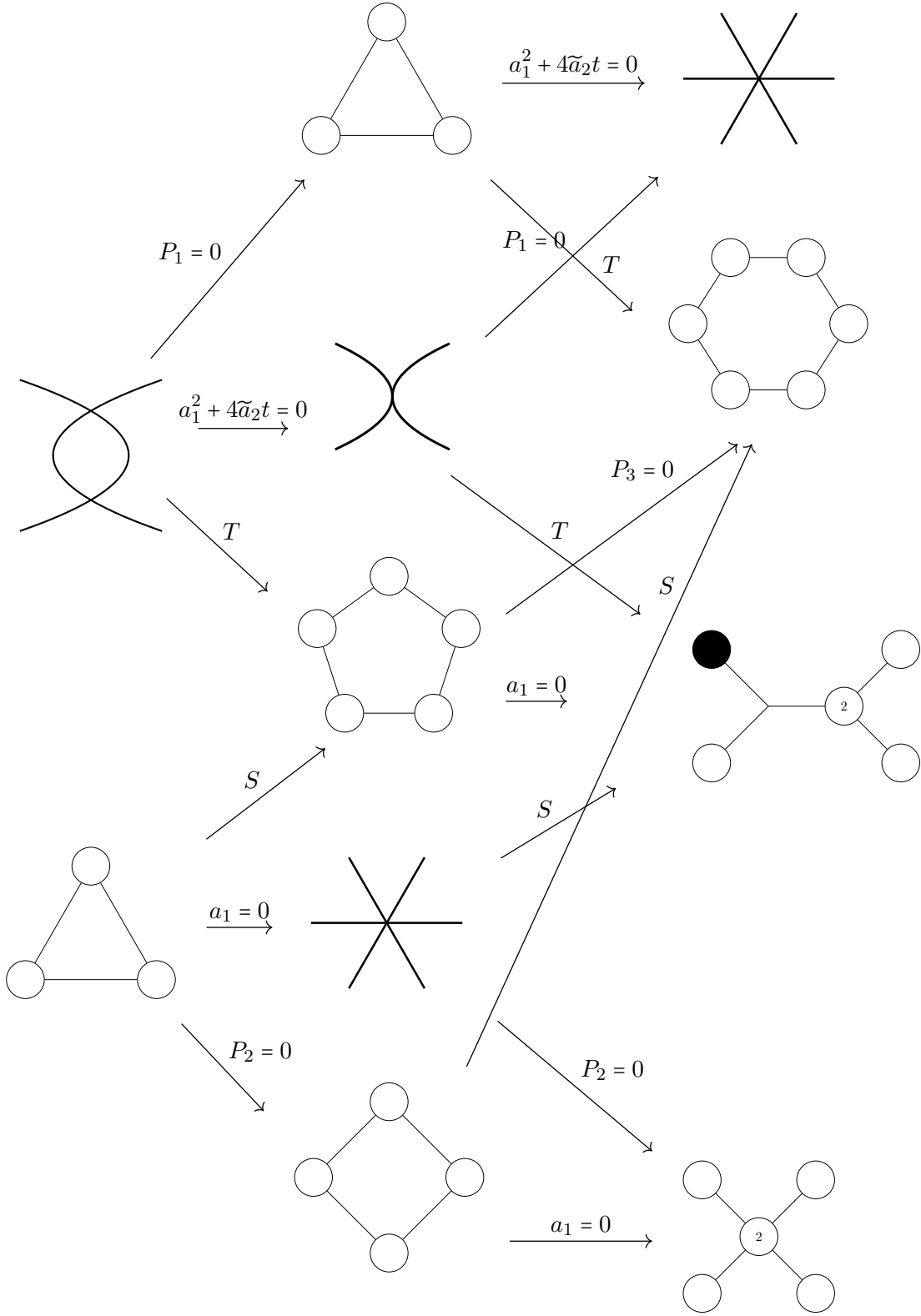


Table 19: $I_2^{\text{ns}} + I_3^{\text{s}}$ Resolution II. $P_1 = -2\tilde{a}_1^2 t + 4\tilde{a}_2 \tilde{a}_6 t + a_1^2 \tilde{a}_6 - 2\tilde{a}_2 \tilde{a}_3^2$, $P_2 = \tilde{a}_3^3 s - a_1 \tilde{a}_2 \tilde{a}_3^2 + a_1^2 \tilde{a}_3 \tilde{a}_4 - a_1^3 \tilde{a}_6$, and $P_3 = \tilde{a}_2 \tilde{a}_3^2 s - a_1 (a_1 \tilde{a}_6 - \tilde{a}_3 \tilde{a}_4)$. The non-Kodaira fiber is a contraction of an I_1^* .

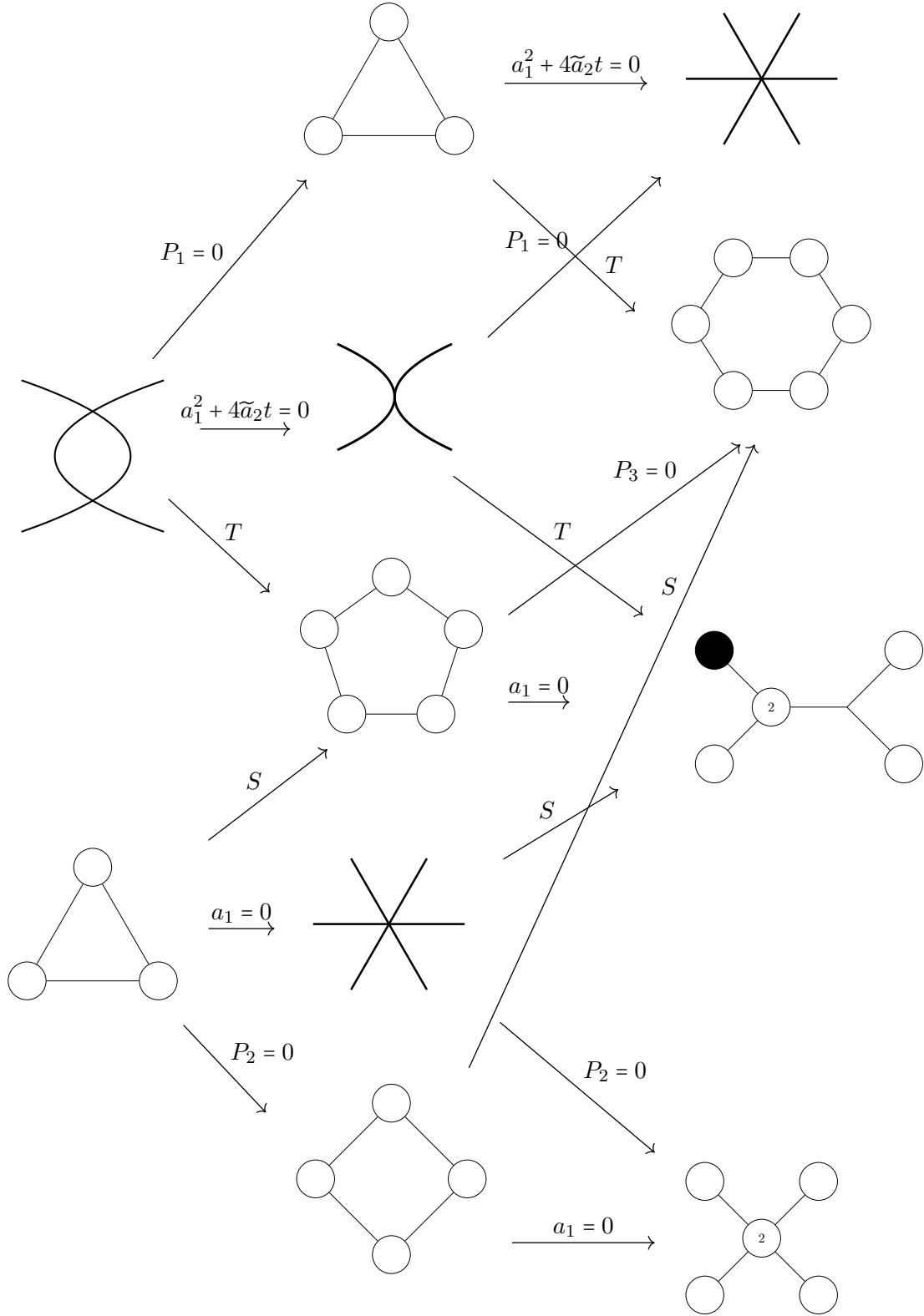


Table 20: $I_2^{\text{ns}} + I_3^{\text{s}}$ Resolution III. $P_1 = -2\tilde{a}_4^2 t + 4\tilde{a}_2 \tilde{a}_6 t + a_1^2 \tilde{a}_6 - 2\tilde{a}_2 \tilde{a}_3^2$, $P_2 = \tilde{a}_3^3 s - a_1 \tilde{a}_2 \tilde{a}_3^2 + a_1^2 \tilde{a}_3 \tilde{a}_4 - a_1^3 \tilde{a}_6$, and $P_3 = \tilde{a}_2 \tilde{a}_3^2 s - a_1 (a_1 \tilde{a}_6 - \tilde{a}_3 \tilde{a}_4)$. The non-Kodaira fiber is a contraction of an I_1^* .

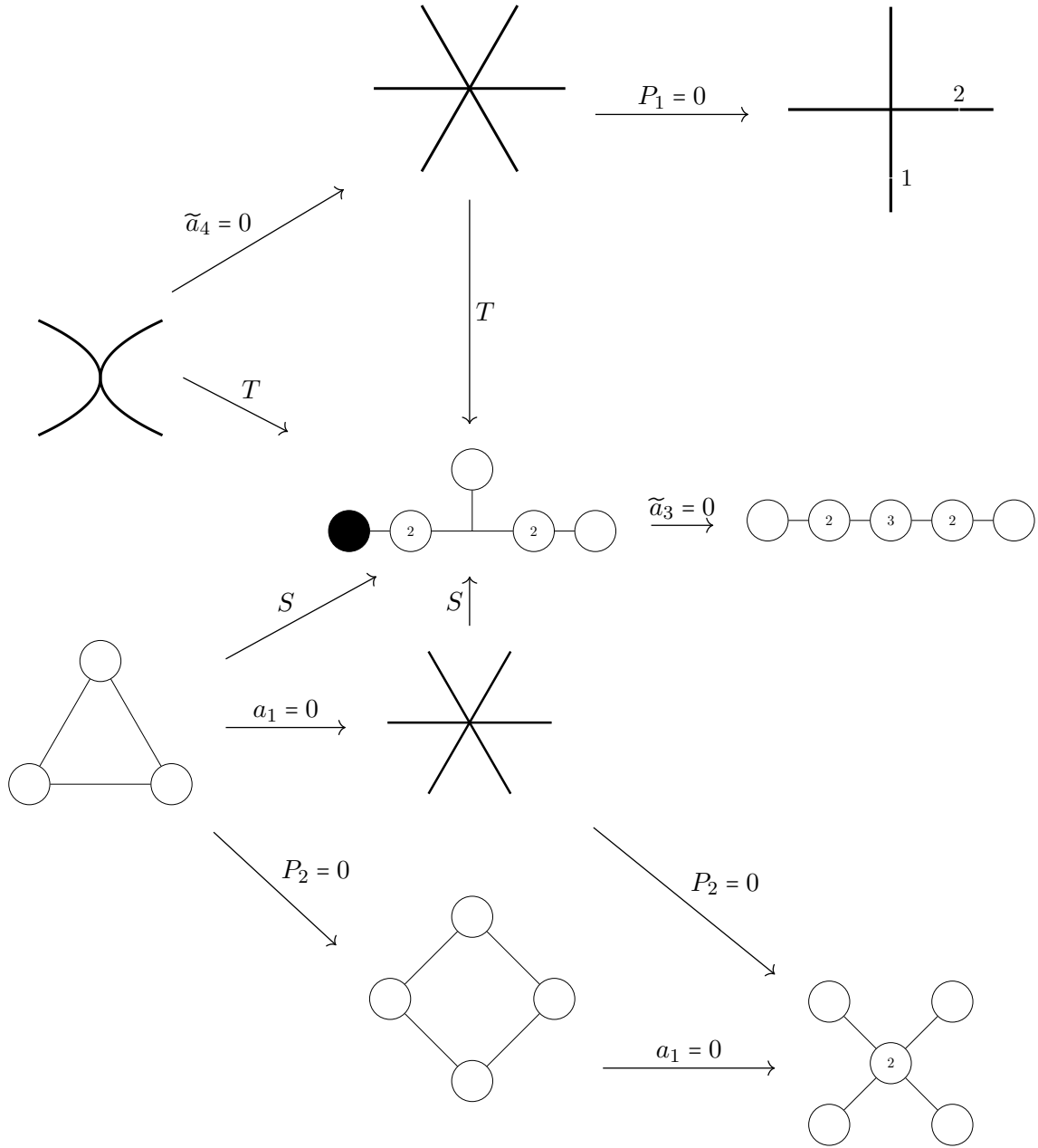


Table 21: III + I₃^s Resolution I. $P_1 = \tilde{a}_3^2 + 4\tilde{a}_6t$ and $P_2 = \tilde{a}_3^3 - \tilde{a}_1\tilde{a}_2\tilde{a}_3^2s + \tilde{a}_1^2\tilde{a}_3\tilde{a}_4s - \tilde{a}_1^3\tilde{a}_6s^2$

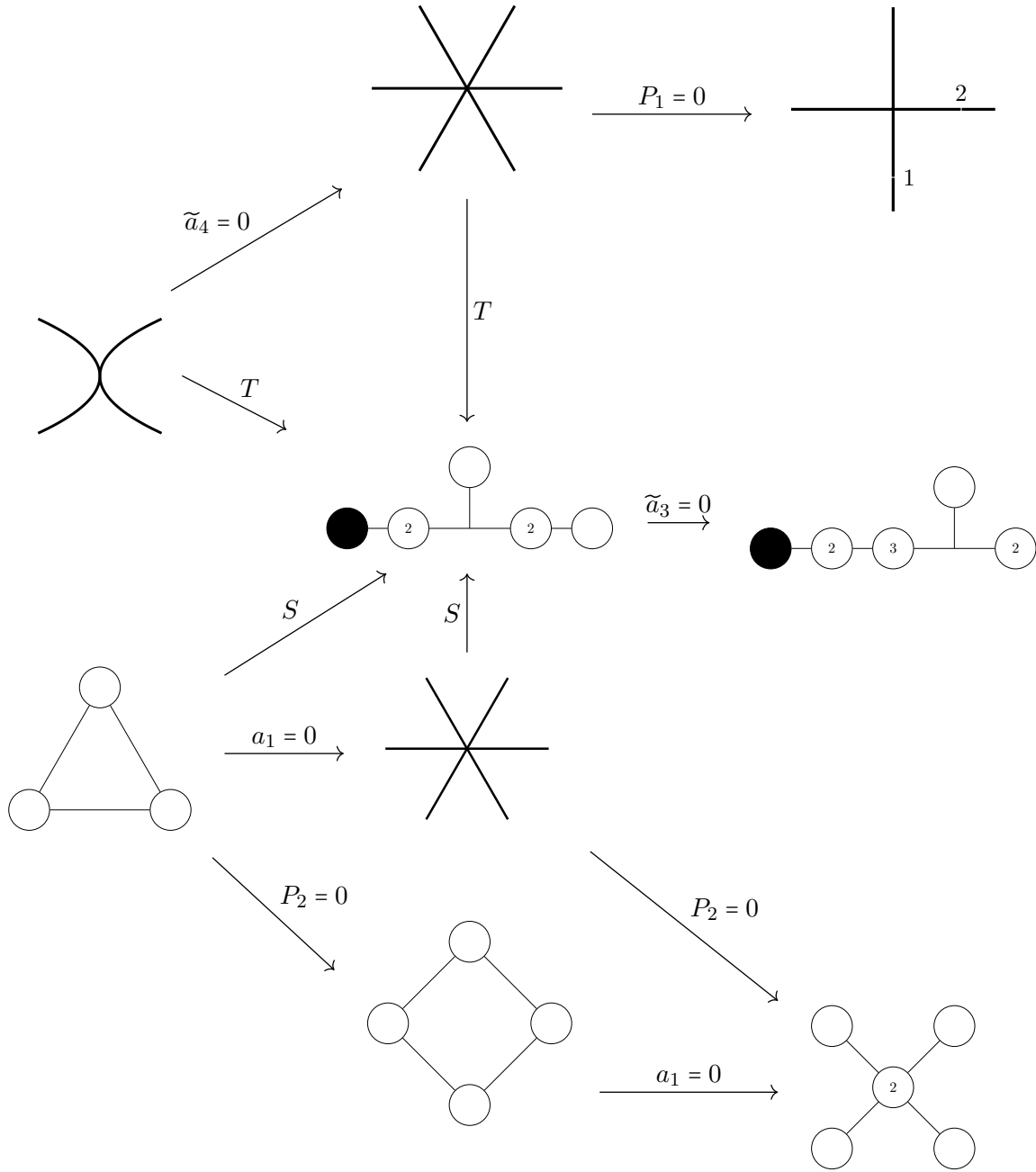


Table 22: III + I₃^s Resolution II. $P_1 = \tilde{a}_3^2 + 4\tilde{a}_6 t$ and $P_2 = \tilde{a}_3^3 - \tilde{a}_1 \tilde{a}_2 \tilde{a}_3^2 s + \tilde{a}_1^2 \tilde{a}_3 \tilde{a}_4 s - \tilde{a}_1^3 \tilde{a}_6 s^2$

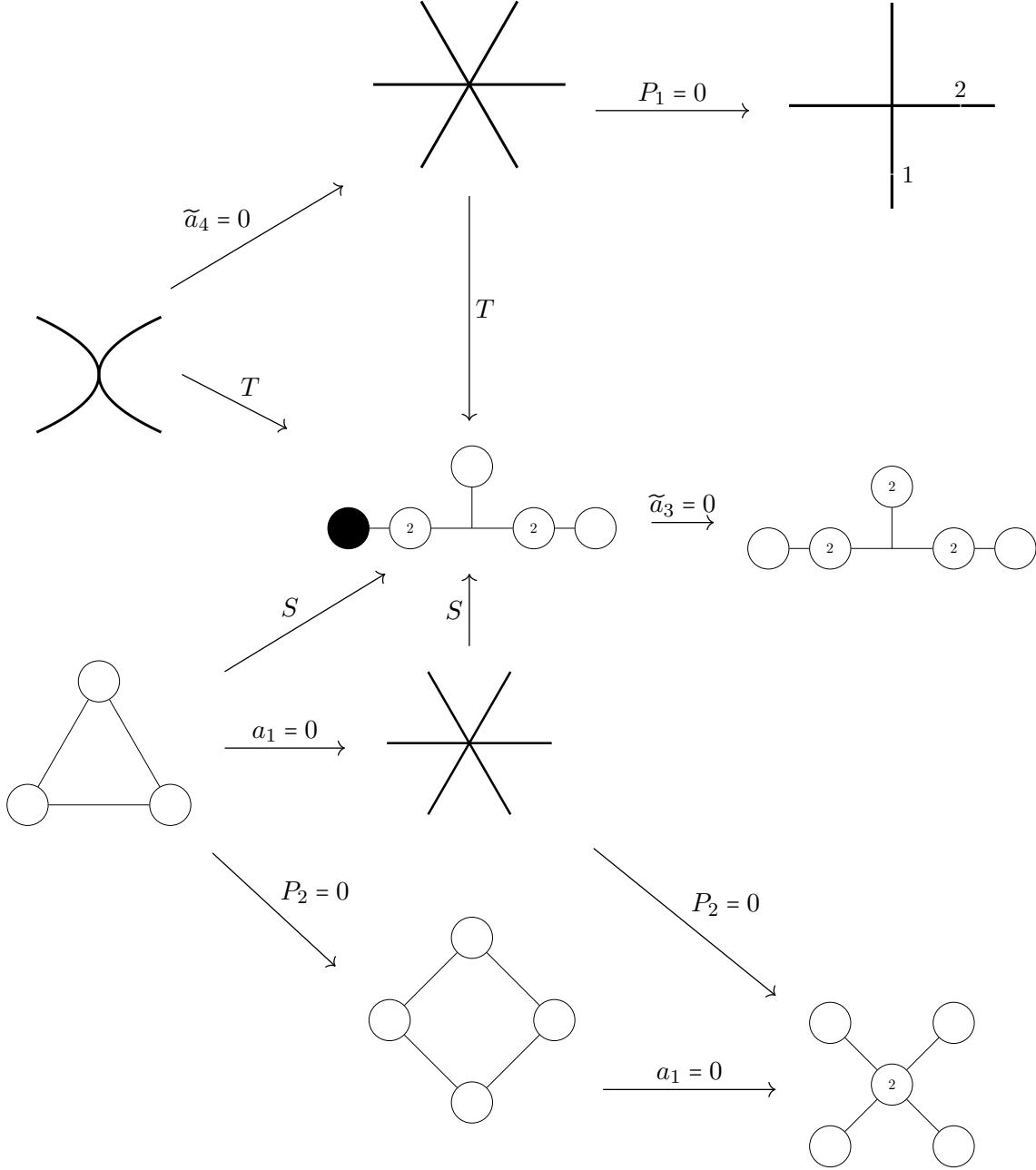


Table 23: III + I₃^s Resolution III. $P_1 = \tilde{a}_3^2 + 4\tilde{a}_6t$ and $P_2 = \tilde{a}_3^3 - \tilde{a}_1\tilde{a}_2\tilde{a}_3^2s + \tilde{a}_1^2\tilde{a}_3\tilde{a}_4s - \tilde{a}_1^3\tilde{a}_6s^2$

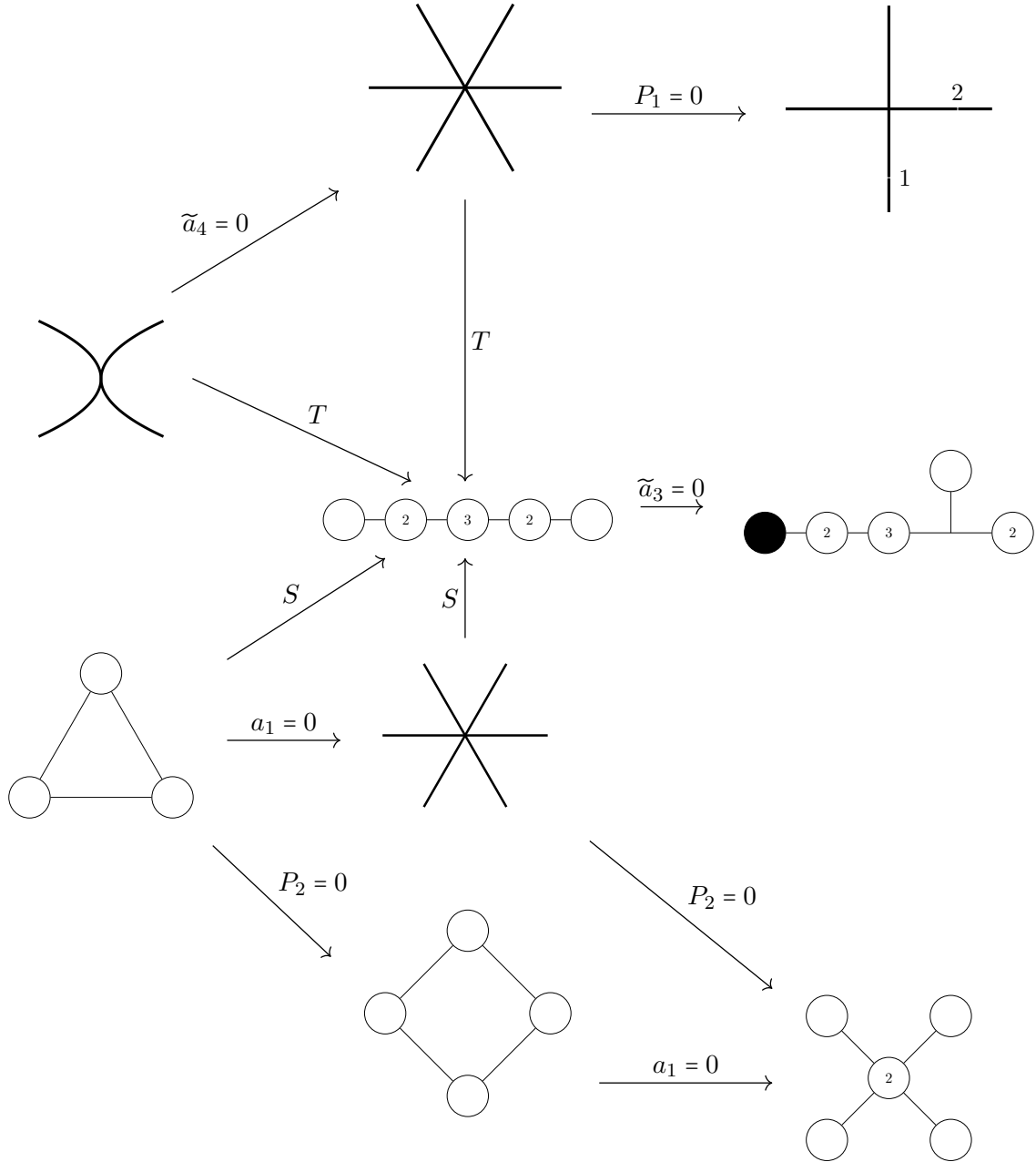


Table 24: III + \mathbb{I}_3^s Resolution IV. $P_1 = \tilde{a}_3^2 + 4\tilde{a}_6 t$ and $P_2 = \tilde{a}_3^3 - \tilde{a}_1 \tilde{a}_2 \tilde{a}_3^2 s + \tilde{a}_1^2 \tilde{a}_3 \tilde{a}_4 s - \tilde{a}_1^3 \tilde{a}_6 s^2$

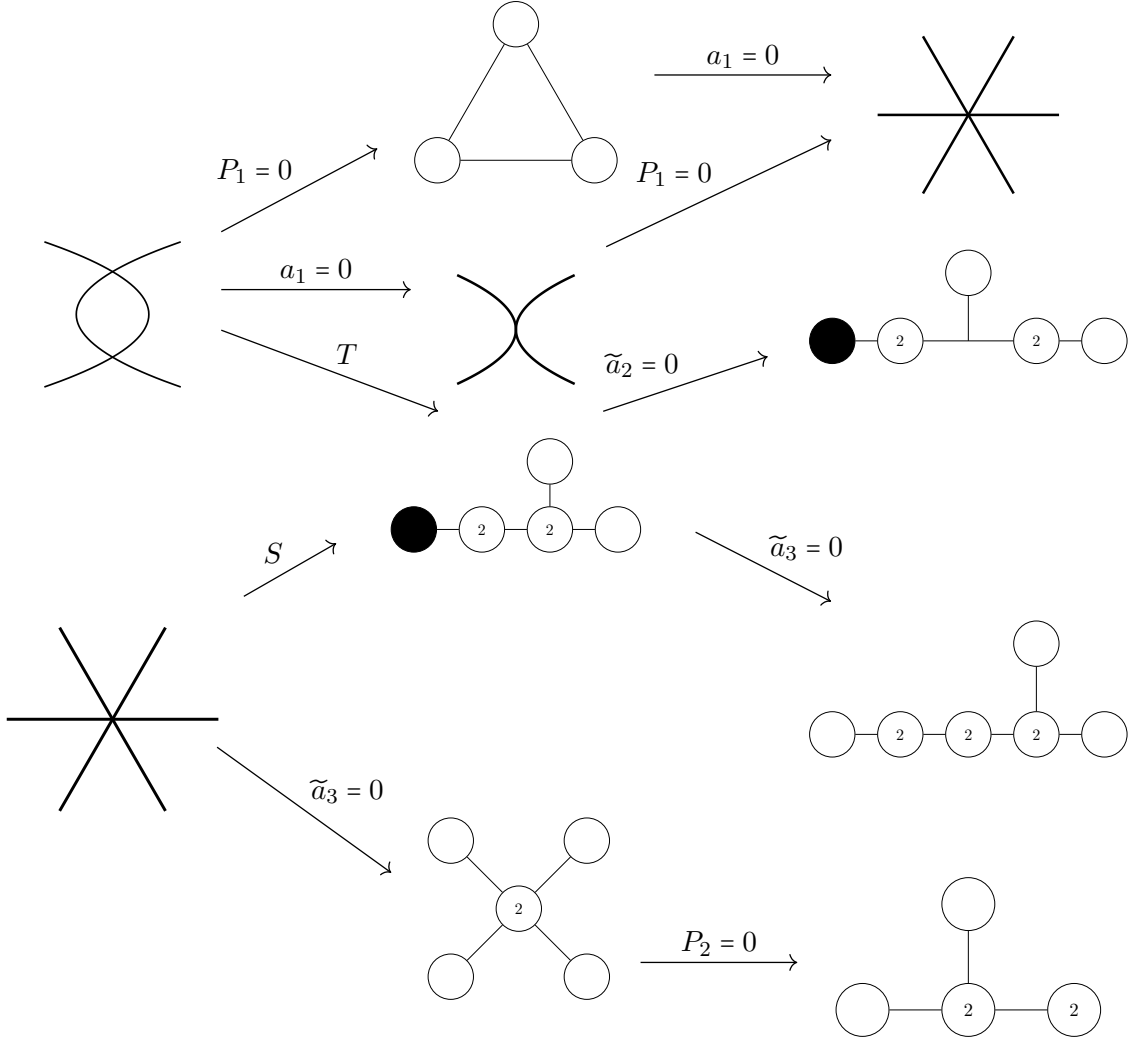


Table 25: $I_2^{\text{ns}}+IV^{\text{s}}$ or $I_2^{\text{s}}+IV^{\text{s}}$, Resolution I. $P_1 = \tilde{a}_4^2 - \tilde{a}_1^2 \tilde{a}_6 t$ and $P_2 = \tilde{a}_2^2 \tilde{a}_4^2 - 4\tilde{a}_4^3 s - 4\tilde{a}_2^3 \tilde{a}_6 + 18\tilde{a}_2 \tilde{a}_4 \tilde{a}_6 s - 27\tilde{a}_6^2 s^2$ for $I_2^{\text{ns}}+IV^{\text{s}}$, $P_2 = \tilde{a}_2^2 \tilde{a}_4^2 s - 4\tilde{a}_4^3 - 4\tilde{a}_2^3 \tilde{a}_6 s^2 + 18\tilde{a}_2 \tilde{a}_4 \tilde{a}_6 s^2 - 27\tilde{a}_6^2 s$ for $I_2^{\text{s}}+IV^{\text{s}}$.

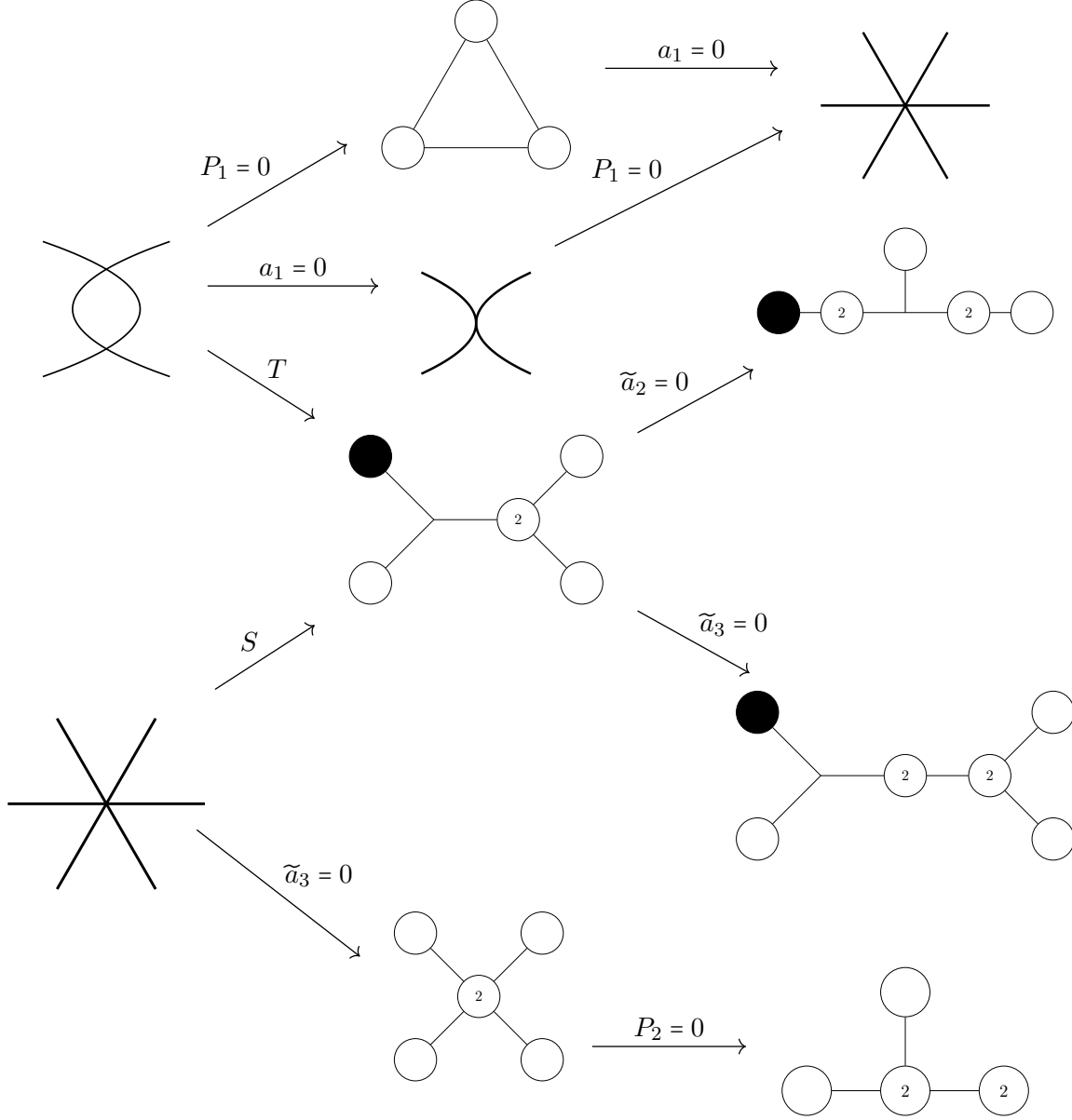


Table 26: $I_2^s + IV^s$ or $I_2^{ns} + IV^s$, Resolution II. $P_1 = \tilde{a}_4^2 t - a_1^2 \tilde{a}_6$ and $P_2 = \tilde{a}_2^2 \tilde{a}_4^2 - 4\tilde{a}_4^3 s - 4\tilde{a}_2^3 \tilde{a}_6 + 18\tilde{a}_2 \tilde{a}_4 \tilde{a}_6 s - 27\tilde{a}_6^2 s^2$ for $I_2^{ns} + IV^s$, $P_2 = \tilde{a}_2^2 \tilde{a}_4^2 s - 4\tilde{a}_4^3 - 4\tilde{a}_2^3 \tilde{a}_6 s^2 + 18\tilde{a}_2 \tilde{a}_4 \tilde{a}_6 s^2 - 27\tilde{a}_6^2 s$ for $I_2^s + IV^s$.

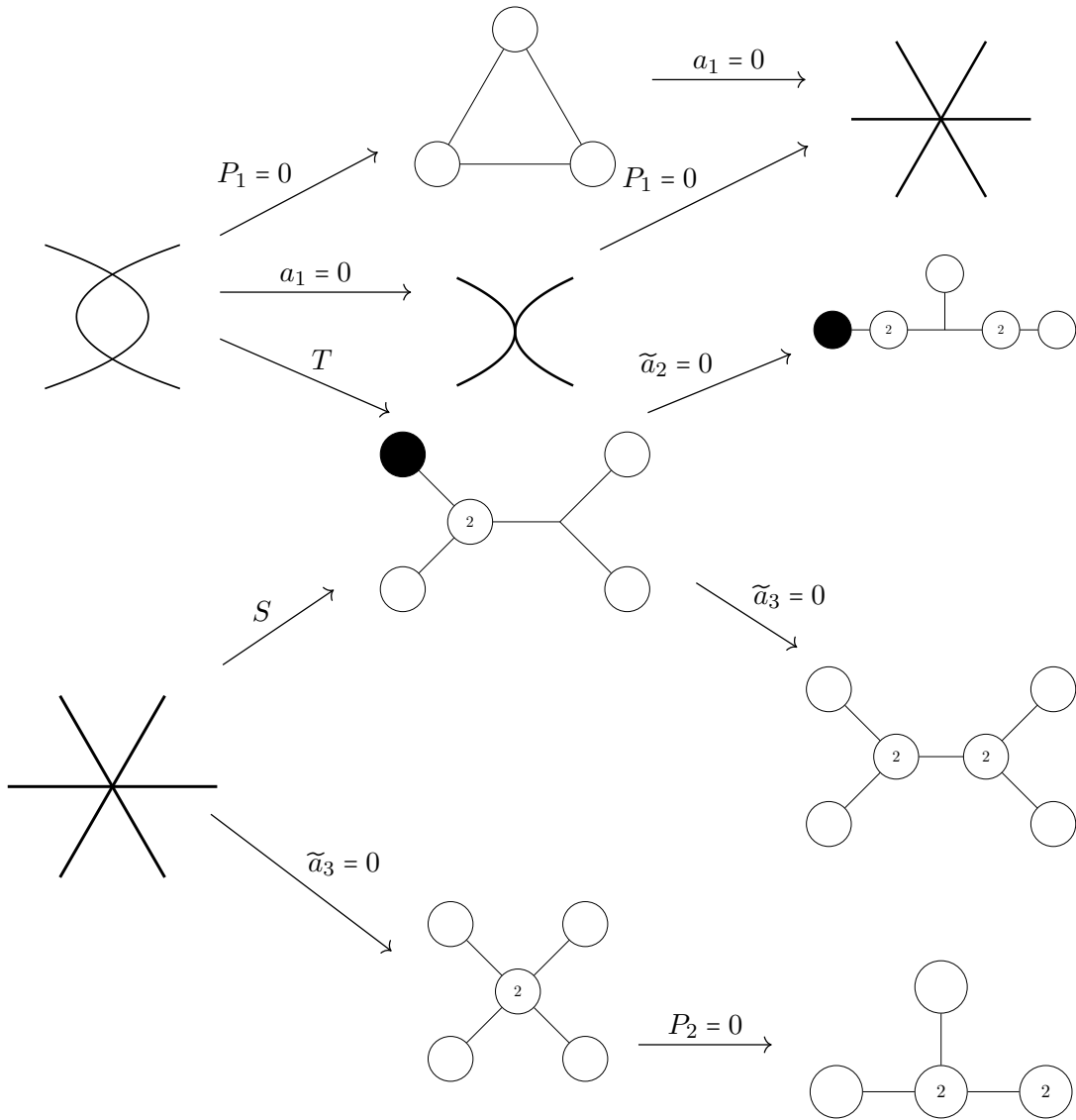


Table 27: $I_2^{\text{ns}} + IV^s$ or $I_2^s + IV^s$, Resolution III. $P_1 = \tilde{a}_4^2 t - a_1^2 \tilde{a}_6$ and $P_2 = \tilde{a}_2^2 \tilde{a}_4^2 - 4\tilde{a}_4^3 s - 4\tilde{a}_2^3 \tilde{a}_6 + 18\tilde{a}_2 \tilde{a}_4 \tilde{a}_6 s - 27\tilde{a}_6^2 s^2$ for $I_2^{\text{ns}} + IV^s$, $P_2 = \tilde{a}_2^2 \tilde{a}_4^2 s - 4\tilde{a}_4^3 - 4\tilde{a}_2^3 \tilde{a}_6 s^2 + 18\tilde{a}_2 \tilde{a}_4 \tilde{a}_6 s^2 - 27\tilde{a}_6^2 s$ for $I_2^s + IV^s$.

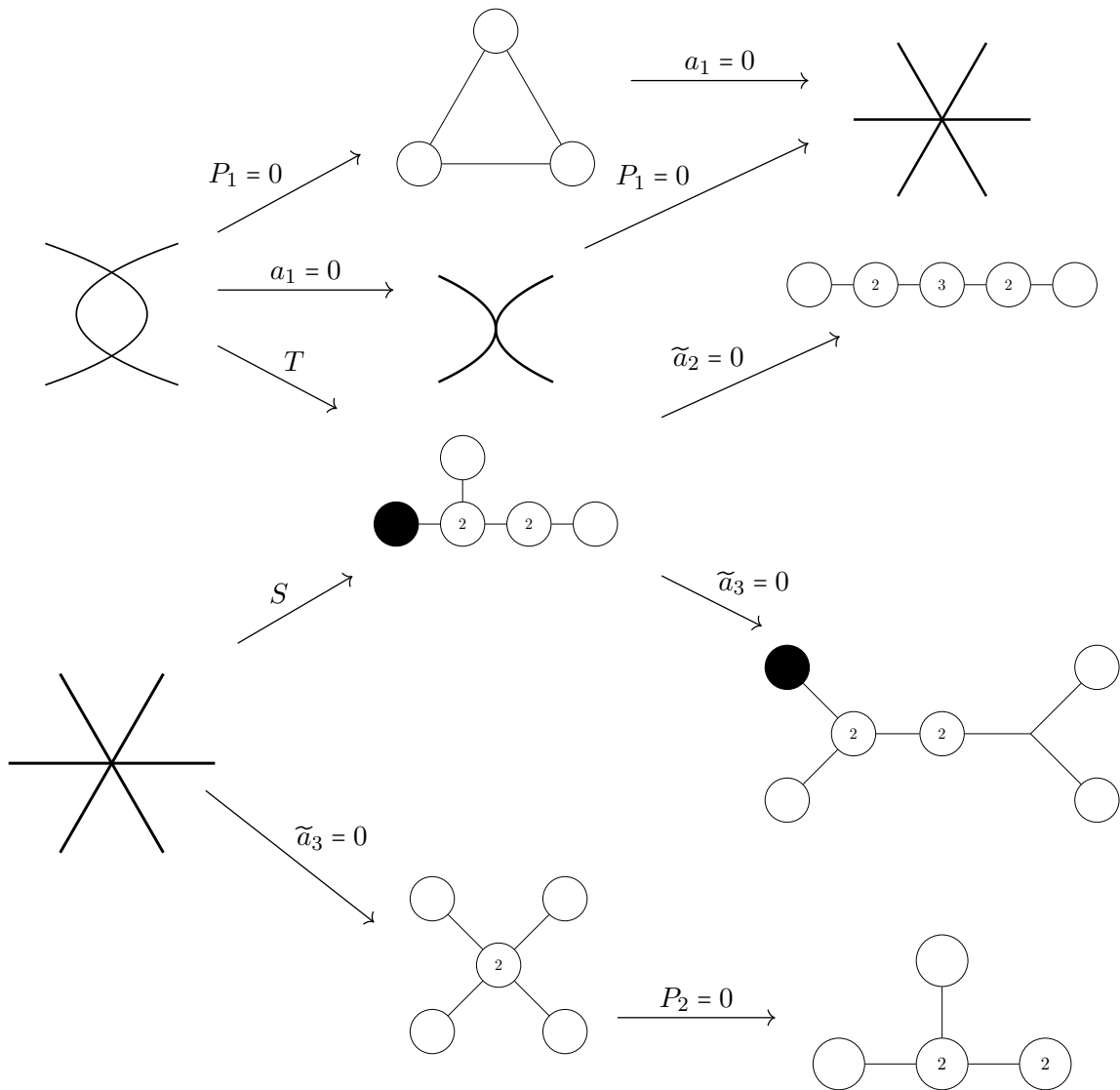


Table 28: $I_2^s + IV^s$ or $I_2^{ns} + IV^s$, Resolution IV. $P_1 = \tilde{a}_4^2 t - a_1^2 \tilde{a}_6$ and $P_2 = \tilde{a}_2^2 \tilde{a}_4^2 - 4\tilde{a}_4^3 s - 4\tilde{a}_2^3 \tilde{a}_6 + 18\tilde{a}_2 \tilde{a}_4 \tilde{a}_6 s - 27\tilde{a}_6^2 s^2$ for $I_2^{ns} + IV^s$, $P_2 = \tilde{a}_2^2 \tilde{a}_4^2 s - 4\tilde{a}_4^3 - 4\tilde{a}_2^3 \tilde{a}_6 s^2 + 18\tilde{a}_2 \tilde{a}_4 \tilde{a}_6 s^2 - 27\tilde{a}_6^2 s$ for $I_2^s + IV^s$.

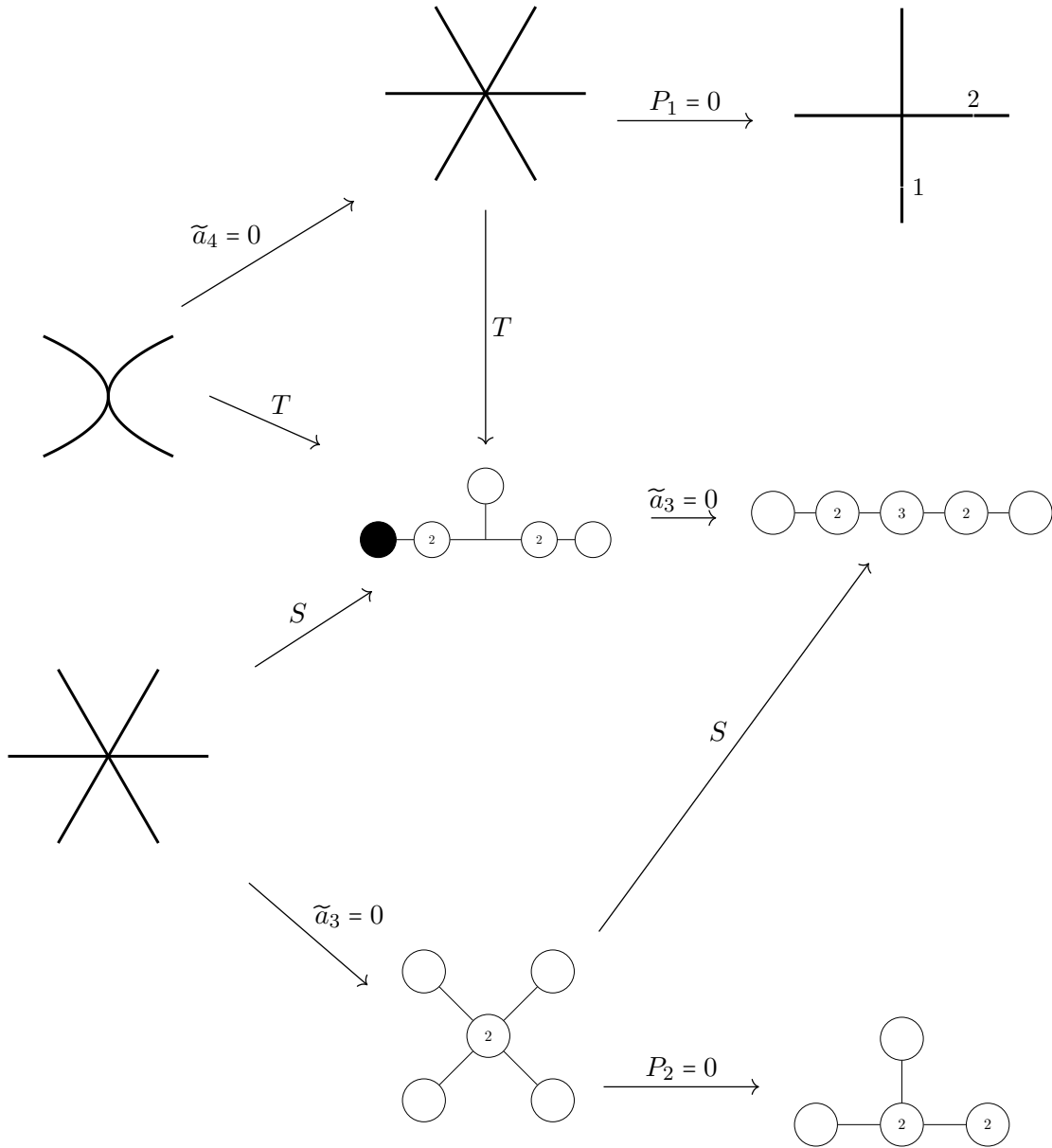


Table 29: III + IV^s, Resolution I. $P_1 = \tilde{a}_3^2 + 4\tilde{a}_6 t$ and $P_2 = \tilde{a}_2^2 \tilde{a}_4^2 s - 4\tilde{a}_4^3 - 4\tilde{a}_2^3 \tilde{a}_6 s^2 + 18\tilde{a}_2 \tilde{a}_4 \tilde{a}_6 s - 27\tilde{a}_6^2 s$.

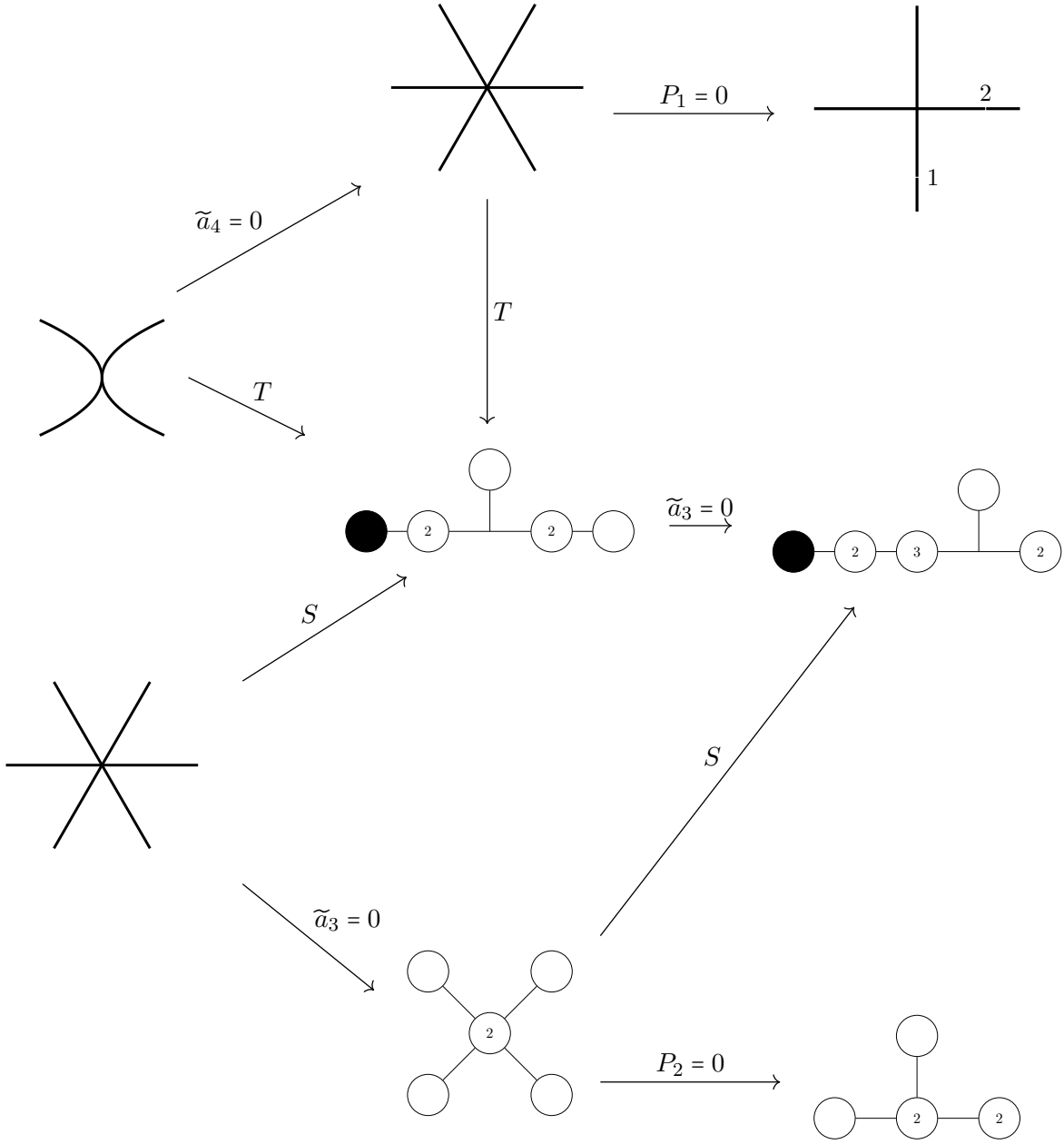


Table 30: III + IV^s Resolution II. $P_1 = \tilde{a}_3^2 + 4\tilde{a}_6 t$ and $P_2 = \tilde{a}_2^2 \tilde{a}_4^2 s - 4\tilde{a}_4^3 - 4\tilde{a}_2^3 \tilde{a}_6 s^2 + 18\tilde{a}_2 \tilde{a}_4 \tilde{a}_6 s - 27\tilde{a}_6^2 s$.

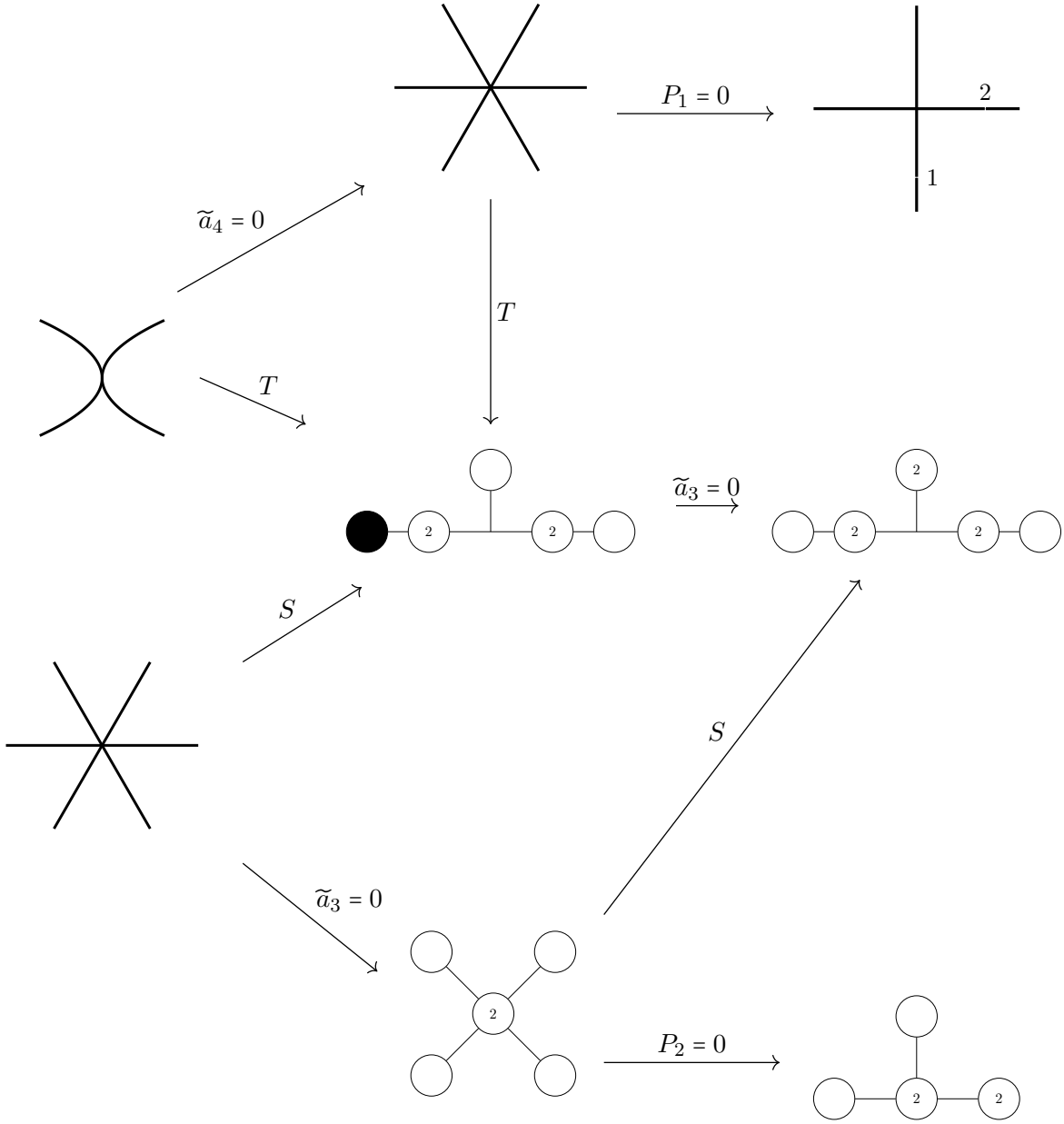


Table 31: III + IV^s, Resolution III. $P_1 = \tilde{a}_3^2 + 4\tilde{a}_6 t$ and $P_2 = \tilde{a}_2^2 \tilde{a}_4^2 s - 4\tilde{a}_4^3 - 4\tilde{a}_2^3 \tilde{a}_6 s^2 + 18\tilde{a}_2 \tilde{a}_4 \tilde{a}_6 s - 27\tilde{a}_6^2 s$. The non-Kodaira fiber in codimension-two is a contraction of a IV* and its specialization in codimension-three is a contraction of a III*.

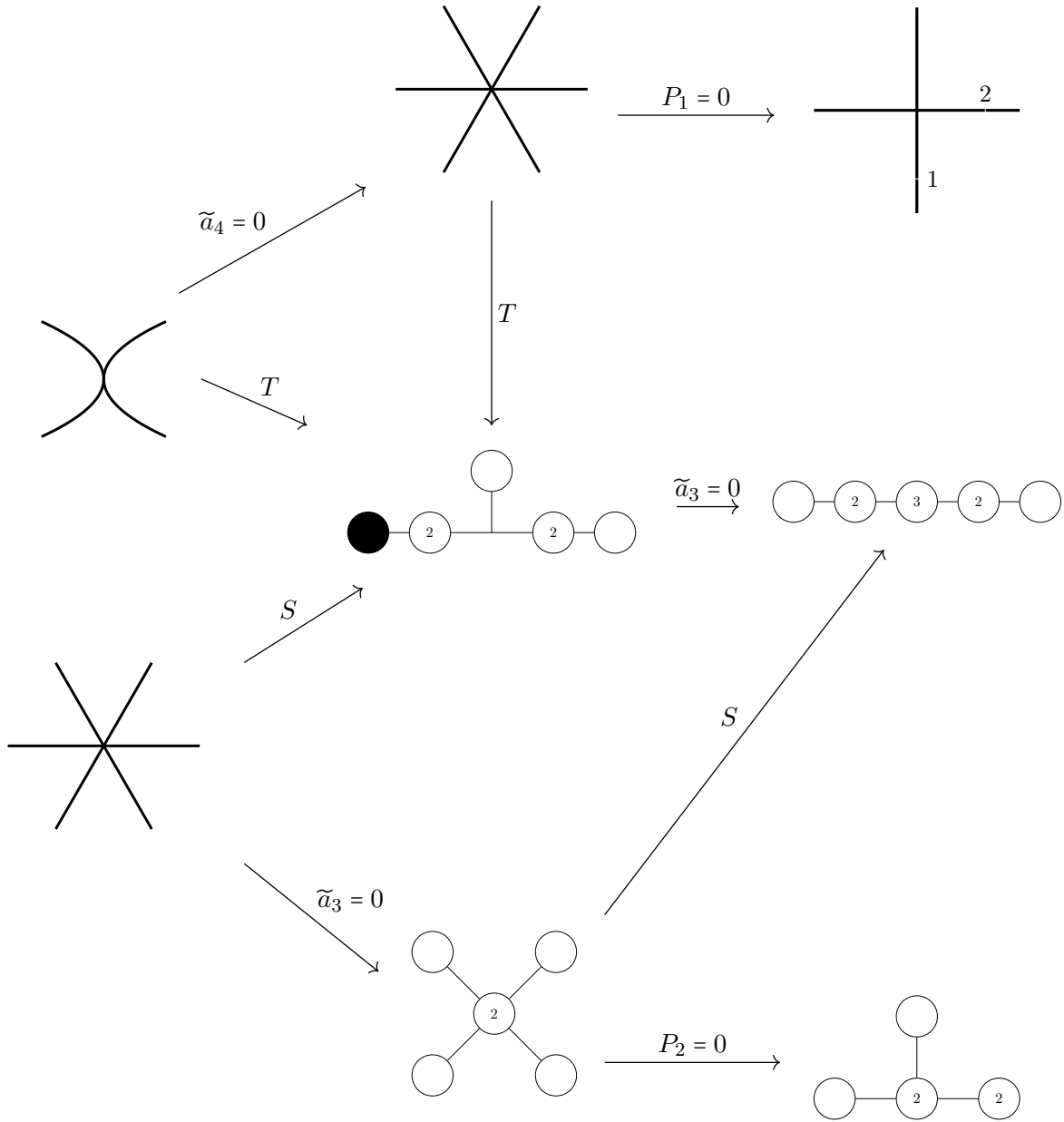


Table 32: III + IV^s, Resolution IV. $P_1 = \tilde{a}_3^2 + 4\tilde{a}_6 t$ and $P_2 = \tilde{a}_2^2 \tilde{a}_4^2 s - 4\tilde{a}_4^3 - 4\tilde{a}_2^3 \tilde{a}_6 s^2 + 18\tilde{a}_2 \tilde{a}_4 \tilde{a}_6 s - 27\tilde{a}_6^2 s$. The non-Kodaira fiber in codimension-two is a contraction of a IV* and its specialization in codimension-three is a contraction of a III*.

References

- [1] P. Aluffi. Chern classes of blowups. *Math. Proc. Cambridge Philos. Soc.*, 148(2):227–242, 2010.
- [2] P. Aluffi and M. Esole, Chern class identities from tadpole matching in type IIB and F-theory. *JHEP*, 03:032, 2009.
- [3] P. Aluffi and M. Esole, New Orientifold Weak Coupling Limits in F-theory. *JHEP*, 02:020, 2010.
- [4] L. B. Anderson, M. Esole, L. Fredrickson and L. P. Schaposnik, Singular Geometry and Higgs Bundles in String Theory, *SIGMA* **14** (2018) 037.
- [5] P. C. Argyres and M. R. Douglas, New phenomena in SU(3) supersymmetric gauge theory, *Nucl. Phys. B* **448**, 93 (1995)
- [6] P. Arras, A. Grassi and T. Weigand, Terminal Singularities, Milnor Numbers, and Matter in F-theory, *J. Geom. Phys.* **123**, 71 (2018)
- [7] S. D. Avramis and A. Kehagias, A Systematic search for anomaly-free supergravities in six dimensions, *JHEP* **0510**, 052 (2005).
- [8] J. C. Baez and J. Huerta, “The Algebra of Grand Unified Theories,” *Bull. Am. Math. Soc.* **47**, 483 (2010)
- [9] V. V. Batyrev. Birational Calabi-Yau n -folds have equal Betti numbers. In *New trends in algebraic geometry (Warwick, 1996)*, volume 264 of *London Math. Soc. Lecture Note Ser.*, pages 1–11. Cambridge Univ. Press, Cambridge, 1999.
- [10] C. W. Bernard, N. H. Christ, A. H. Guth and E. J. Weinberg, Instanton Parameters for Arbitrary Gauge Groups, *Phys. Rev. D* **16**, 2967 (1977).
- [11] M. Bershadsky, K. A. Intriligator, S. Kachru, D. R. Morrison, V. Sadov, and C. Vafa, Geometric singularities and enhanced gauge symmetries. *Nucl. Phys.*, B481:215–252, 1996.
- [12] M. Bershadsky and A. Johansen, Colliding singularities in F theory and phase transitions, *Nucl. Phys. B* **489**, 122 (1997)
- [13] M. Bershadsky and C. Vafa, “Global anomalies and geometric engineering of critical theories in six-dimensions,” hep-th/9703167.
- [14] C. Birkar, P. Cascini, C. D. Hacon and J. McKernan, Existence of minimal models for varieties of log general type, *J. Amer. Math. Soc.* **23** (2010), 405-468
- [15] A. C. Cadavid, A. Ceresole, R. D’Auria and S. Ferrara, Eleven-dimensional supergravity compactified on Calabi–Yau threefolds, *Phys. Lett. B* **357**, 76 (1995)
- [16] A. Cattaneo. Crepant resolutions of Weierstrass threefolds and non-Kodaira fibers. [arXiv:1307.7997v2](https://arxiv.org/abs/1307.7997v2) [math.AG].
- [17] A. Collinucci, F. Denef, and M. Esole. D-brane Deconstructions in IIB Orientifolds. *JHEP*, 02:005, 2009.

- [18] P. Deligne, Courbes elliptiques: formulaire d'après J. Tate. (French) *Modular functions of one variable, IV (Proc. Internat. Summer School, Univ. Antwerp, Antwerp, 1972)*, pp. 53–73. Lecture Notes in Math., Vol. 476, Springer, Berlin, 1975.
- [19] M. Esole, *Introduction to Elliptic Fibrations*, In: Cardona A., Morales P., Ocampo H., Paycha S., Reyes Lega A. (eds) *Quantization, Geometry and Noncommutative Structures in Mathematics and Physics*, pp 247–276, Mathematical Physics Studies. Springer, Cham, 2017.
- [20] M. Esole, J. Fullwood, and S.-T. Yau. D_5 elliptic fibrations: non-Kodaira fibers and new orientifold limits of F-theory. *Commun. Num. Theor. Phys.* **09**, no. 3, 583 (2015).
- [21] M. Esole, S. G. Jackson, R. Jagadeesan, and A. G. Noël. Incidence Geometry in a Weyl Chamber I: GL_n , arXiv:1508.03038 [math.RT].
- [22] M. Esole, S. G. Jackson, R. Jagadeesan and A. G. Noël, Incidence Geometry in a Weyl Chamber II: SL_n , arXiv:1601.05070 [math.RT].
- [23] M. Esole, R. Jagadeesan and M. J. Kang, The Geometry of G_2 , Spin(7), and Spin(8)-models, arXiv:1709.04913 [hep-th].
- [24] M. Esole, P. Jefferson and M. J. Kang, The Geometry of F_4 -Models, arXiv:1704.08251 [hep-th].
- [25] M. Esole, P. Jefferson and M. J. Kang, Euler Characteristics of Crepant Resolutions of Weierstrass Models, arXiv:1703.00905 [math.AG].
- [26] M. Esole and S. Pasterski, D_4 -flops of the E_7 -model, arXiv:1901.00093 [hep-th].
- [27] M. Esole and M. J. Kang, Characteristic numbers of elliptic fibrations with non-trivial Mordell–Weil groups, arXiv:1808.07054 [hep-th].
- [28] M. Esole and M. J. Kang, Characteristic numbers of crepant resolutions of Weierstrass models, arXiv:1807.08755 [hep-th].
- [29] M. Esole and M. J. Kang, The Geometry of the $SU(2) \times G_2$ -model, *JHEP* **1902**, 091 (2019)
- [30] M. Esole and M. J. Kang, Flopping and Slicing: $SO(4)$ and Spin(4)-models, arXiv:1802.04802 [hep-th].
- [31] M. Esole, M. J. Kang and S. T. Yau, Mordell–Weil Torsion, Anomalies, and Phase Transitions, arXiv:1712.02337 [hep-th].
- [32] M. Esole, M. J. Kang and S. T. Yau, A New Model for Elliptic Fibrations with a Rank One Mordell–Weil Group: I. Singular Fibers and Semi-Stable Degenerations, arXiv:1410.0003 [hep-th].
- [33] M. Esole and R. Savelli, Tate Form and Weak Coupling Limits in F-theory, *JHEP* **1306**, 027 (2013)
- [34] M. Esole and S. H. Shao, M-theory on Elliptic Calabi–Yau Threefolds and 6d Anomalies, arXiv:1504.01387 [hep-th].
- [35] M. Esole, S.-H. Shao, and S.-T. Yau. Singularities and Gauge Theory Phases. *Adv. Theor. Math. Phys.*, 19:1183–1247, 2015.

- [36] M. Esole, S. H. Shao and S. T. Yau, Singularities and Gauge Theory Phases II, *Adv. Theor. Math. Phys.* 20, 683 (2016)
- [37] M. Esole and S. T. Yau, Small resolutions of SU(5)-models in F-theory, *Adv. Theor. Math. Phys.* 17, no. 6, 1195 (2013)
- [38] J. Erler, Anomaly cancellation in six-dimensions, *J. Math. Phys.* **35**, 1819 (1994)
- [39] S. Ferrara, R. R. Khuri and R. Minasian, M theory on a Calabi–Yau manifold, *Phys. Lett. B* **375**, 81 (1996)
- [40] J. Fullwood. On generalized Sethi-Vafa-Witten formulas. *J. Math. Phys.*, 52:082304, 2011.
- [41] E. G. Gimon and J. Polchinski, Consistency conditions for orientifolds and d manifolds, *Phys. Rev. D* **54**, 1667 (1996)
- [42] A. Grassi and T. Weigand, On topological invariants of algebraic threefolds with (\mathbb{Q} -factorial) singularities, arXiv:1804.02424 [math.AG].
- [43] A. Grassi, J. Halverson, J. Shaneson and W. Taylor, Non-Higgsable QCD and the Standard Model Spectrum in F-theory, *JHEP* **1501**, 086 (2015)
- [44] A. Grassi and D. R. Morrison. Group representations and the Euler characteristic of elliptically fibered Calabi–Yau threefolds. *J. Algebraic Geom.*, 12(2):321–356, 2003.
- [45] M. B. Green, J. H. Schwarz and P. C. West, Anomaly Free Chiral Theories in Six-Dimensions, *Nucl. Phys. B* **254**, 327 (1985).
- [46] H. Hayashi, C. Lawrie, D. R. Morrison and S. Schafer-Nameki, Box Graphs and Singular Fibers, *JHEP* **1405**, 048 (2014) doi:10.1007/JHEP05(2014)048
- [47] K. A. Intriligator, D. R. Morrison, and N. Seiberg. Five-dimensional supersymmetric gauge theories and degenerations of Calabi–Yau spaces. *Nucl.Phys.*, B497:56–100, 1997.
- [48] S. Katz, D. R. Morrison, S. Schäfer-Nameki, and J. Sully. Tate’s algorithm and F-theory. *JHEP*, 1108:094, 2011.
- [49] S. H. Katz and C. Vafa, Matter from geometry, *Nucl. Phys. B* **497**, 146 (1997)
- [50] Y. Kawamata. Flops connect minimal models, *Publ. RIMS, Kyoto Univ.* 44 (2008), 419–423
- [51] Y. Kawamata, On the cone of divisors of Calabi-Yau fibre spaces, *Internal J. Math.* 8 (1997), 665–687.
- [52] Y. Kawamata. Crepant blowing-up of 3-dimensional canonical singularities and its application to degenerations of surfaces. *Ann. of Math. (2)*, 127(1):93–163, 1988.
- [53] Y. Kawamata, and K. Matsuki, The Number of the Minimal Models for a 3- Fold of General Type is Finite, *Math. Ann.* 276, 595–598, 1987.
- [54] K. Kodaira. On compact analytic surfaces. II, III. *Ann. of Math. (2)* 77 (1963), 563–626; *ibid.*, 78:1–40, 1963.
- [55] J. Kollár and S. Mori, Birational geometry of algebraic varieties, *Cambridge Tracts in Mathematics*, vol. 134, Cambridge University Press, Cambridge, 1998.

- [56] S. Kováč, Quotient singularities with no crepant resolution?, URL (version: 2011-06-03): <https://mathoverflow.net/q/66702>
- [57] S. Krause, C. Mayrhofer and T. Weigand, G_4 flux, chiral matter and singularity resolution in F-theory compactifications, Nucl. Phys. B **858**, 1 (2012) doi:10.1016/j.nuclphysb.2011.12.013 [arXiv:1109.3454 [hep-th]].
- [58] V. Kumar, D. R. Morrison and W. Taylor, Global aspects of the space of 6D $N = 1$ supergravities, JHEP **1011**, 118 (2010)
- [59] C. Lawrie and S. Schäfer-Nameki, The Tate Form on Steroids: Resolution and Higher Codimension Fibers, JHEP **1304**, 061 (2013).
- [60] K. Matsuki, Weyl groups and birational transformations among minimal models, *Mem. Amer. Math. Soc.* **116** no. 557, (1995) vi+133.
- [61] K. Matsuki, Introduction to the Mori program, Universitext, Springer-Verlag, New York, 2002
- [62] C. Mayrhofer, D. R. Morrison, O. Till and T. Weigand, Mordell–Weil Torsion and the Global Structure of Gauge Groups in F-theory, JHEP **1410**, 16 (2014)
- [63] R. Miranda. Smooth models for elliptic threefolds. In *The birational geometry of degenerations (Cambridge, Mass., 1981)*, volume 29 of *Progr. Math.*, pages 85–133. Birkhäuser Boston, Mass., 1983.
- [64] S. Monnier, G. W. Moore and D. S. Park, “Quantization of anomaly coefficients in 6D $\mathcal{N} = (1, 0)$ supergravity,” JHEP **1802**, 020 (2018)
- [65] D. R. Morrison and W. Taylor, Matter and singularities, JHEP **1201**, 022 (2012)
- [66] D. R. Morrison and W. Taylor, Classifying bases for 6D F-theory models, Central Eur. J. Phys. **10**, 1072 (2012)
- [67] D. R. Morrison and C. Vafa. Compactifications of F theory on Calabi–Yau threefolds. 2. *Nucl. Phys.*, B476:437–469, 1996.
- [68] D. Mumford and K. Suominen, *Introduction to the theory of moduli*, in Algebraic Geometry, Oslo 1970, Proceedings of the 5th Nordic summer school in Math, Wolters-Noordhoff, 1972, 171-222.
- [69] D. S. Park, Anomaly Equations and Intersection Theory, JHEP **1201**, 093 (2012)
- [70] S. Randjbar-Daemi, A. Salam, E. Sezgin and J. A. Strathdee, An Anomaly Free Model in Six-Dimensions, Phys. Lett. **151B**, 351 (1985).
- [71] V. Sadov, Generalized Green-Schwarz mechanism in F theory, Phys. Lett. B **388**, 45 (1996).
- [72] A. Sagnotti, A Note on the Green-Schwarz mechanism in open string theories, Phys. Lett. B **294**, 196 (1992)
- [73] J. H. Schwarz, Anomaly - free supersymmetric models in six-dimensions, Phys. Lett. B **371**, 223 (1996)

- [74] S. Sethi, C. Vafa and E. Witten, Constraints on low dimensional string compactifications, Nucl. Phys. B **480**, 213 (1996)
- [75] M. G. Szydło. *Flat regular models of elliptic schemes*. ProQuest LLC, Ann Arbor, MI, 1999. Thesis (Ph.D.)—Harvard University.
- [76] R. Tatar and W. Walters, GUT theories from Calabi–Yau 4-folds with SO(10) Singularities, JHEP **1212**, 092 (2012) doi:10.1007/JHEP12(2012)092 [arXiv:1206.5090 [hep-th]].
- [77] J. Tate, Algorithm for determining the type of a singular fiber in an elliptic pencil. *Modular functions of one variable, IV (Proc. Internat. Summer School, Univ. Antwerp, Antwerp, 1972)*, pp. 33–52. Lecture Notes in Mathematics 476, Springer-Verlag, Berlin, 1975.
- [78] T. van Ritbergen, A. N. Schellekens and J. A. M. Vermaseren, Group theory factors for Feynman diagrams, Int. J. Mod. Phys. A **14**, 41 (1999)
- [79] E. Witten, Phase transitions in M theory and F theory, Nucl. Phys. B **471**, 195 (1996).
- [80] E. Witten, String theory dynamics in various dimensions, Nucl. Phys. B **443**, 85 (1995)
- [81] E. Witten, An SU(2) Anomaly, Phys. Lett. B **117**, 324 (1982) [Phys. Lett. **117B**, 324 (1982)].